Recent (0-40 years) environmental und climate change as interpreted from the spatial and temporal distribution of organic matter (LOI) in sediment cores from seven tributary fjords of the Sognefjord, Western Norway

Jana Altenkirch

Bachelor thesis submitted in fulfilment of the requirements for the degree of Bachelor of Science (B.Sc.) in Climate Change Mitigation and Adaptation

Western Norway University of Applied Sciences, Sogndal

(Høgskulen på Vestlandet)

Department of Environmental Sciences

Supervisors: Matthias Paetzel, Torbjørn Dale

University of Applied Sciences, Bingen

(Technische Hochschule Bingen)

Department 1 – Life Sciences and Engineering

Supervisor: Elke Hietel

30.05.2022

TH BINGEN University of Applied Sciences

Høgskulen på Vestlandet

Abgabedatum:

abgegeben bei: ………………………………….

(Name)

Arbeit angenommen:

Bingen, den ………………………………….

(TH Bingen Prof. Dr. Elke Hietel)

Betreuer (TH): Prof. Dr. Elke Hietel

Betreuer (extern): Assoc. Prof. Dr. Matthias Paetzel,
Western Norway University of Applied Sciences,
Department of Environmental Sciences

Acknowledgements

This thesis is the final outcome of two wonderful semesters at the University of Applied Sciences in Sogndal. This place became so much more than only a place to study, and I will be forever grateful that I had the opportunity to spend the last year of my bachelors as an exchange student here in Norway. I would warmly like to thank my supervisor from HVL, Matthias Paetzel. Your patience and unlimited support helped me finishing this thesis and kept me motivated throughout the entire writing process. I learned a lot from you, and your approach about how to build up and structure a scientific work will always stay in the back of my head. Many thanks as well to my supervisor at my home university in Bingen, Prof. Elke Hietel, for the easy handling and communication between you and Matthias. I really appreciate your complete trust in the working process at HVL. Furthermore, I would like to thank the international office at TH Bingen, who helped with all the organising it requires to spend a semester abroad. Last but not least, I would like to thank my family and friends for the continuously support, never mind which decision I chose to make. A special appreciation goes to my dutch girl Lynn, you gave me the physical and mental support I needed to finish my work in the last week before the submission.

Sogndal, 30.05.2022

Table of Contents

List of Abbreviations

LIA:	Little Ice Age
LOI:	Loss On Ignition
OM:	Organic Matter
OC:	Organic Carbon
TOC:	Total Organic Carbon
NOA:	North Atlantic Oscillation
XRF:	X-Ray Fluorescence
HVL:	Høgskulen på Vestlandet
UiB:	University of Bergen
CTD:	Conductivity Temperature Depth
NCCS:	Norwegian Centre for Climate Services
MET:	Norwegian Meteorological Institute

List of Figures

List of Tables

Abstract

Over the past 10 years, various sediment cores have been retrieved in seven tributary fjords of the Sognefjord, Western Norway, namely the Fjærlandsfjord, the Sogndalsfjord, the Barsnesfjord system, the Ikjefjord, the Arnafjord system, the Nærøyfjord and the Aurlandsfjord.

As a standard procedure the organic matter content has been analysed, using the method called "loss-on-ignition" (LOI). The occurrence of organic matter in the respective fjords basins is used in this thesis to get a signal of environmental and climate change over the past four decades.

Possible influencing factors for altering environmental conditions in the fjord systems are considered to be hydropower, man-made construction work and climate change. The north and south side location of the tributary fjords of the Sognefjord plays a distinct role regarding the glacial influence from the Jostedalsbreen on the hydrographical and meteorological variables influencing the fjord systems.

Spatial and temporal variations in the LOI content of the sediment samples of the tributary fjord basins of the Sognefjord can be observed. The overall trend states an increase in LOI concentrations since the 1980s until today for the north-located tributary fjords, whereas the southern tributary fjord basins experience an overall decrease in the LOI development.

The variations can be mainly explained by the link to climate change and glacial impact on the northern side of the Sognefjord, resulting in more runoff and primary production, and the link to human-induced environmental change through hydropower, resulting in significantly less runoff and primary production on the southern side of the Sognefjord.

Unique local fjord features, such as oxygen availability, are not the major controlling factor for the observed trend. The regional influence of the northern and southern location outweighs the intended individuality of each tributary fjord basin of the Sognefjord.

A simple box model has been developed to illustrate the influencing processes and factors on the organic matter supply system.

1. Introduction

Various sediment cores have been retrieved from seven tributary fjords of the Sognefjord, Western Norway and are used in this thesis to discuss environmental and climate change in the respective areas during the past four decades.

1. Background

Fjord sediments have been proven to provide historical archives of environmental and climate change (e.g., Faust et al., 2016; Howe et al., 2010; Paetzel and Dale, 2010). Overall enhanced sedimentation rates ranging between millimetres to centimetres per year (Howe et al., 2010) make fjords ideal depositional environments for gaining continuous records of changing marine, terrestrial and atmospheric conditions with a high temporal resolution, which can be in extreme cases close to a daily frequency (Howe et al., 2010).

According to the IPCC (2021), recent changes in the climate system give rise to concern for future living conditions with predictions of shifting temperature regimes. Overall, there is no doubt of a warming in the climate system since the Little Ice Age (LIA) Maximum around 1750 A.D. (e.g. Nesje and Dahl 2003). In addition, each of the last four decades has been successively warmer than any decade since 1850 (IPCC, 2021). The intensity of many of the climate extreme events such as heatwaves, heavy precipitation and droughts have strengthened and became more frequent since the 1950s (IPCC, 2021). In the climate evaluation for Norway, Hanssen-Bauer et al. (2017) confirmed that the temperature rise during the past four decades has been very distinctive and accompanies with a significant increasing trend in annual precipitation.

It is well-known that climate change will have potentially wide-ranged impacts on marine ecosystems (e.g., Keeling et al., 2010; Doney et al., 2009). Even though the natural ecosystem functions such as nutrient cycling and primary production are not directly affected by shifts in the structure of marine environments in the first place, rising temperatures might lead to changes in sea level, ocean stratification and circulation, precipitation, and freshwater input (Doney et al., 2012).

In the framework of environmental change, climate change might interact with a range of processes that are altering the environment – such as landslides or artificial supply of nutrients – and thus be linked on a certain level (Vitousek, 1992). This implies that it can be challenging to separate climate and environmental change from each other and involves that there is ever the need to consider various kinds of drivers for altering environmental conditions. In the past two decades, the focus has increased on the possible impacts of the recent changing climate and environmental conditions in fjord ecosystems (e.g., Molina-Navarro et al., 2018; Howe et al., 2010; Paetzel and Dale, 2010)

Fjords can be considered as a transition zone between terrestrial and marine environments and are often categorized as estuaries (Asknes et al., 2019). With their special hydrography and morphology, they have a unique way of functioning as water bodies, as submarine sills often create semi-enclosed basins as a characteristic feature of fjords that might affect physical and biochemical processes (Syvitski et al., 1987). This feature gives an opportunity to investigate fjords as a miniature ocean basin laboratory (Howe et al., 2010).

Fjord sediments can be used for providing evidence of environmental change, including e.g., diatoms, mineral grain sizes or the organic matter concentration (Paetzel and Schrader, 1992). The variable of focus for this thesis is the occurrence of organic matter. This can be measured through the standardized method called "Loss on Ignition" (LOI), a widely used approach to state the total organic matter concentration of sediments (Dean, 1974).

For the past ten years, there has been sampled a collection of LOI data from seven tributary fjords of the Sognefjord, Western Norway, namely the Fjærlandsfjord, the Sogndalsfjord, the Barsnesfjord system, the Ikjefjord, the Arnafjord system, the Nærøyfjord and the Aurlandsfjord (*Figure 1*).

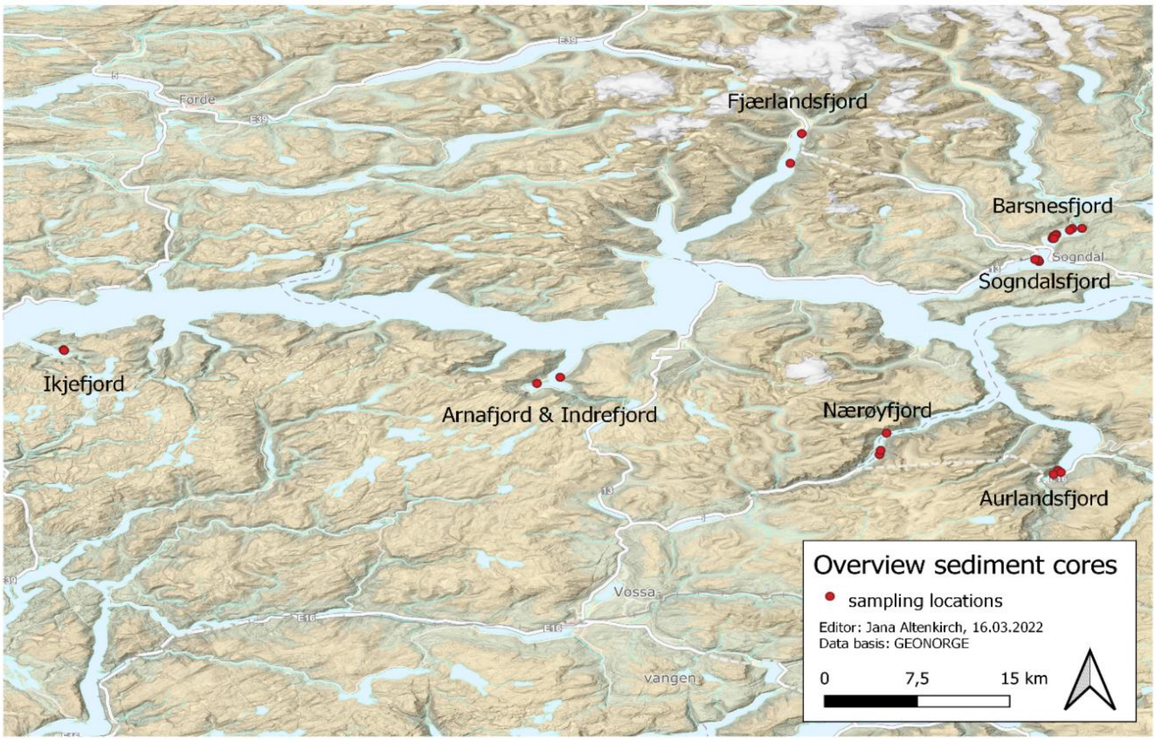

Figure 1: Overview over the Sognefjord and its tributary fjord locations. The dotted line represents existing ferry routes, the white line represents streets.

In previous studies around the Sognefjord, the LOI has been used among other as a proxy variable to see how sediments respond to local climate and environmental change (e.g., Koek and Van Doorn, 2018; Dybo et al., 2016; Timmers, 2014). These investigations focused mainly on the LOI distribution in the single tributary fjords. The thesis at hand is trying to interpret the regional LOI distribution pattern by comparing the northern tributary fjords of the Sognefjord (the Fjærlandsfjord, the Sogndalsfjord and the Barsnesfjord system) and southern tributary fjords of the Sognefjord (the Ikjefjord, the Arnafjord system, the Nærøyfjord and the Aurlandsfjord) in relation to their hydrography and geographical position to elaborate the climatic and environmental influence over the past four decades.

Generally, the aim is to gain an understanding on which factors are controlling the amount of organic matter in the fjord sediments. This also includes a documentation of the temporal development of the organic matter content in these sediments back to the late 1970s. Either degradation or accumulation of organic matter is a possible scenario due to changing biogeochemical processes in the marine sediments (Arndt et al., 2013). This would also include a change in hydrographic variables such as oxygen and its relation to the preservation of organic matter, depending on the depositional environment.

A connection between decreasing oxygen (O_2) concentrations in water bodies and rising temperatures, implying that O_2 is less soluble in warmer water, is well-known and can be seen as a direct impact of climate change on the marine systems (Keeling et al., 2010). However, other causes for a rapid transition in environmental conditions in fjords at all levels, meaning on a hydrographical, biological or geochemical scale, were taken into account by several studies earlier (e.g., Bucher, 2020; Van Rossum, 2018; Bøthun et al., 2014). Therefore, for this thesis, besides climate change, the further selected possibly controlling factors for the organic matter load in fjord sediments are hydropower and construction work impacts.

1.1 Objectives and Objective Explanations

The results of this study might form a basis for further interpretations in terms of enhancing the understanding about impacts of factors which are altering the environmental conditions in fjord systems. Regarding the expectations and assumptions, the subsequent research leads to the following objectives:

a) Are there spatial and temporal variations in the LOI content of the tributary fjord sediment samples of the Sognefjord?

In earlier studies, the focus has been on environmental change and the LOI content restricted to each single tributary fjord. The approach of the thesis at hand is to compare the different study area locations and see if the distribution differs between the tributary fjords, related to their northern and southern location. The classification in north and south is related to the glacial occurrence, with possible implications on the organic matter supply in the respective fjord basins. Whereas the tributary fjords on the northern side of the Sognefjord are connected to the Jostedalsbreen glacier, the southern located tributary fjords do not have any relation to the impacting glacier system. LOI variations can be either temporal or spatial or both.

In the first place, the analysis is going to be carried out by looking into the LOI development within the sediment cores of the single tributary fjords, with the aim to gain insight on temporal variation. This is possible due to the continuous sedimentary records in the samples and therefore the chance on dating the sediment layers in a specific depth to an estimated year. Afterwards, these results can be compared to the other tributary fjords, in order to find possible distribution patterns related to the geographical locations.

It is proposed to see a change in the internal, and thus temporal LOI development within the sediment core. The extent of this change might depend on the fjord features and the study area, including hydrographical and meteorological factors. As these factors differ from fjord to fjord, depending on the geographical location, it is also proposed to get a spatial distribution pattern of the LOI content by comparing the single tributary fjords with each other. Especially the influence of the north and south-side location of the tributary fjords at the Sognefjord might play a role for a first distinction, as affected by glacial occurrence.

b) If so, is it possible to relate these LOI variations to environmental and climate change in the respective fjords?

Noticeable changes in environmental conditions in ecosystems do always have triggers. This also accounts for the LOI variations in the sediment.

Possible influencing factors for altering environmental conditions in fjord systems as discussed in this thesis are considered to be hydropower, man-made construction work and the changing climate. Relating certain changes in the LOI content in the sediments to any of the considered factors requires to look into representative variables. Therefore, precipitation and air temperature trends will be observed in order to get a signal of changing climatic conditions during the past four decades. In addition, hydrographical variables such as oxygen and water temperature in the tributary fjord basins might provide insight about changing features in the fjord systems.

It is proposed to see a significant change in the LOI content related to changing oxygen conditions. If fjord basins do get more depleted in oxygen due to rising water temperatures, which in turn can be linked to the global warming, organic matter accumulated in the sediments will be less effectively decomposed. An increase in precipitation might influence the terrestrial runoff and therefore affect the inflow of organic and inorganic particulate matter with the water flux. Furthermore, rising air temperatures are affecting the speed of the glacier melt, which in turn might also result in an increased meltwater flux and thus more transportation of particles of glaciofluvial origin. Apart from that it might be possible to see changes in the LOI development by comparing the LOI content in the sediments before and after the start of hydropower influence in the respective fjord basins. The same accounts for human made construction work such as delta and harbour building.

c) Do such LOI controlling factors account for the entire Sognefjord region, or do they depend on the uniqueness of each tributary fjord?

The earlier investigation is supposed to show if, how and why the LOI content in the respective tributary fjord basins of the Sognefjord is changing. After pointing out the actual controlling factors, it might be possible to gain insight about how these factors are affecting the single fjord systems. It is mandatory to get a sufficient understanding of how the environment changes, to derive possible implications for the entire ecosystem. Since fjords are considered to be unique waterbodies with special features (e.g. Syvitski et al., 1987), it is interesting to observe whether there is an overall controlling factor for the spatial and temporal LOI change in the tributary fjord sediments.

The analysis can be done in the first place by comparing the single fjord features, regarding hydrological and/or meteorological variables, with the area of the Sognefjord where the tributary fjords are located. It might then be possible to see any further correlation between the areas and the proposed controlling factors.

Generally, it is expected that the LOI controlling factors are rather dependent on the uniqueness of each fjord system. Concerning this prospect, the variation and distribution of the LOI in the sediments might be more a combination of several influences instead of only one significant influence. All of these influences are most likely depending on the actual local area and eventually cannot be widened to the entire Sognefjord area.

1.2 Environmental Setting

1.2.1 Description of the Study Areas

The thesis at hand deals with the Sognefjord, Western Norway and seven of their associated smaller tributary fjords. The Sognefjord is Norway’s longest and deepest fjord, extending eastwards into land with 205 km length, and reaching 1308 m below sea level at its deepest point (Manzetti and Stenersen, 2010).

The physical distribution of the considered tributary fjords can be divided into a northern and southern area. The northern part of the Sognefjord includes the Fjærlandsfjord, the Sogndalsfjord and the Barsnesfjord system (including the Inner and Outer Barsnesfjord).

These north-located fjords are reaching toward the mountain area of Jotunheimen, central Norway. This is where the Jostedalsbreen, which is the largest ice cap in mainland Europe, is located (*Figure 2*). With an extent of 458 km^2 in 2019 (Andreassen et al., 2022), the glacier continuously has diminished and thinned since the LIA maximum (Carriviak et al., 2022).

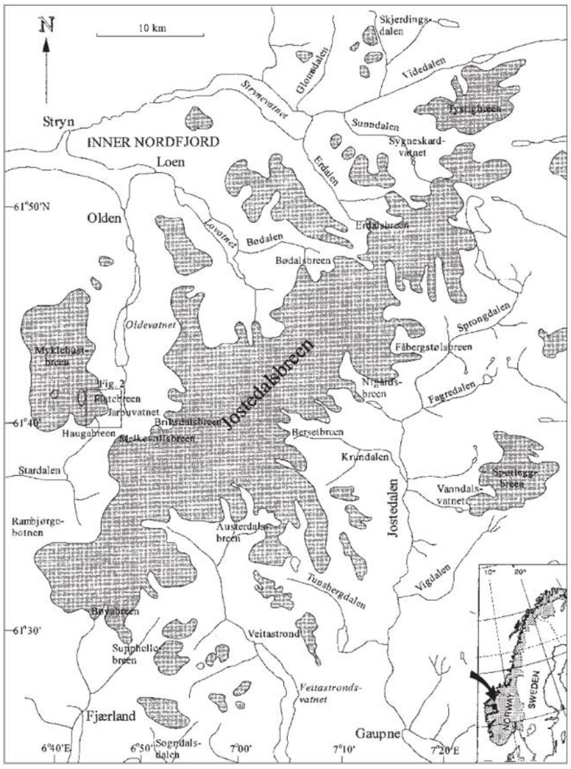

Figure 2: Location map of the Jostedalsbreen area. Reprinted from Nesje et al. (2001).

During the Holocene (counted from 11500 years ago until today) there have been several climatic fluctuations, which controlled mainly the glaciations during this time. Nesje et al. (2008) stated that all the Norwegian glaciers melted away at least once during the mid/early Holocene. In terms of the LIA Maximum, most of the glaciers reached their maximum extent around mid-eighteenth century, although it can differ depending on the location (Nussbaumer et al., 2011).

Glacial runoff and precipitation are controlling the sediment flux into the northern fjord systems, and in this way playing a key role in the distribution of particulate matter supply into the northern tributary fjords (e.g. Paetzel and Dale, 2010). Basically, with the glacial influence of the Jostedalsbreen, it is proposed that the northern tributary fjord basins might have a dependency on climatic and environmental factors controlling the glacier system, in addition to possible human induced environmental change.

The tributary fjords on the southern side of the Sognefjord, i.e. the Ikjefjord, the Arnafjord system (including the Arnafjord and the Indrefjord), the Nærøyfjord and the Aurlandsfjord are not exposed to direct glacial influence. Here, runoff from precipitation and man-made construction work like hydropower plants may play a more distinct role (e.g., Van Rossum, 2018; Koek and Van Doorn, 2018; Bucher, 2020).

To summarize, a first distinguishment can be made through the northern and southern location side of the tributary fjords of the Sognefjord. Another significant distinction is dividing the tributary fjords by their recent hydrographic conditions since some are considered oxic and others are anoxic, respectively. It is outlined in *Table 1*.

Table 1: First distinction of the considered tributary fjord basins of the Sognefjord.

Fjords	**OXIC**	**ANOXIC or SUBOXIC**
GLACIAL INFLUENCED	Fjærlandsfjord Sogndalsfjord	Inner Barsnesfjord Outer Barsnesfjord
NON-GLACIAL INFLUENCED	Arnafjord System Inner Aurlandsfjord	Inner Ikjefjord Inner Nærøyfjord

The general spatial distribution of the selected fjord basins, with a spread across a total length of about 90 km of the entire Sognefjord, can therefore provide a good starting point for investigating the controlling factors for organic matter in the sediments.

The Fjærlandsfjord

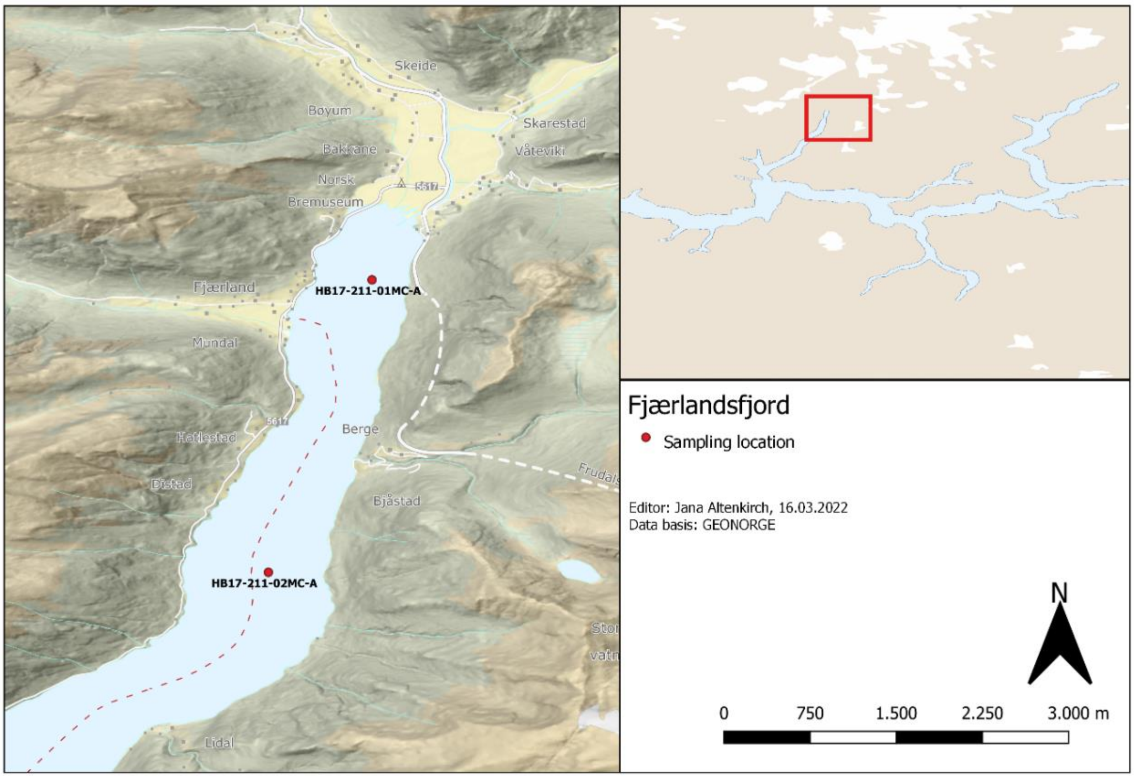

Figure 3: Location map of the Fjærlandsfjord. The red-dotted line represents a ferry route, the white line represents a street.

On the northern side of the Sognefjord, the tributary Fjærlandsfjord (*Figure 3*) is located in north-east direction. It has a length of 25 km and the township of Fjærland is located on the inner end part of the fjord (Askheim, 2020). The glaciers Bøyabreen and Supphellebreen are reaching into the adjacent valleys, fed by the main Jostedalsbreen glacier. The inner fjord basin reaches at its deepest point an approximate water depth of 182m.

The fjord basin leads at their innermost part to a delta at Bøyaøyra, which consists of brackish water and receives freshwater supply by the Storelvi river. This river in turn was formed by the tributaries Bøyaelvi and Supphelleelvi, coming from the nearby glacier valleys of Bøyadalen and Supphelledalen (Vangsnes, 1981).

Due to the location near to the glacier system, the main source for the terrestrial sediment influx into the Fjærlandsfjord is therefore glaciofluvial material from the Jostedalsbreen glacier and runoff material from the fjord sides. It can be either deposited at the delta outlet, or material can be transported further into the fjord basin.

The meteorological station in Fjærland (Station ID: SN55840/SN55820) provides the only available continuous dataset on air temperature development over the past 40 years (as shown in Figure 19), referring directly to one of the considered fjord basins. This dataset is used as an overall reference value for the entire region of the Sognefjord.

The Sogndalsfjord

The 20 km long Sogndalsfjord (*Figure 4*) is a north-east/south-west orientated tributary of the Sognefjord (Askheim, 2020). The township of Sogndal is located at the innermost end of the fjord.

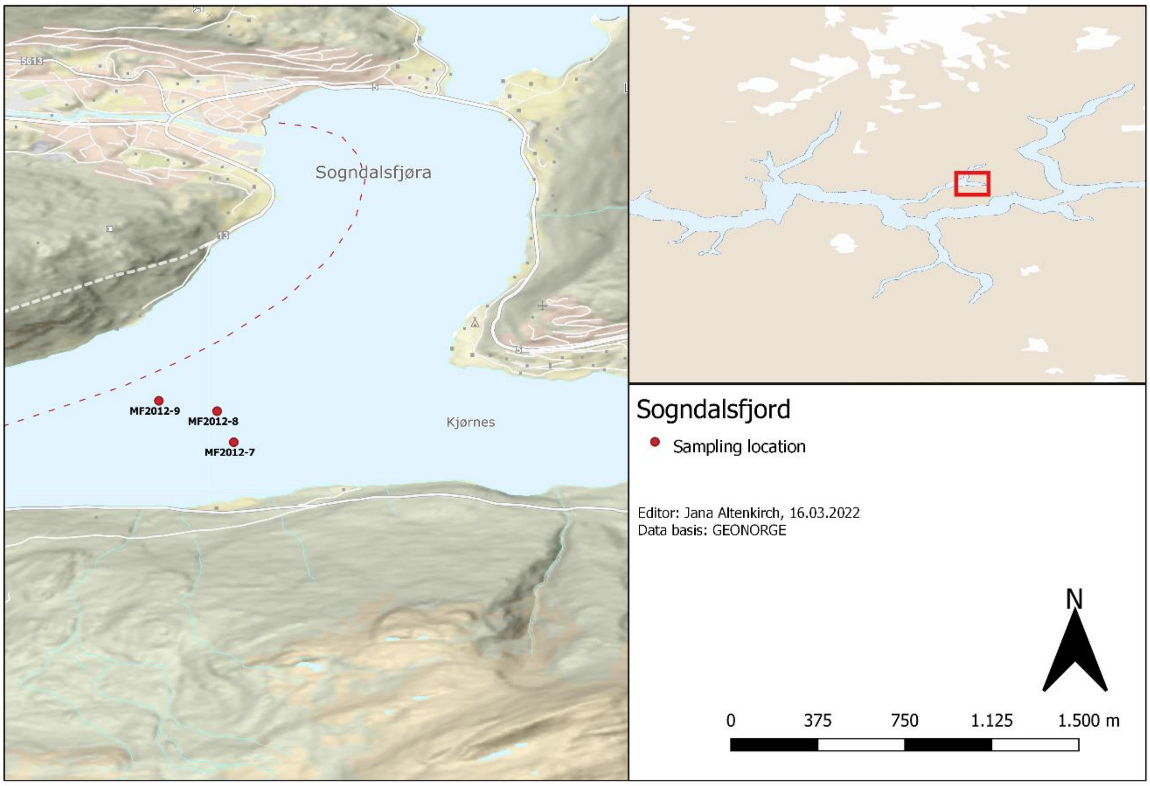

Figure 4: Location map of the Sogndalsfjord. The red-dotted line represents a ferry route, the white lines represent streets.

At the outermost part in south-west direction, a 25 m deep sill separates the Sogndalsfjord basin from the 900 m deep Sognefjord. Another 7,5 m shallow sill is connecting the

Sogndalsfjord basin with the Outer Barsnesfjord basin of 80 m water depth, transition in north-east direction (Paetzel and Dale, 2010).

The Sogndalsfjord has a maximum water depth of 260 m with overall oxic water conditions (Paetzel and Dale, 2010), even though new findings propose that the water is getting more and more depleted in oxygen over the past decades, and that values are closing in towards the critical value 2 mgO_2/l (Grieger, 2021).

The main freshwater supply is ensured by the river Sogndalselv with a catchment area of 178 km^2, including the lake Dalavatnet (Paetzel and Dale, 2010). The river is entering the fjord at the township of Sogndal. Dale and Hovgaard (1993) estimated the annual freshwater inflow with 0,5 km^3 and overall water volume of the Sogndalsfjord with 1,9 km^3. In addition, the Sogndalsfjord gets freshwater supply by the Årøyelv river at the northern part of the Barsnesfjord.

Thus, the main transport of terrestrial inorganic and organic particles comes from these two river outlets. Since the Sogndalsfjord happens to be the last sedimentation basin for particles originating from the Jostedalsbreen glacier, mostly silt sized particles are transported all the way into the Sogndalsdfjord.

Unlike the Barsnesfjord, the Sogndalsfjord is only indirect influenced by the hydropower plant at Årøy.

The Barsnesfjord

The Barsnesfjord is a north-east tributary of the Sogndalsfjord, which is connected to the Sognefjord in further south-east orientation. The Barsnesfjord consists of two parts, the Outer (*Figure 5*) and Inner (*Figure 6*) Barsnesfjord basin. These basins are separated by a 29 m deep sill. The entire fjord system has a total length of 5 km (Paetzel and Schrader, 1992)

The Inner Barsnesfjord reaches a maximum water depth of 66 meter at its basin and extends from the Årøy river inlet until the fjord narrowing between Barsnes and Kvam. The outer basin reaches 80 m at its deeptest part and ends at the town of Sogndal in the south. There, 7,5 m deep still is connecting the Outer Barsnsfjord with the Sogndalsfjord (Paetzel and Dale, 2010).

As a result of the limited water exchange opportunity due to the shallow sill between the Outer Barsnesfjord basin and the oxic basin of the Sogndalsfjord, both the Inner and Outer basin represent more or less anoxic conditions. The Inner Barsnesfjord basin is permanently anoxic

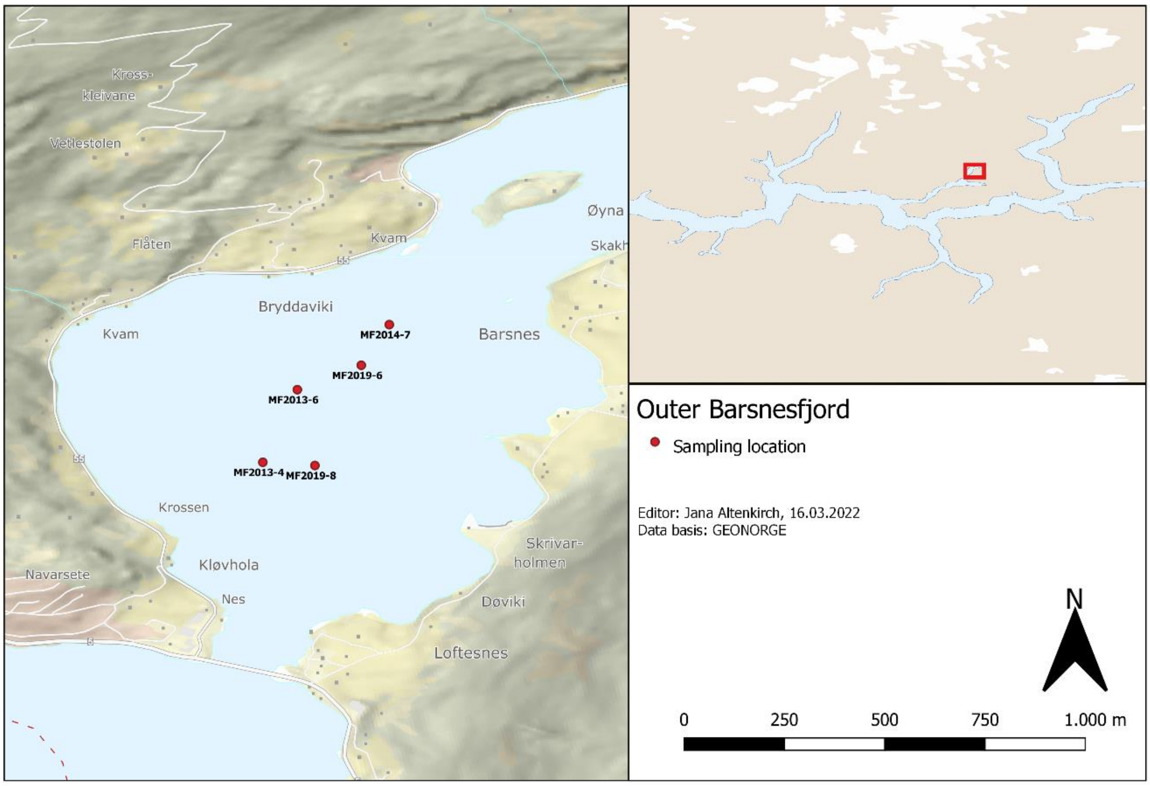

Figure 6: Location map of the Outer Barsnesfjord. The red-dotted line represents a ferry route, the white lines represent streets.

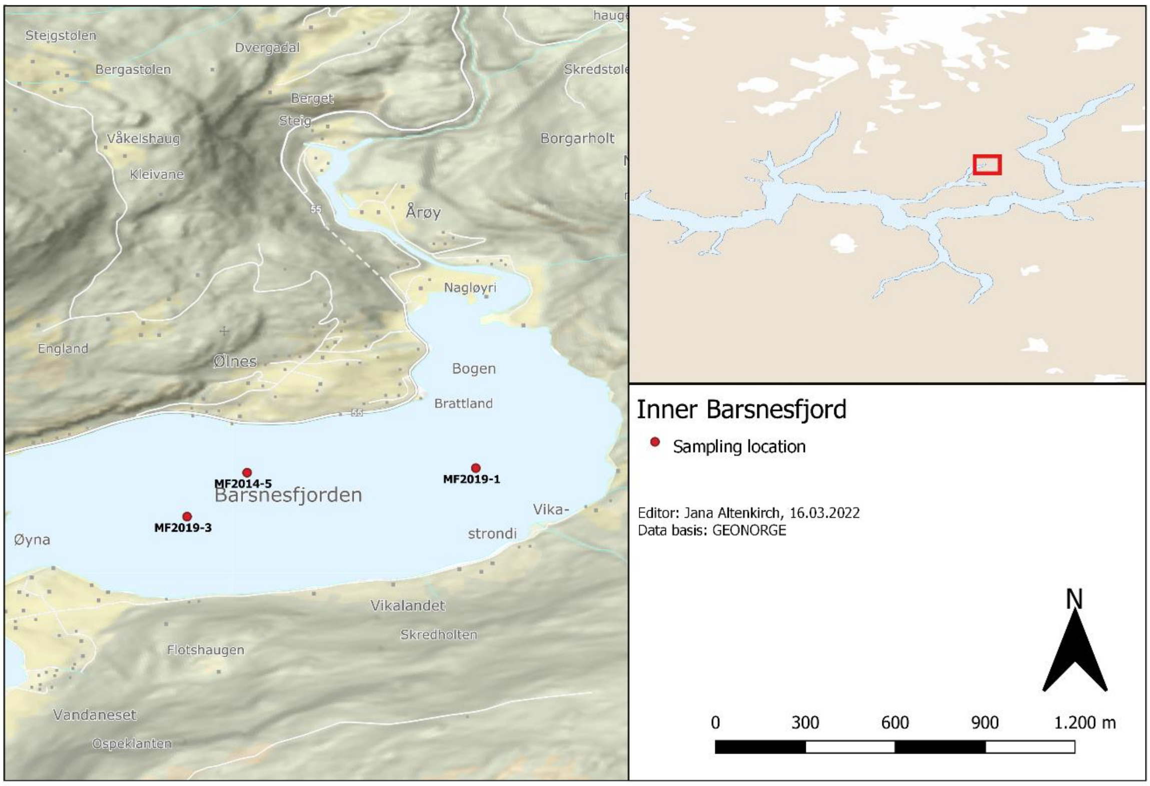

Figure 5: Location map of the Inner Barsnesfjord. The white lines represent streets.

below approximately 60 m water depth, while the Outer Barsnesfjord basin has periodically anoxic (suboxic) features (Paetzel and Schrader, 1991).

The main freshwater supply is ensured by the Årøyelv in the north, flowing via the Inner Barsnesfjord into the Outer Barsnesfjord. The river catchment area of 429 km^2 reaches up to the Jostedalsbreen glacier system, passing the lakes Veitastrondvatnet and Hafslovatnet on its way (Paetzel and Dale, 2010). The Årøyelv river is therefore the final outlet before freshwater is entering the Barsnesfjord system (Paetzel and Schrader, 1992). Dale and Hovgaard (1993) estimated the annual freshwater supply originating from the Årøyelv with 1,0 km^3.

Since the Veitastrondvatnet and the Hafslovatnet are working as a pre-sedimentation basin for coarse-grained (sand and coarse silt) material originating from the Jostedalsbreen glacier, only small (medium to very fine silt and clay) sediment particles will enter the Barsnesfjord system throughout the inflowing river (Paetzel and Schrader, 1992).

The Hafslovatnet has being dammed the first time in year 1905 and the Veitastrondvatnet was regulated in 1982. A second damming of the Hafslovatnet happened in connection with the construction of the Årøy hydropower plant in 1983. This changed the recent way of the water flow since the water is passing through a tunnel from Hafslovatnet to the hydropower station and is getting released later to the river (Paetzel and Schrader, 1992). However, the natural annually freshwater inflow rate is imitated artificially and thus at a similar level (Paetzel and Dale, 2010).

The Inner Ikjefjord

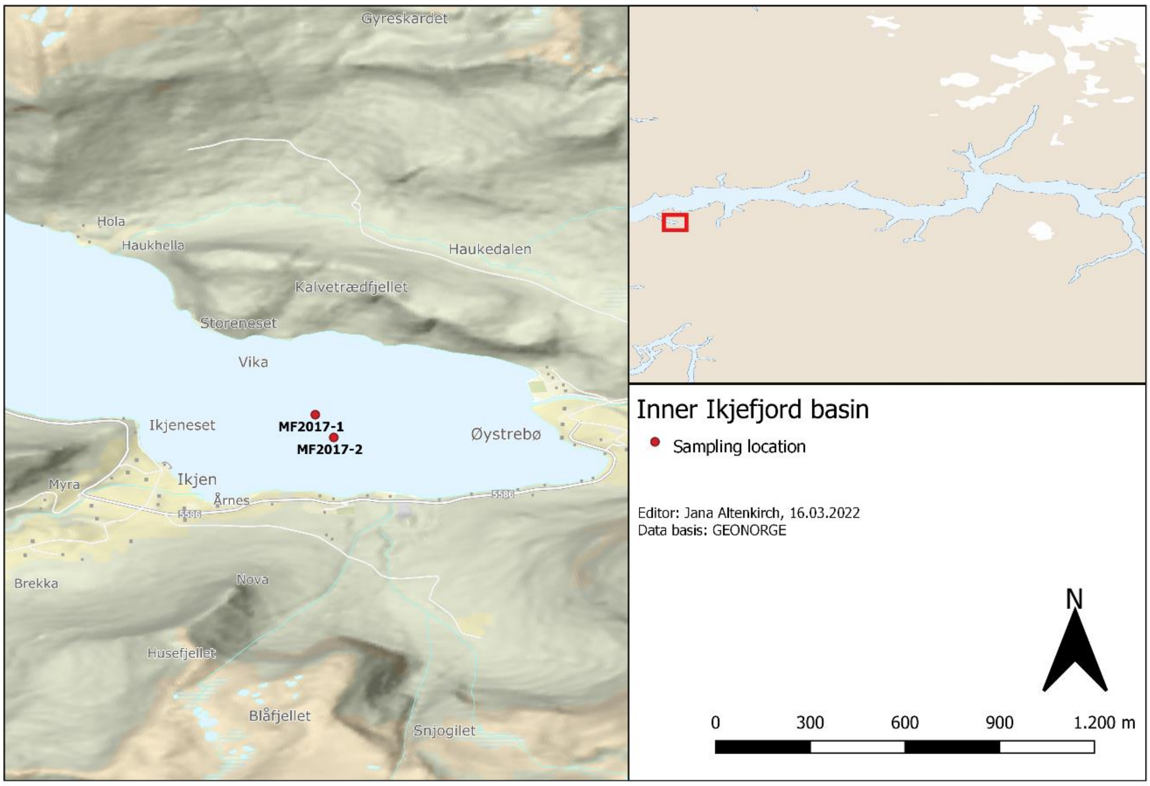

Figure 7: Location map of the Inner Ikjefjord basin. The white lines represent streets.

The Ikjefjord is located in the municipality of Høyanger, Western Norway and has a length of 5 km. It is tending in southeast direction of the Sognefjord. Of all the considered tributary fjords for this thesis, the Ikjefjord is located in most western direction at the Sognefjord.

The Ikjefjord is divided into an Inner and an Outer Basin, separated by a 53 m deep sill. The Inner basin, as shown in *Figure 7*, has a maximum water depth of around 90 m.

Several anthropogenic activities in the Ikjefjord system in the 1970s might have caused a change in the environmental conditions. The damming of the lake Stølsvatnet in 1971 reduced the freshwater input into the Ikjefjord (Schedel et al., 2015) and the fjord water circulation was impacted by the building of a bridge at the fjord outlet between 1973 to 1977 (Massnes, 2016).

Besides, a natural freshwater overflow event occurred in 1983 at the dam of the lake Stølsvatnet. As a result, uncontrolled water masses have been released into the Ikjefjord within a short amount of time. This event might have had an impact on the sediment deposition in the fjord basin.

The freshwater supply was originally ensured by the rivers Storelva, Snjogilet and the Øystrebøelva. The runoff into the fjord is system changed with the construction of the hydropower plant in 1971 in Masfjorden, south of the Ikjefjord. Since then, the rivers are regulated through several damming and tunnels, and the freshwater flows now in opposite direction, away from the Ikjefjord and towards the hydropower plant (Solbakken et al., 2011). This resulted in a reduced freshwater runoff into the Ikjefjord via the river Øystrebøelva by over 60% after the first redirection activity, followed by a 40% reduction of freshwater runoff through the regulation of the river Storelva (Schedel et al., 2015; Åtland et al., 1998).

The Arnafjord System

The Arnafjord system is located in Vik municipality, Western Norway. It has a length of approximate 9 km (Askheim, 2020). The Arnafjord system consists of the Arnafjord in the north, the Framfjord in the southeast and the Indrefjord in the southwest. For this study, only the Arnafjord basin and the Indrefjord have been considered, as shown in *Figure 8*.

In the Arnafjord basin, the water depth is approximately 109 m, the Indrefjord has a maximum water depth of 68 m.

Hydrographical measurements state that the oxygen concentrations in the Arnafjord system are in a good condition (Bucher, 2020).

The freshwater inflow into the fjord system is ensured by several rivers, the Sleipa river in the southwest and the rivers Dalelvi und Tura in the southeast. These south-eastern rivers have been regulated since the building of the Refsdal hydropower plant, located in the western nearby valley of Øvrisdalen, in 1968 (Appelgren and Ledje, 2016). Since then, the water supply has been majorly impacted and resulted in a reduction of freshwater inflow about 75% to 80% (Dårflot and Nævdal, 2020; Appelgren and Ledje, 2016).

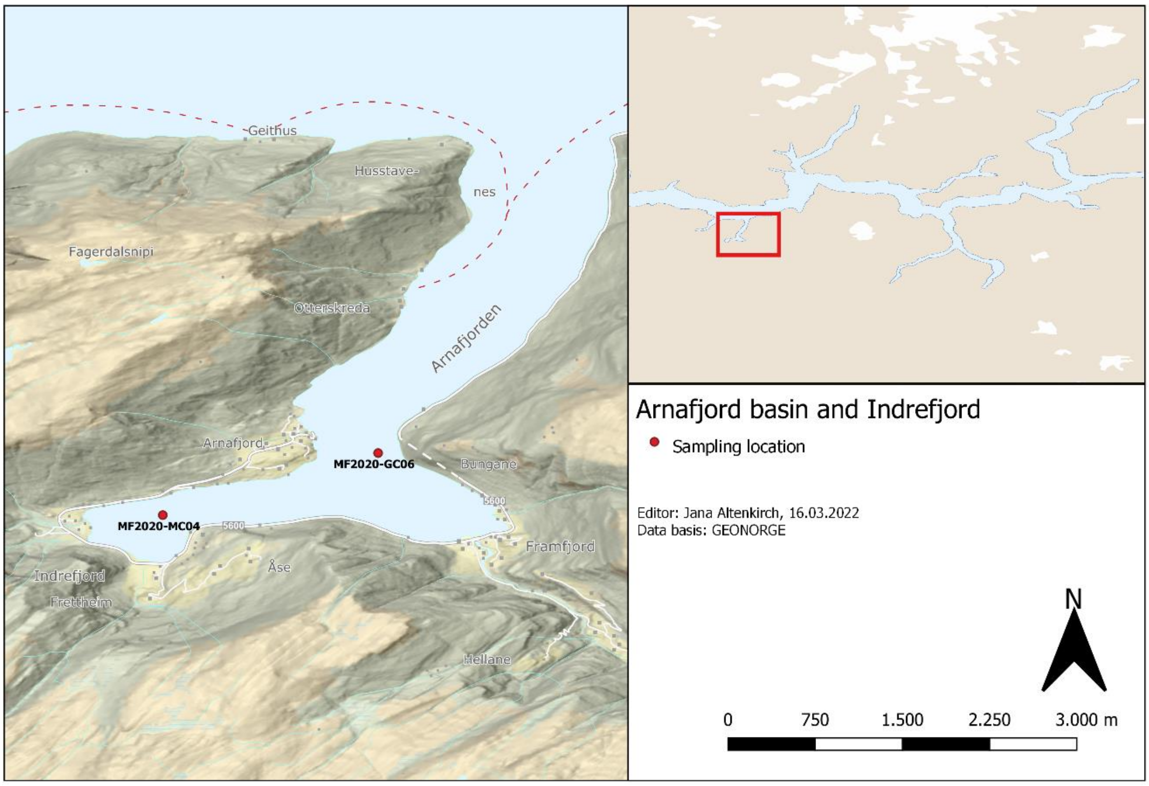

Figure 8: Location map of the Arnafjord system. The red-dotted lines represent ferry routes, the white lines represent streets.

The Nærøyfjord

The Nærøyfjord is a fjord system in the Aurland municipality. It is a southwestern side arm of the Aurlandsfjord, which is connected to the Sognefjord to the north and has a length of 19 km (Thorsnæs, 2021). It consists of the Inner Nærøyfjord (*Figure 9*), the sill area of the shallow Bakka basin and the Outer Nærøyfjord. The most narrow and shallow point of the entire Nærøyfjord is at Bakka, with a width of 250 m.

The Inner Nærøyfjord is permanently anoxic with a basin depth of 75 m. Between Bakka and the basin at the town of Gudvangen, a 11 m deep sill is separating these two parts from each other.

The Nærøyfjord is Norway’s narrowest fjord. It is included in the UNESCO List of World Natural Heritage and together with the Geirangerfjord it is a typical location for a fjord

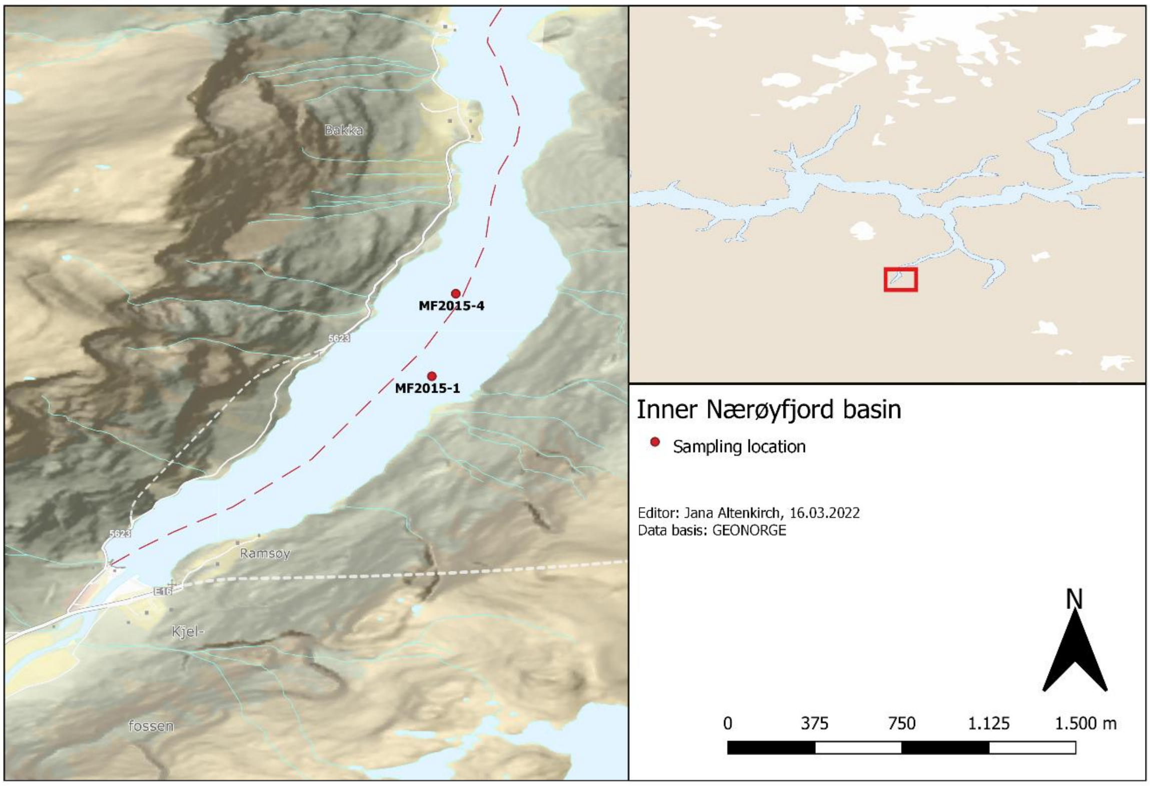

Figure 9: Location map of the Inner Nærøyfjord basin. The red-dotted line represents a ferry route, the white lines represent streets.

landscape (Thorsnæs, 2021). With the start of cruise ship traffic in Norway around 1890, the Nærøyfjord became a popular tourist destination.

Figure 10: Development of the river delta in Gudvangen from 1971 (left picture) to 2013 (right picture). Reprinted from Dybo et al. (2016).

The little township of Gudvangen is located at the southern end of the Inner Nærøyfjord at the delta where the river Nærøydalselva is flowing into the fjord basin. Between 1986-1991 the natural river delta was destroyed to improve the local infrastructure by building a main road across the delta and locating tourist attraction onto the delta (Klamer, 2017), as shown in *Figure 10*.

The main freshwater supply comes from the river Nærøydalselvi at Gudvangen and with less extent from runoff from the steep mountain sides around the fjord.

Although the Nærøyfjord is located in an area that is known for a high production of hydroelectricity, is has no hydropower plants directly influencing the fjord system (Manzetti and Stenersen, 2010).

The Aurlandsfjord

The Aurlandsfjord is located in Aurland municipality, Western Norway. It splits after about 12 km in southern extension into the Nærøyfjord. The fjord is surrounded by steep mountains (Selland, 2021). At the innermost part of the Aurlandsfjord (*Figure 11*), the village of Flåm is located. It is well known as a popular touristic destination for cruise ship traffic and the Flåmsbanen railway line.

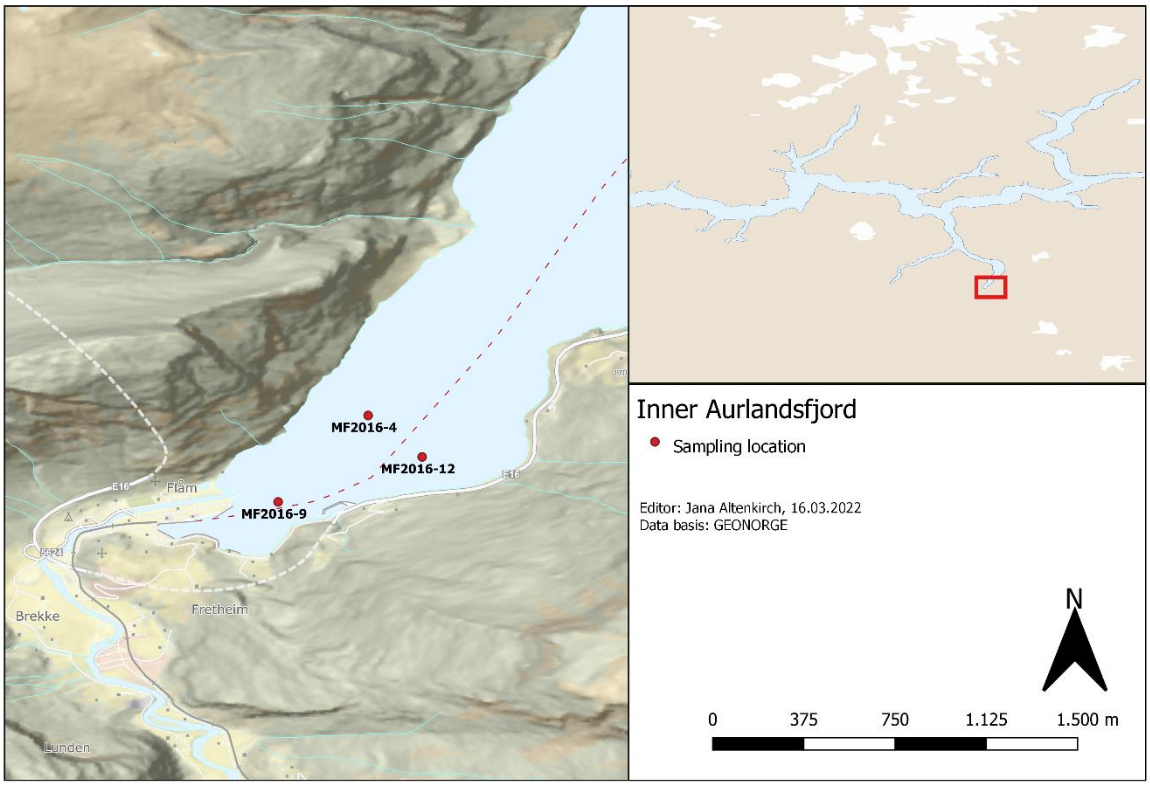

Figure 11: Location map of the Inner Aurlandsfjord. The red line represents a ferry route, the white lines represent streets.

The topography of the Inner Aurlandsfjord is dividing the fjord into different environments. Different water depths can be found which are varying between 25 to 70 m. These ranges in water depths at the fjord bottom are most likely due to landslide events, what has been found out after geological mapping from bathymetric and seismic surveys (Midttømme et al., 2017).

A historical report on hydrographic conditions in the Aurlandsfjord states that the available oxygen has been classified into a good condition (Johannesen and Lønning, 1988).

The most important sediment flux source for the Inner Aurlandsfjord is the river Flåmselvi. It is extending southwards into the valley of Flåmsdalen. The river is regulated and impacted by two hydropower plants at Leinafossen and Kjosfossen.

Between 1981 to 1985, the natural delta has been destroyed by depositing sediments from a tunnel construction: The development is shown in *Figure 12*. In 1999, a cruise ship quay was established additionally (Klamer, 2017).

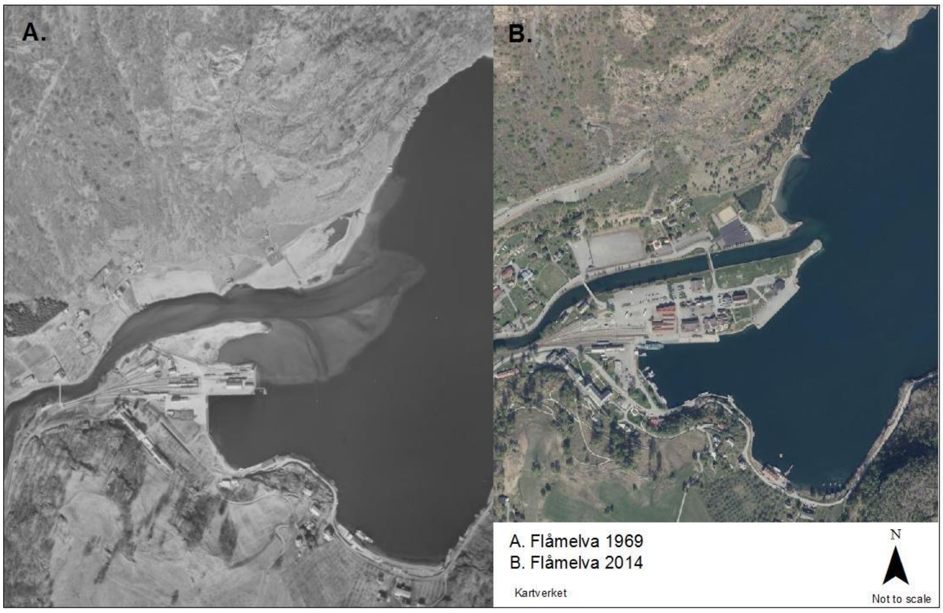

Figure 12: Development of the river delta in Flåm from 1969 (left picture) to 2014 (right picture). Reprinted from Midttømme et al. (2017).

Western Norway was affected by a flood period in October 2014, major caused by heavy precipitation. Flåm was here especially impacted by this century flood.

1.2.2 Fjord Formation

A fjord is described as a deep estuary, which has been or is presently being altered by land-based ice (Syvitski et al., 1987). They can be found as mid to high latitude fjord belts along both hemispheres (Howe et al., 2010).

The formation of the fjord in Western Norway, as illustrated in *Figure 13*, began with the uplift of the Norwegian landmass during the Tertiary period, forming a highland plateau called the Paleic surface (Holtedahl, 1967). During the uplift, fluvial and aerial erosional processes were forming V-shaped valleys, following zones of weakness in the bedrock (Syvitski et al., 1987). The following Quaternary glaciations deepened and widened the valleys and transferred them to U-shaped valleys (Nesje and Whillans, 1994). As soon as the glacial erosion reached sea level, the erosion continued below sea level, resulting in an over-deepening process. Such over-deepened and sea water filled glacial valleys are then called fjords (Howe et al., 2010).

Regarding the history of fjord formation with significant geomorphic features, they can be seen as immature and non-steady-state systems, developing and changing over relatively short time scales (Bianchi et al., 2020). Therefore, their succession of erosion and deposition is dynamic and can be related to glacial and interglacial history, also expected to continue throughout future glacial and interglacial processes (Syvitski et al, 1987).

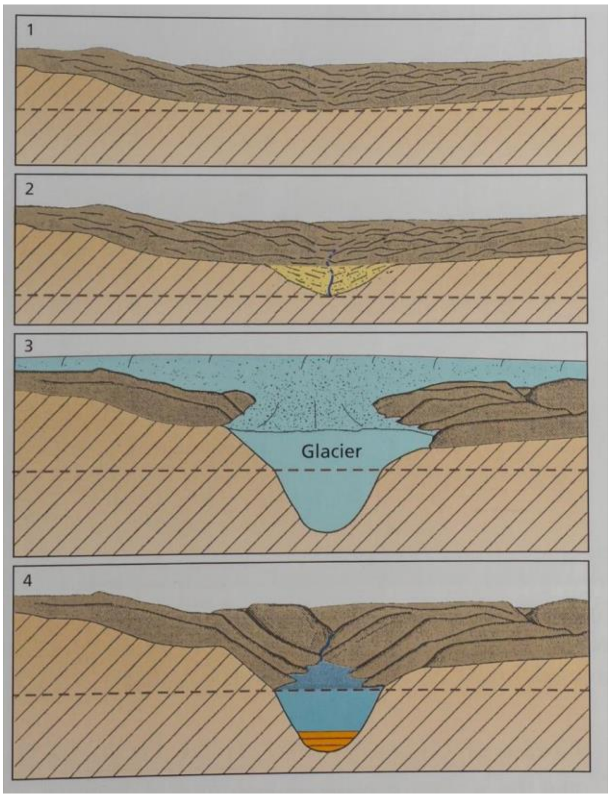

Figure 13: Illustration of the principal fjord formation. Reprinted from Ramberg et al. (2008)
(1) uplift of the paleic surface, (2) riverine erosion in the bedrock, (3) over-deepening by glaciers below sea level, (4) sea water filled valleys as the final fjord landscape.

1.2.3 General Fjord Hydrography

The hydrographic cycle of a fjord system can be divided into freshwater input and marine water exchange and give an insight into recent land-ocean interactions on a local scale (Faust et al., 2017).

One typical feature is decisive for the hydrographical system of a fjord. Overall, submarine sills are separating a fjord basin from the open ocean (Asknes et al., 2019). In the case of the considered tributary fjord basins, shallow sills outline the threshold between the fjord outlet at its outermost part and the Sognefjord. The presence of a sill can lead to a limited water exchange between the coastal water (the Sognefjord) and the basin water (the tributary fjords) and can result in oxygen depletion, and eventually either periodically or even permanently anoxic fjord basin water conditions (Howe et al., 2010). However, depending on the geomorphological development of the fjord, there are some fjords with multiple sills and some with no sill at all (Syvitski et al., 1987)

Since fjords are considered as a type of estuary, their semi-enclosed costal waterbody still has a free connection to the open sea water. Thus, the near-shore sea water is diluted with freshwater from land drainage (Syvitski et al., 1987). Since freshwater and coastal water - or in the case of this thesis, the more saline waters of the main Sognefjord - do have different densities, a salinity gradient is created in the water body and leading to a stratification into different water layers of the tributary fjords. This implies an estuarine circulation, meaning that the less dense brackish water on the surface is flowing out of the tributary fjords, while the more saline and thus denser coastal or Sognefjord water is flowing into the fjord basin, creating deeper water layers (Howe et al., 2010). The general structure of a fjord waterbody is illustrated in *Figure 14*.

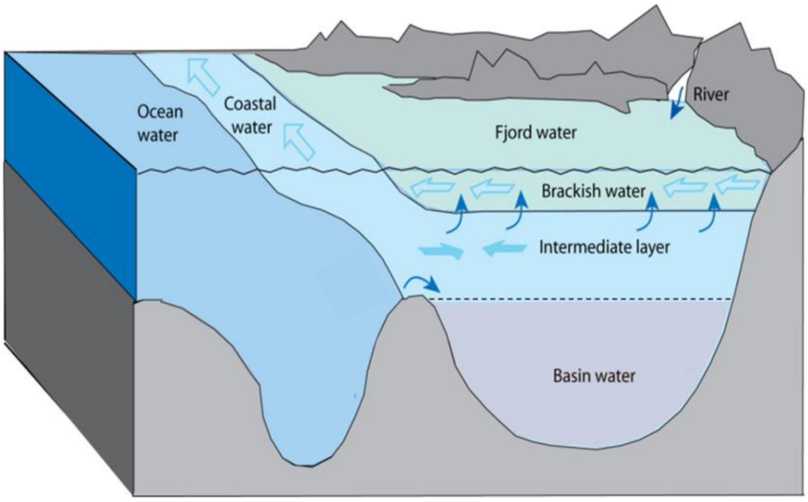

Figure 14: Vertical water layers in a silled fjord system and the associated water circulation. Modified from Asknes et al. (2019).

In case of direct or indirect glacial influence on the northern tributary fjords, the respective hydrographical systems would get a significant freshwater supply, especially during melting periods. The amount of released meltwater by shrinking glaciers is in turn dependant on climatic conditions controlling the glacier system, such as precipitation and air temperature (e.g. Nesje et al., 2008).

For the southern located tributary fjords, glacial meltwater runoff does not play a distinctive role regarding freshwater supply into the fjord system. Here, other factors happen to control the hydrographical system. Generally, water input due to riverine runoff from rainfall catchment is a possible freshwater supply process, whereas direct rainfall on the fjord water surface has a negligible effect on most fjords (Inall and Gillibrand, 2010). All the southern tributary fjords, except the Nærøyfjord, are directly influenced by hydropower plants in the nearby areas, including sometimes several damming and regulating of the rivers in the respective catchment areas. Overall, the hydropower production in these fjord basins might therefore have a hydrographic impact which needs to be considered.

1.2.4 Organic Matter Supply and Decomposition

The different environmental settings for the respective fjord systems (here the tributary fjords of the Sognefjord) usually affect their biological processes, including the organic matter supply (Syvitski et al., 1987).

Generally, organic matter (OM), often simplified as organic carbon (OC), can be classified into two main categories within marine or fjord environments, allochthonous and autochthonous. The autochthonous organic matter derives mainly from local marine primary production in the photic zone of the marine or fjord waterbody. The allochthonous organic carbon originates from external sources, such as terrestrial organic material transported by rivers, runoff, or glaciers (Bianchi et al., 2020). Together, they form the total organic carbon (TOC) fraction in sediments.

Primary production in fjords is mainly dependant on nutrient supply and solar radiation available for photosynthesis (Bianchi et al., 2020). During a snow melting season there is an increased river discharge of dissolved mineral nutrients what triggers the annual spring bloom of phytoplankton and thus implies primary production in the surface the respective waterbodies (Faust et al., 2016). Additionally, macroalgae can also add organic material to the primary production.

There are three major blooms which are of significance (Erga, 1989). The first spring bloom around March/April is triggered by light and utilizing the unused nutrients that accumulated in the water column during the non-productive winter period. The second spring bloom in May/June is triggered by nutrient supply during the melting season. The fall bloom around September/October is triggered by nutrient supply through runoff due to the fall precipitation season.

The marine organic matter flux within the water column is acting as a driving force, the so called "biological pump" (Kulinski et al., 2014). Therefore, Smith et al. (2015) hypothesized fjords as global hotspots of organic carbon burial. The usual characteristically fjord basins features – deep and dark, with a low availability on oxygen – make them ideal environments for preserving organic matter. Minimal disturbance and high annual amounts of about 18 Mt OC buried in fjord sediments on a global scale account for estimated 11% of the entire annual marine organic carbon burial (Smith et al., 2015).

Apart from that, the decomposition of OM in the water column and the surface sediments accompanies with a consumption of oxygen (Syvitski et al., 1987). Due to the sill-restricted water exchange and thus limited ventilation of the basin water body, the degradation of organic matter leads to further oxygen depletion in the fjord system.

Sediments in anoxic environments have the advantage that they are not affected by vertical bioturbation and thus stay undisturbed at the transition zone between water and the sediment surface (Howe et al., 2010). As a result, all organic matter that reaches an anoxic fjord bottom will be preserved and thus accumulate in a stronger degree compared to oxic and oganic matter decomposing fjord bottom environments (Syvitski et al., 1987).

1.2.5 Environmental and Climate Change

The near-land fjord settings make them particularly interesting for industry and getting economically valuable (Howe et al., 2010). The Sognefjord is a popular destination for cruise ship traffic, visiting the famous touristic hotspots around the Nærøyfjord and the Aurlandsfjord. Besides, hydropower production has become a significant promotion for a growing economy in many municipalities (Manzetti and Stenersen, 2010).

Hydropower

The Sognefjord shore hosts many hydropower plants, including the chosen tributary fjords. The Sogndalsfjord and the Nærøyfjord are the onlyfjord basins only indirectly impacted by hydropower plants (as illustrated in *Table 8*). Some villages around the Sognefjord area rely on the production and export of hydroelectrical power to major populated cities as the capital Oslo or Bergen. In addition, this industry ensures job security for thousands of people working at the hydropower stations (Manzetti and Stenersen, 2010).

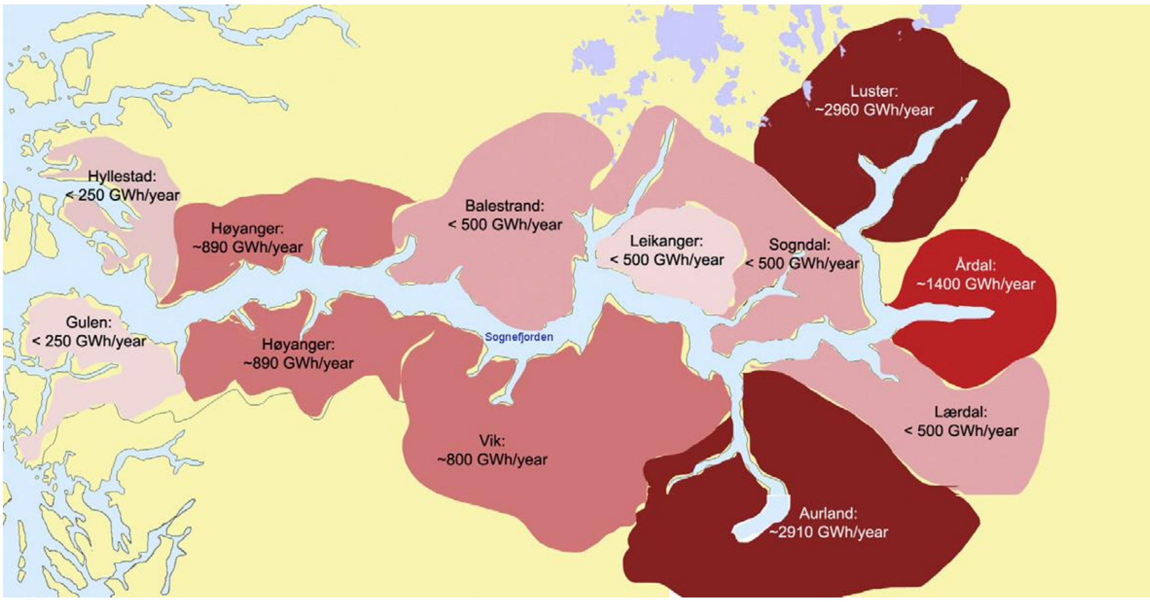

Figure 15: Illustration of the hydropower production activity around the shores of the Sognefjord and its municipalities. Reprinted from Manzetti and Stenersen (2010).

Figure 15 illustrates the hydroelectric power production along the Sognefjord area, indicating an increase in intensifying the colours from pink to red. Here it is visible that the northern tributary fjords (Fjærlandsfjord, Sogndalsfjord and Barsnesfjord) are located in an area that produces < 500 GWh/year. In contrast, on the southern side, the Ikjefjord and the Arnafjord system are located in an area that produces between 800-900 GWh/year. Moreover, the Nærøyfjord and the Aurlandsfjord are located in the majorly hydropower impacted area, producing an amount of approximately 2900 GWh/year. The estimated hydropower energy production of the entire Sognefjord region was estimated by Manzetti and Stenersen (2010) to 8 TWh on an annual scale.

Earlier studies suggest that the hydropower production has an impact on the hydrographic system of the Sognefjord and its tributary fjords, resulting in 248% more freshwater entering the fjord in winter compared to times without any regulation, and correspondingly less freshwater reaches the fjord during the summer season (Berg et al., 2017). However, some fjords might be more affected by others. Kaufmann (2014) and Ress (2016) documented such effect on the seasonal discharge changing the runoff patterns into the fjord system. This development is basically the opposite of the natural regime, and thus lead to implications on associated hydrological factors. However, some fjords might be more affected as others.

Fjord delta development

Another anthropogenic impact, which is causing increasing pressure on the fjord ecosystems, is the development of harbours and the associated destruction of the fjord deltas for enhancing the touristic attraction (Klamer, 2017).

Since the Sognefjord and their tributary fjords are especially known for their cruise ship traffic, they are receiving over 200 visits from big touring ships (Manzetti and Stenersen, 2010) showing tourists popular destinations such as the UNESCO Natural World Heritage fjord regions around the harbours of Flåm and Gudvangen. As shown in *Figure 10* and *12*, the natural river deltas of Flåm and Gudvangen have been destroyed to constructing quays for the cruise ships. Klamer (2017) concluded in his study about the development of river deltas in the Inner Sognefjord region, that eight out of ten deltas experienced major changes between the 1960s and the 2010s to create more areas for industry, tourism, mobility and agriculture.

This drastic physical change in the catchment area might be reflected in recent sedimentary deposits in the fjord basins (Howe et al., 2010). This could include changing sedimentation rates, as well as changing organic and inorganic particulate matter supply.

Climate change

Besides the human-induced impacts, challenges due to the recent climate change and the implications for the fjord ecosystem have been discussed lately.

There is no doubt that the climate is recently changing, on a global scale as well as on the local scale (IPCC, 2021). The Sognefjord region of Western Norway is therefore affected by changes in the climatic conditions as well (Hanssen-Bauer et al., 2017).

Representative for the entire area, three meteorological stations were picked to analyse the climate change signal in terms of air temperature. Additionally, each tributary fjord basin was assigned to a near meteorological station in terms of observing the local precipitation pattern. An overview about all the considered meteorological stations for the respective tributary fjord basins is shown in *Table 2*, and the locations of all stations are illustrated in *Figure 16*.

Table 2: Overview over the considered nearest meteorological stations to the respective associated tributary fjords in the Sognefjord area and the two additional meteorological stations.

Nearest meteorological station	Meters above sea level (masl)	Station ID	Associated tributary fjord	Available data
Fjærland - Skarestad	10 m	SN55840	Fjærlandsfjord	Precipitation + Air Temperature
Fjærland - Bremuseet	3 m	SN55820		
Sogndal - Selseng	421 m	SN55730	Sogndalsfjord	Precipitation
Hafslo	246 m	SN55550	Barsnesfjord System	Precipitation
Sørebø	4 m	SN52970	Inner Ikjefjord	Precipitation
Vik I Sogn III	65 m	SN53070	Arnafjord System	Precipitation
Jordalen - Nåsen	614 m	SN53160	Inner Nærøyfjord	Precipitation
Aurland	15 m	SN53700	Inner Aurlandsfjord	Precipitation
Additionally picked meteorological stations:				
Vangsnes I	51 m	SN53100	-	Air temperature
Vangesnes II	49 m	SN53101	-	
Takle	34 m	SN52860	-	Air temperature

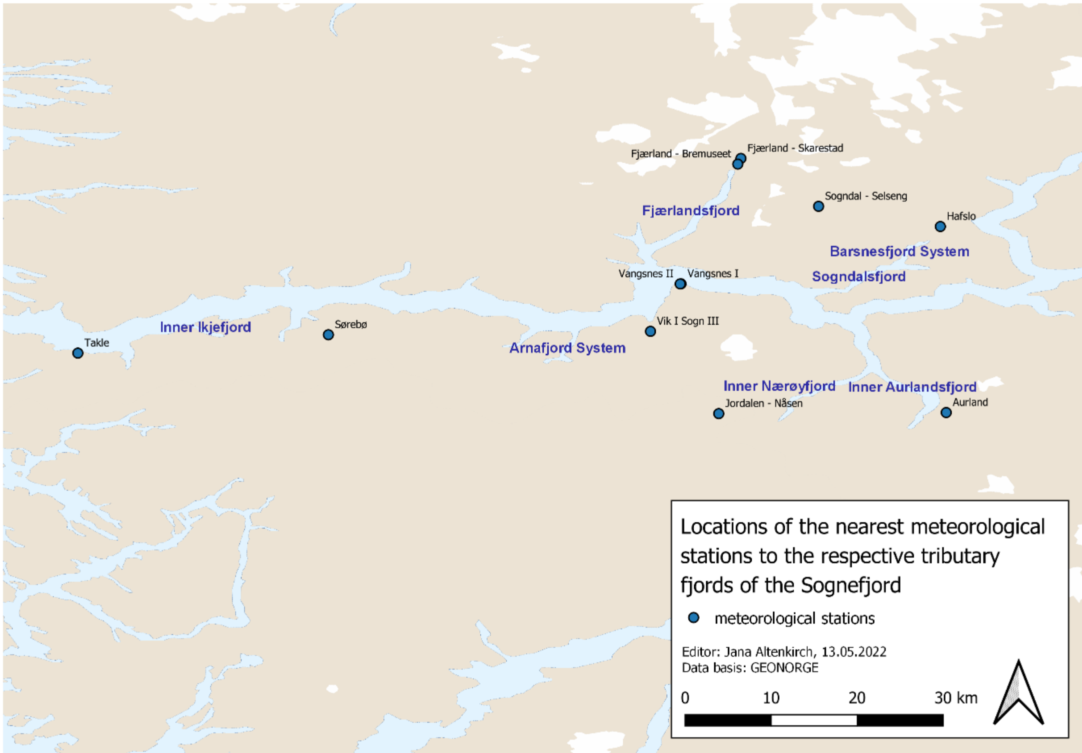

Figure 16: Locations of the nearest meteorological stations to the respective tributary fjords of the Sognefjord.

The air temperature development is pictured for the meteorological stations in Takle (*Figure 17*), Vangsnes (*Figure 18*), and Fjærland (*Figure 19*).

It is visible that in all considered locations the air temperature increased significantly over the past 40 years. Generally, the meteorological station in Fjærland shows the lowest average air temperature. That can be explained by the glacial influence resulting in a generally cooler environment. The annual temperatures increased between 1-1,5°C at these locations throughout the last four decades.

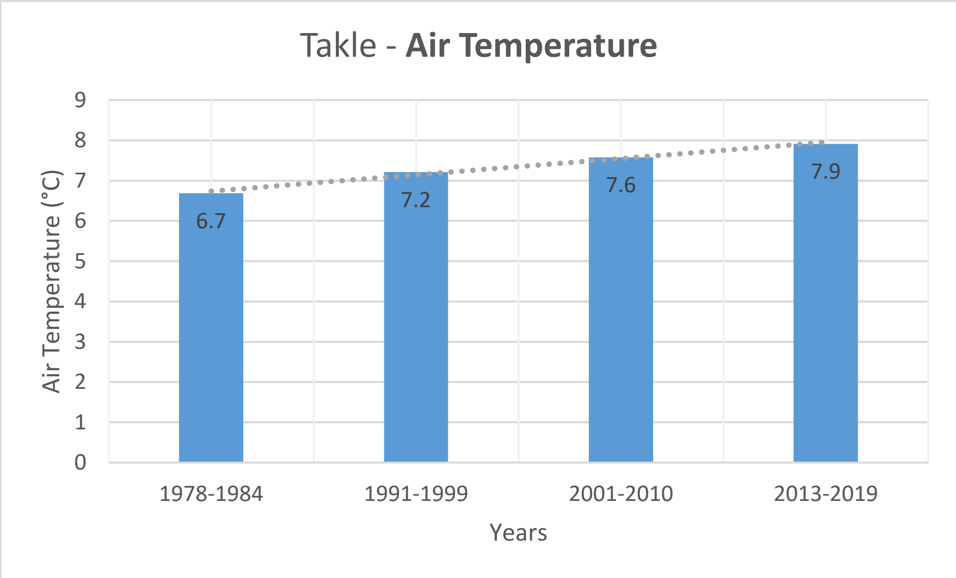

Figure 18: Air temperature trend at the meteorological station in Takle.

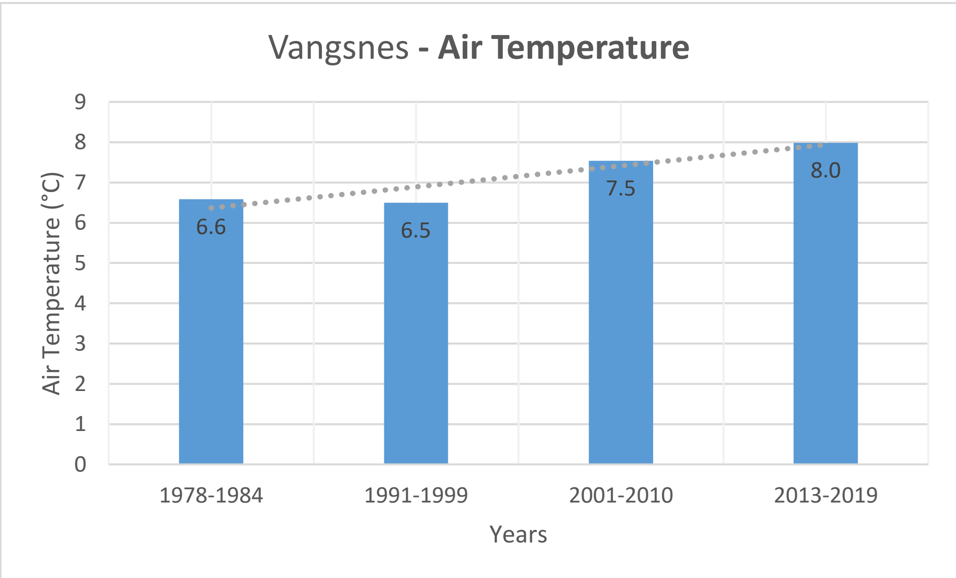

Figure 17: Air temperature trend at the meteorological station in Vangsnes.

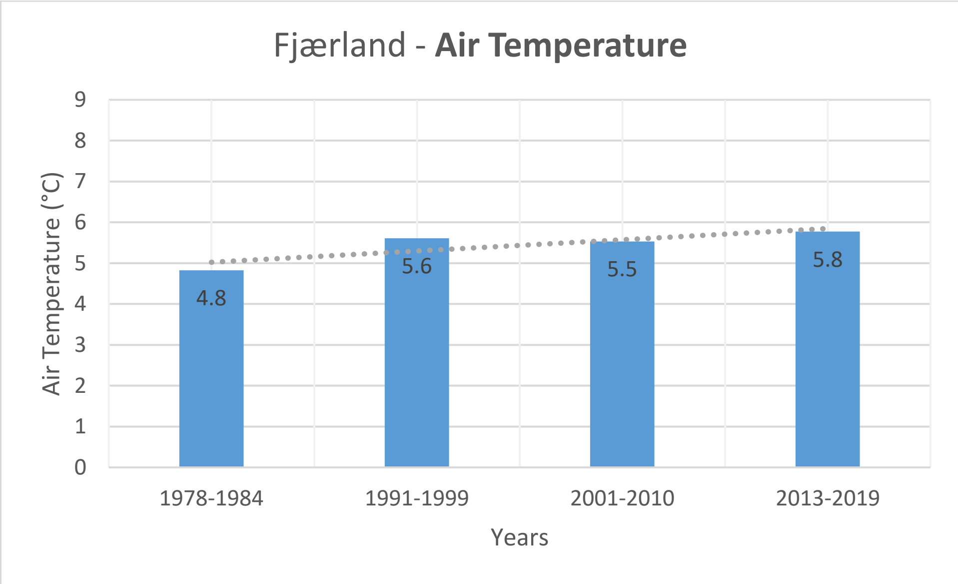

Figure 19: Air temperature trend at the meteorological station in Fjærland.

The choice of the considered timing throughout the past four decades (1978-1984, 1991-1999, 2001-2010, 2013-2019) corresponds with the choice of the later used time horizons for the analysis of the LOI, as well as for the hydrographical data. That is the reason for the in-continuous progression throughout the years, as pictured in the graphs.

Rising air temperatures might have implications for the living environment since the fjord ecosystem conditions do change with this altering factor. It results in increasing water temperatures and possible oxygen depletion, which in turn can affect the nutrient cycling and biological interactions regarding primary production (Doney et al., 2012) and thus organic matter supply.

Additionally, the precipitation pattern can also be used to observe a signal of climate change. The annual precipitation was estimated to be highest in the central part of Western Norway, where the tributary fjords of the Sognefjord are located. Regarding further climate projections until the end of the 21st century, the largest absolute increase in millimetres precipitation is expected to happen in this area as well (Hanssen-Bauer et al., 2017).

To get a more precise frame of the precipitation pattern at the respective tributary fjord locations, available data from the nearest meteorological stations have been analysed. The overall trend shows only a significant increase in the annual precipitation for the meteorological stations concerning the Sogndalsfjord (*Figure 21*) and the Nærøyfjord (*Figure 25*). The values for the other fjords remain either stable or are fluctuating around a certain quantity (see *Figure 20, 22, 23, 24, 26*).

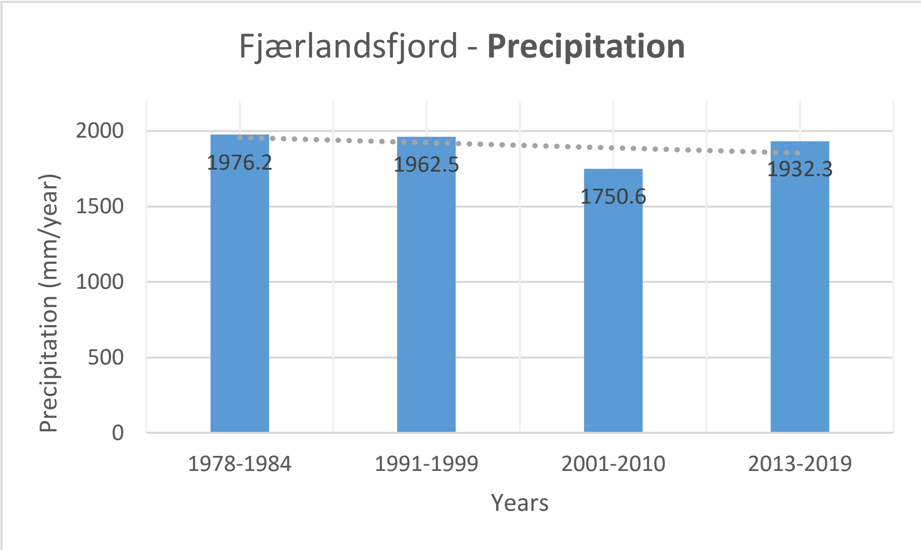

Figure 22: Precipitation trend in the Fjærlandsfjord.

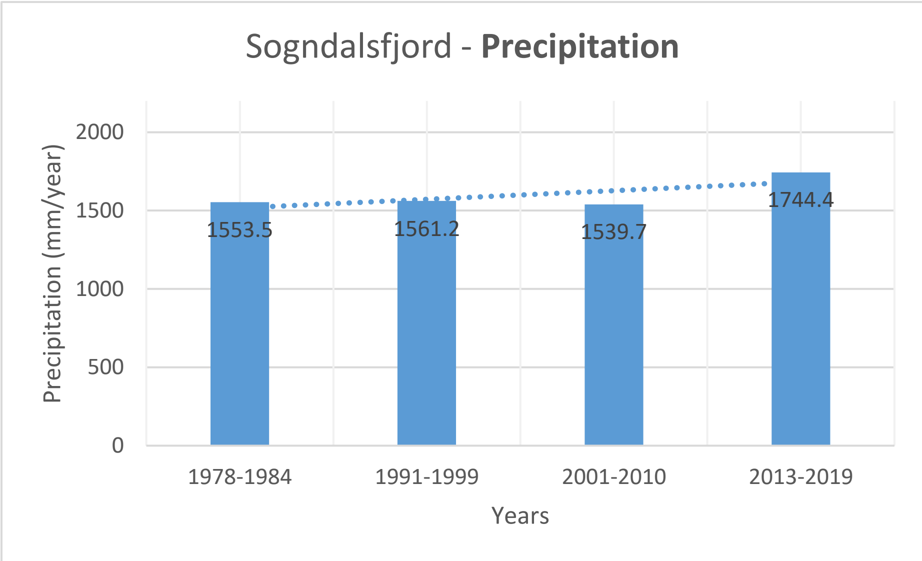

Figure 21: Precipitation trend in the Sogndalsfjord.

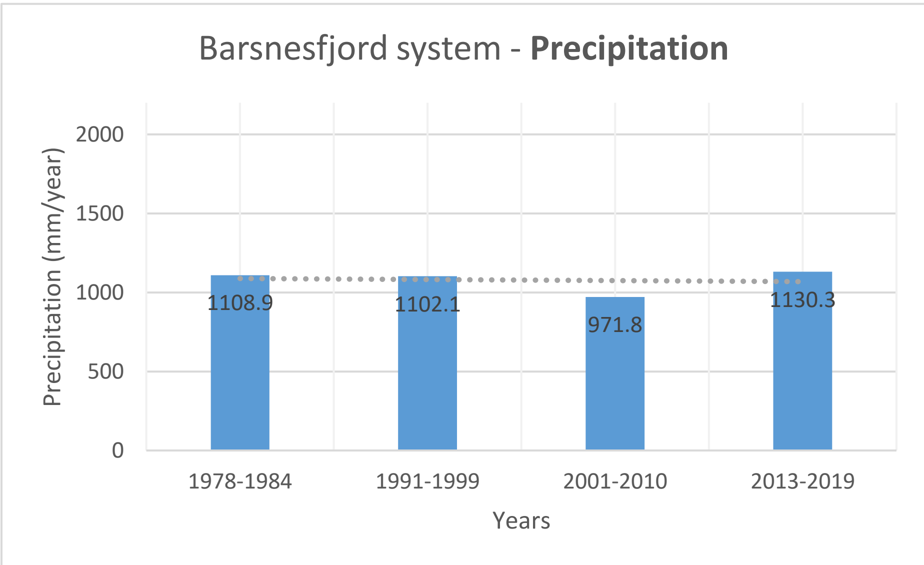

Figure 20: Precipitation trend in the Barsnesfjord system.

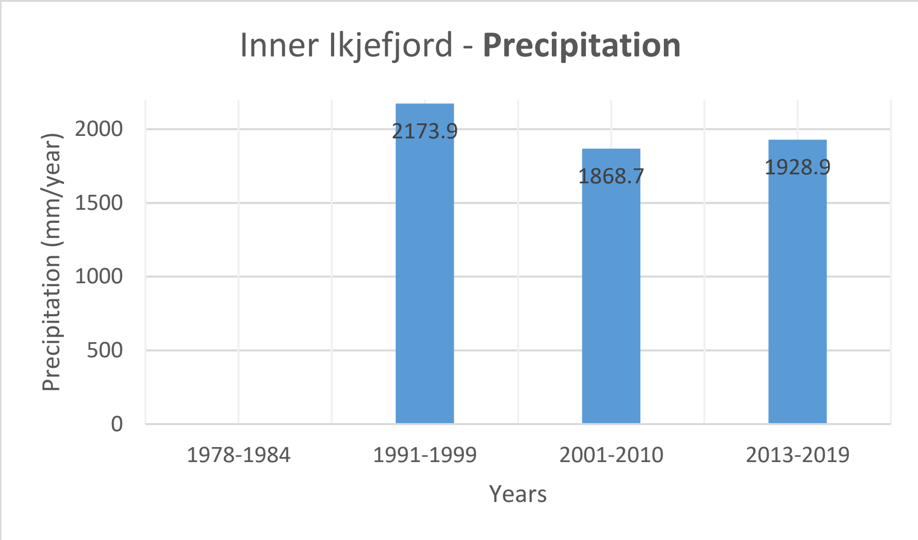

Figure 25: Precipitation trend in the Inner Ikjefjord.

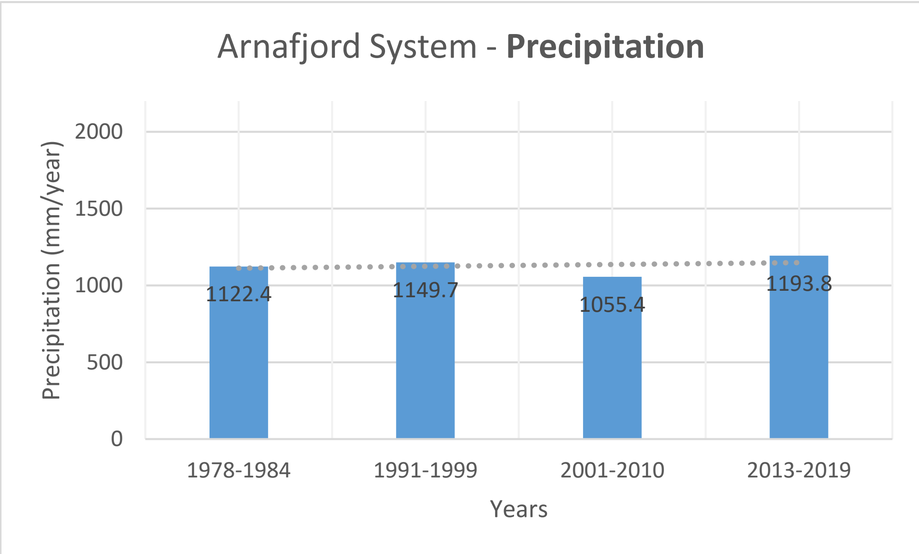

Figure 24: Precipitation trend in the Arnafjord system.

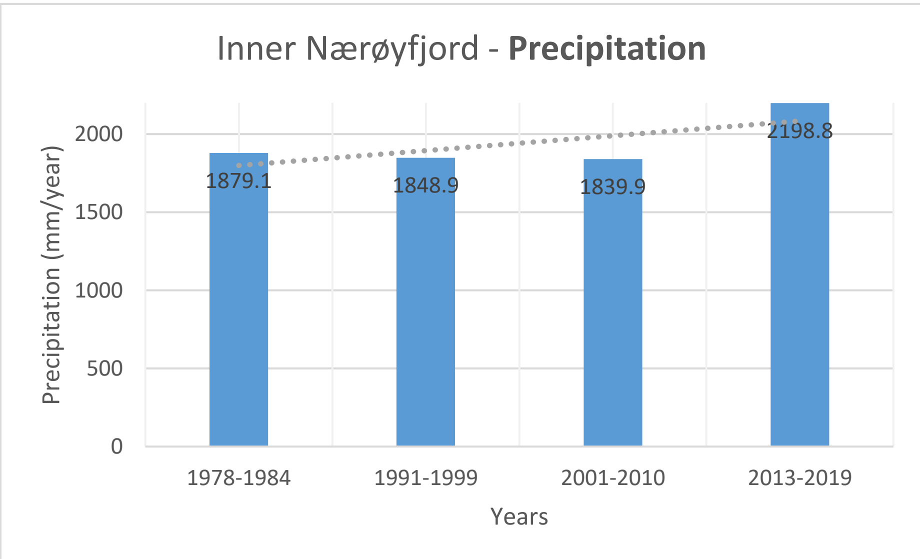

Figure 23: Precipitation trend in the Inner Nærøyfjord.

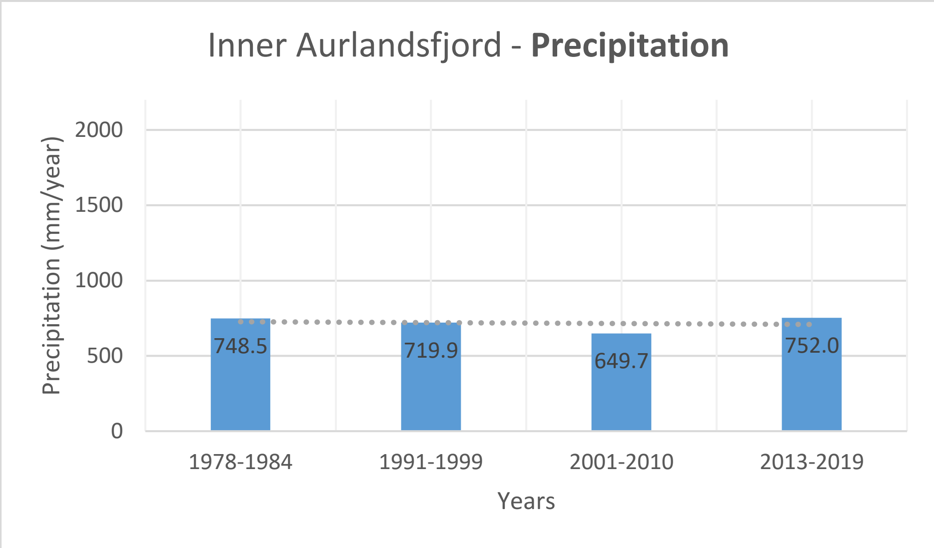

Figure 26: Precipitation trend in the Inner Aurlandsfjord.

A changing precipitation pattern is relevant for the freshwater inflow due to increasing precipitation and thus an increased runoff into the fjord system. Terrestrial runoff plays an important role in the terrestrial organic matter supply and in the supply of mineral nutrients for primary production of marine organic material in the fjord waterbodies.

In conclusion, it can be summarized that different factors are able to alter environmental conditions in fjord ecosystems. Human-induced environmental change, as shown in hydropower production and delta construction work, might play a distinctive role, as well as climate change implications controlling hydrographical processes. Thus, fjords are recently facing increasing pressure, especially from the challenges of environmental and climate change (Howe et al., 2010).

1.3 Scientific Setting

Following is an overview about relevant scientific papers or studies, which have been published concerning organic matter in fjord sediments as proxies for climate and environmental change. Only relevant studies in the Sognefjord area are taken into consideration.

Paetzel & Schrader (1992): Recent environmental changes recorded in anoxic Barsnesfjord sediments, Western Norway

This paper aims to determine the marine organic and mineral matter composition and its origin in the sediment depositions in the Barsnesfjord. Accumulation and changes in sedimentation rates were observed prior to the hydropower construction in 1982 and compared to recent sediment composition to relate these to altering environmental conditions. Paetzel and Schrader (1992) concluded that the multiple damming and regulation of the influencing river did not have a significant influence on the sediment structure of the fjord.

Paetzel & Dale (2010): Climate proxies for recent fjord sediments in the Inner Sognefjord region, Western Norway

The authors use variations of mineral clay particles, total organic matter fraction and freshwater diatoms as climate proxies for the last 20 year. High-resolution sediment cores from the Inner and Outer Barsnesfjord and the Sogndalsfjord are analysed to identify a signal of climate variation, corresponding to regional patterns of precipitation, temperature, cloud cover, and insolation. They developed a simple box model to illustrate their results. Paetzel and Dale (2010) associated observed sediment changes to changes in the solar activity, the North Atlantic Oscillation (NAO), and the regional climate development.

Timmers (2014): Sediment response to post Little Ice Age climate change in the Sogndalsfjord, Western Norway

Three high-resolution sediment cores were taken to investigate fjord responses to environmental and climate change since the maximum glacial advance at the end of the Little Ice Age (LIA) around 1750. The observed parameters for indicating altering environmental conditions are the mineral grain size (sand, silt, and clay), the terrestrial and marine organic matter content, the organic carbon concentration, and the diatom composition. The author concluded that the parameters do indicate environmental and climate change since the LIA maximum, even though they do not confirm the recent and exponential temperature increase throughout the past decades, as suggested by the IPCC (2013) to be caused by anthropogenic influences.

Bøthun et al. (2014): Innflytelse av endringer i hydrografi på avsetning av organisk karbon i Barsnesfjorden, Vest-Norge

The authors aim to observe how hydrographic changes are affecting the deposition of organic carbon in fjord sediments. They are using the loss-on-ignition technique to state the organic carbon content over the past 30 years. Due to a new bridge construction work across the Barsnesfjord in 2014, they assume a change in hydrographical conditions. As a result they are simulating a future fjord environment, depending on a possible changing water flow and furthermore changing oxygen and temperature values in the fjord basin waterbody.

Tysnes et al. (2015): Changes in sediment composition of the Barsnesfjord, Western Norway, throughout the last 50 years

The composition of the sediment before the 1980s has been compared with the sediment composition after the 1980s, with focus on the impacts of the hydropower plant construction in Årøy. Therefore, sediment cores were taken and analysed from the Inner and Outer Barsnesfjord. They found that the organic matter has increased in both basins with a significant amount between 35-60% over the past 50 years.

Dybo et al. (2016): Analysis of recent sediment cores in the anoxic Nærøyfjord, Western Norway

Three sediment cores have been retrieved to reconstruct environmental change in the Nærøyfjord. The parameters used for the investigation are visual analysis, density measurements, grain distribution, X-ray imaging, loss-on-ignition and XRF (X-ray fluorescence) elemental analysis. They linked these parameters to precipitation data and runoff reconstructions from the freshwater diatom record. The interpretation focuses on the impacts of the delta construction work at the township of Gudvangen during the time between 1986-1991.

Midttømme et al. (2017): Deposits from historic events in the Aurlandsfjord, Western Norway, over the last 40 years – part I. The sedimentological records

This study aims to trace back the fjord sediment signals to historical events of significant influence on the environmental conditions in the Aurlandsfjord. The specific event of interest has been the century flood in 2014, which is proposed to affect the sediment composition. The investigated key factors for linking the sediment to its source of origin are diatoms, foraminifera, grain sizes, organic matter, and mineral matter. The authors found that traces from historic events can be observed in the respective sediment samples.

Langeng & Slinning (2018): A 400 year historical sediment record from the Fjærlandsfjord, Western Norway

Two sediment cores have been taken with the purpose to relate sediment signals to climate and anthropogenic changes during the last 400 years. The analysis was implemented using an XRF scanner, a multi-sensor core logger (for the magnetic susceptibility record), loss-on-ignition and smear slides. They found that the sedimentary deposits clearly changed, in terms of a reduction in minerogenic material and an increase in organic material. The authors presented their results in a box model, linked to several occurring changes such as glacier retreat and increased runoff.

Koek & Van Doorn (2018): Investigating environmental change in the micro-organism distribution of anoxic Ikjefjord sediments since the 1960s, Western Norway

This research has been carried out to investigate the influence of building activities on the environmental conditions in the Ikjefjord. Focus hereby is the construction of dams for hydropower production in the local area as well as the building of the Ikjefjord bridge. Freshwater and planktonic marine diatoms and benthic foraminifera are used as proxies for environmental change. To relate the species abundance to the amount of organic matter in the sediments, LOI measurements were taken. They found that both the benthic and the pelagic environment has been influenced and changed, as indicated by the microorganism species composition.

Bucher (2020): Recent environmental change as recorded in sediments from the Arnafjord system, Western Norway

Three sediment cores have been retrieved from the Arnafjord system, including the Framfjord, the Indrefjord and the Arnafjord basin, with the aim to get a signal of recent environmental change. The considered altering factors are talc mining from 1907-1984, hydropower energy production since 1968, and the start of a fish hatchery in 1986. These influencing events result in a change of marine organic matter concentration and concentration of freshwater diatoms, as well as the grain size distribution in the sediments. A simple box model was developed to show possible transport pathways for the different sediment parameters during the last 120 years.

2. Methods

In order to gain data on the LOI content in the sediments for the tributary fjords of the Sognefjord, it is necessary to extract sediment cores from the different fjord basins. Sediment cores were taken each year as part of the science project within the "From Mountain to Fjord" course at HVL in Sogndal. These cores were later analysed by the students and the LOI data was gathered over the years. It must be noted that the differing experienced level of researchers may be a potential source of a systematic error, for the data collection as well as for the data analysis part.

2.1 Sediment Sampling

The sediment cores were taken by students under appropriate supervision at HVL. The Fjærlandsfjord (2017) and Arnafjord (2020) cores were taken by the Department of Earth Science from the University of Bergen (UiB).

Most of the sediment cores were extracted by a Niemistö (1974) gravity corer as shown in *Figure 27*. On occasion, a Multicorer was used as well for retrieving the sediment. The advantage of using a Multicorer is that multiple undisturbed sediment samples can be retrieved at the same time, although the penetration depth is lower (Monsen, 2017). Both the gravity corer and the Multicorer allow to retrieve sediment with intact sediment-water interfaces and in intact stratigraphical order. Thus, the sediment on the surface corresponds to the year of deposition and retrieval. Also, the time resolution within the sediment core remains consistent (Niemistö, 1974).

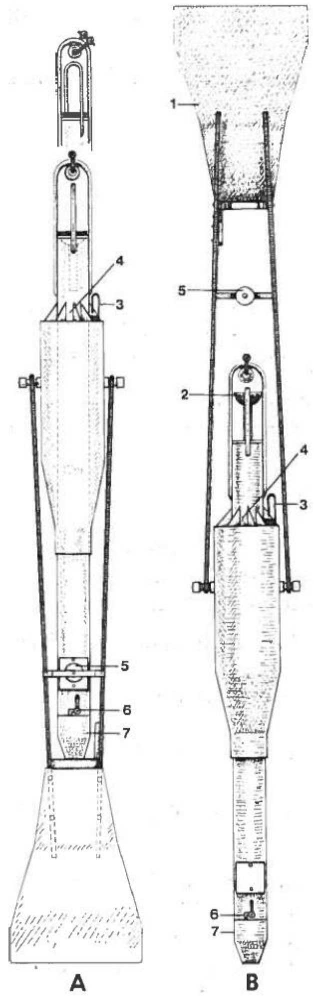

Figure 27: Schematic illustration of the gravity corer. Reprinted from Niemistö (1974).

After sampling, the cores were sealed and transported vertically with the fjord bottom water on top of the sediment. This prevents the surface from drying out and getting disturbed during the transport. The plastic pipes with the sampled sediment are usually stored in a cool environment to prevent degradation.

Back in the laboratory the sediment cores have been prepared for further analysis by creating subsamples. The cores were opened, and the bottom water was drained of the sediment surface. Afterwards the core was placed horizontally and cut in two halves from the bottom to the top.

Prior to the analysis in the laboratory, continuous slices of a certain thickness must be created. The thickness of the slices varies between 0.5 and 2 cm, depending on the present core. It might happen that some subsamples could not be analysed, either because of mistakes during the sampling or during the followed laboratory work. Thus, the LOI method is sometimes not continuously applied throughout the entire sediment core.

2.2 The Loss-on-Ignition (LOI) Technique

The amount of organic matter in sediments can be determined by the standardized loss-on-ignition (LOI) method. It is common and widely used and provides fast and inexpensive results (Dean, 1974).

The LOI is stated in percentage of the dry weight of the analysed sediment. In a first step, it has thus to be oven-dried for usually 12 to 24 hours until it reaches a constant weight at 105°C (Heiri et al., 2001). Then the organic fraction is getting burned at a temperature of 550°C in a muffle oven.

Both the burning temperature and the exposure time in the oven and are varying as there is no overall established value. It needs to be considered that these factors as well as the position of the crucibles in the oven might have an influence on the results (Heiri et al., 2001). Dean (1974) recommended to use a burning temperature between 500 and 550°C to get the best results. A reasonable exposure time at 550°C would be 4 h, it may depend on the sediment however (Heiri et al., 2001).

The method is based on the thermal analysis that organic matter begins to ignite at about 200°C and is completely depleted at about 550°C (Santisteban et al., 2004). The organic matter is oxidised to carbon dioxide and ash. During this reaction a weight loss takes place, which can be determined by measuring the weighs of the samples before and after the burning process in the muffle oven (Heiri et al., 2001). The percentage difference in weights after the burning process results in an estimation of organic matter content in the sediment:

$$LOI_{500-550} = ((DW_{105} - DW_{500-550})/(DW_{105} - Tara) * 100$$

$LOI_{500-550}$ represents the LOI content in the sediments as a percentage after the burning process in the muffle oven, DW_{105} the dry weight of the sediment sample before the combustion and $DW_{500-550}$ the dry weight of the sediment after the heating process in the muffle oven. Tara means the single weight of the used crucibles for the method. All values are given in grams (g).

2.3 Applied Hydrography

In addition to the LOI measurements in the sediments of the tributary fjords, hydrographical measurements have been carried out in some fjord basins over the past years, with some data going back to the year 1912. Gathering all the available data is necessary to use them for the further analysis regarding the LOI controlling factors, as proposed in the objective explanation. The historical hydrographical datasets were earlier refurbished and summarized by Grieger (2021) and thus the used data for this thesis at hand is retrieved from the raw data of this reference.

Hydrographical data is available for the Sogndalsfjord, the Inner and Outer Barsnesfjord, Inner Nærøyfjord and the Inner Ikjefjord. The dataset includes data on dissolved oxygen, water temperature and salinity, measured in different depths in the respective fjord basins. For the subsequent study, only water temperature and oxygen has been considered in the data analysis.

Figure 28: CTD sonde as used for the hydrographical measurements in the tributary fjord basins. Reprinted from SAIV A/S (n.d.).

Generally, the hydrographical data has been gained by using a Conductivity-Temperature-Depth (CTD) sonde, as shown in *Figure 28*. This tool is used in the first place for determining essential physical properties of water columns. The CTD with its attached electrodes is usually fastened to a rope and gets lowered into the water until it hits the fjord basin bottom. Measurements are recorded every couple of seconds in physical units (dissolved oxygen: mg/l; water temperature: °C)

It must be noted that for some measurements in earlier years, other methods than the sampling with the CTD electrode has been applied for determining the dissolved oxygen and temperature in the water body.

2.4 Meteorological Stations

Meteorological data is used to evaluate the climatic conditions in the tributary fjord areas, or moreover stating a representative development for the entire Sognefjord area. Precipitation and air temperature are the variables of interest in the first place when it comes to observing a signal of climate change. The data has been retrieved from the historical statistics database of the Norwegian Centre for Climate Services (NCCS), belonging to the Norwegian Meteorological Institute (MET Norway).

The meteorological stations to gain data on precipitation and temperature are not always directly located at the fjord basins, and thus always the nearest suitable location has been picked. Whilst precipitation data was available for all the considered fjords and their related meteorological stations, that has not been the case for air temperature. To get a more wide-ranged view on the temperature changes, two more meteorological stations around the entire

Sognefjord area were considered for the analysis of the general temperature pattern during the past four decades.

2.5 Data Analysis

All statistical analysis has been executed by using Excel. First step was to gather all the available LOI data in a summarizing dataset. After structuring it by sampling year and location, graphs out of the raw data were created. A map was created to get a geographical overview of the spatial distribution of the sampling locations, as already shown in *Figure 1*.

All maps in this thesis are created with QGIS (Version 3.16.3-Hannover).

In order to interpret the regional LOI distribution pattern and link it to possible influencing factors such as hydrography and geographical position, it is necessary to consider the development of LOI over the past decades. Afterwards it is possible to relate this to changing climatic and environmental influences.

The values of interest for interpreting the regional distribution pattern in the first place are air temperature, oxygen content, water temperature and precipitation. Whether fjords are glacial influenced or not is important for comparing the northern and southern tributary fjords of the Sognefjord. In addition, hydropower as an anthropogenic influence and other significant events resulting in changing environmental conditions are taken into account.

To visualize the changes of all factors in a temporal distribution, graphs were created. By comparing the development of the factors in each fjord basins with each other, it gives an attempt to interpret the changes regarding to climatic and environmental conditions throughout the past decades.

3. Results

This chapter eventually outlines the analysis results of the LOI data, as well as the considered hydrographical factors (oxygen and water temperature) to create a basis for the attempt to interpret the regional LOI distribution pattern by elaborating the climatic and environmental influence over the past four decades.

3.1 Sediment sampling

An overview about all sediment cores, which were used for the LOI analysis is given in *Table 4*. It includes the sampling year, name of the core, sampling location, type of the corer, water depth of sampling and the length of the sediment core.

3.2 Data analysis

An overview about the used data basis for the created maps is given in *Table 3*.

Table 3: Overview over the used data basis for the maps created in QGIS.

Title	Type of map	Version	Copyright
Norges grunnkart	WMS-Service	1.3.0	Statens kartverk 2007
Bakgrunnskart havarealverktøy	WMS-Service	1.3.0	Statens kartverk 2007

The graphs which are showing the development of the LOI within the depths of the individual sediment cores and can be found in the Appendix II, as well as the associated raw data in Appendix I. It must be noted that some values were excluded from the first calculation of the LOI in Appendix I since they were considered as outliers. In addition, sometimes single values are missing due to a mistake while applying the loss-on-ignition method in the laboratory.

Four time horizons were selected to assess the temporal development of LOI, hydrographical and meteorological values, corresponding with the best availability of data. Some fjords are more well-studied than others what results in a lack of data for the following analysis, thus the basis to interpret the results is not equal for every considered fjord. The selected time horizons are 1978-1984, 1991-1999, 2001-2010 and 2013-2019. It must be noted that it was not possible to create equal ranged time horizons, because the LOI data (and meteorological data) had to fit to the existing hydrographical data as a limiting factor.

All single used values and factors for every fjord basin and sediment core are summarized and shown in *Table 5, 6, 7* and *8*.

Table 4: Overview over the sediment cores for the LOI analysis.

Year	Location	Core ID	Latitude / Longitude	Type of corer	Sampling depth	Core length
2012	Sogndalsfjord	MF2012-7	61°12.201' N 07°06.100' E	Niemistö (1974) Gravity corer	260.0 m	48.5 cm
		MF2012-8	61°12.350' N 07°06.020' E			40.5 cm
		MF2012-9	61°12.400' N 07°05.740' E			42.5 cm
2013	Outer Barsnesfjord	MF2013-4	61°14.417' N 07°07.268' E	Niemistö (1974) Gravity Corer	80.0 m	28.5 cm
		MF2013-6	61°14.619' N 07°07.364' E			24.3 cm
2014	Inner Barsnesfjord	MF2014-5	61°15.361' N 07°09.038' E	Niemistö (1974) Gravity Corer	62.2 m	51.25 cm
	Outer Barsnesfjord	MF2014-7	61°14.800' N 07°07.620' E		79.3 m	44.5 cm
2015	Inner Nærøyfjord basin	MF2015-1	60°53.764' N 06°51.993' E	Niemistö (1974) Gravity Corer	76.6 m	40.0 cm
		MF2015-4	60°54.157' N 06°52.107' E		76.5 m	27.0 cm
2016	Inner Aurlandsfjord	MF2016-4	60°52.242' N 07°07.787' E	Niemistö (1974) Gravity Corer	64.1 m	8.0 cm
		MF2016-9	60°51.850' N 07°07.379' E		37.2 m	14.0 cm
		MF2016-12	60°52.054' N 07°08.032' E		55.4 m	12.5 cm
2017	Fjærlandsfjord	HB17-211-01MC-A	61°24.426' N 06°45.139' E	Multicorer	108.0 m	28.0 cm
		HB17-211-02MC-A	61°21.584' N 06°44.128' E		176.0 m	45.0 cm
2017	Inner Ikjefjord basin	MF2017-1	61°03.780' N 05°39.930' E	Niemistö (1974) Gravity Corer	86.0 m	28.0 cm
		MF2017-2	61°03.700' N 05°39.995' E		82.0 m	28.0 cm
2019	Inner Barsnesfjord	MF2019-1	61°15.378' N 07°09.891' E	Niemistö (1974) Gravity Corer	64.1 m	47.0 cm
		MF2019-3	61°15.197' N 07°08.814' E		60.5 m	53.0 cm
	Outer Barsnesfjord	MF2019-6	61°14.687' N 07°07.542' E		80.0 m	43.0 cm
		MF2019-8	61°14.408' N 07°07.413' E		80.7 m	40.5 cm
2020	Arnafjord basin	MF2020-GC06	61°01.147' N 06°23.798' E	Gravity Corer	100.0 m	29.0 cm
	Indrefjord	MF2020-MC04	61°00.556' N 06°21.746' E	Multicorer	68.0 m	21.0 cm

Table 5: Overview over the hydrographical factors and values for the different tributary fjord basins of the Sognefjord.

Sampling year	Fjord name	Core number	Water depth (m)	Temp (°C) 2013-2019	Temp (°C) 2001-2010	Temp (°C) 1991-1999	Temp (°C) 1978-1984	Oxy (mg/l) 2013-2019	Oxy (mg/l) 2001-2010	Oxy (mg/l) 1991-1999	Oxy (mg/l) 1978-1984
2012	Sogndalsfjord	MF2012-7	260	8.3	8.3	7.9	7.4	4.0	3.6	4.2	6.1
		MF2012-8	260	8.3	8.3	7.9	7.4	4.0	3.6	4.2	6.1
		MF2012-9	260	8.3	8.3	7.9	7.4	4.0	3.6	4.2	6.1
2013	Outer Barsnesfjord	MF2013-4	80	7.2	7.7	7.3	6.6	1.8	1.2	2.1	3.6
		MF2013-6	80	7.2	7.7	7.3	6.6	1.8	1.2	2.1	3.6
2014	Inner Barsnesfjord	MF2014-5	62	7.1	7.5	6.8		0.2	1.8	0.0	
	Outer Barsnesfjord	MF2014-7	79	7.2	7.7	7.3	6.6	1.8	1.2	2.1	3.6
2015	Inner Nærøyfjord basin	MF2015-1	77	8.3	8.7	7.8		0.5	2.0	4.3	
		MF2015-4	77	8.3	8.7	7.8		0.5	2.0	4.3	
2016	Inner Aurlandsfjord	MF2016-4	64								
		MF2016-9	37								
		MF2016-12	55								
2017	Fjærlandsfjord	HB17-211-01MC-A	108								
		HB17-211-02MC-A	176								
2017	Inner Ikjefjord basin	MF2017-1	86	7.4				1.2			
		MF2017-2	82	7.4				1.2			
2019	Inner Barsnesfjord	MF2019-1	64	7.1	7.5	6.8		0.2	1.8	0.0	
		MF2019-3	61	7.1	7.5	6.8		0.2	1.8	0.0	
	Outer Barsnesfjord	MF2019-6	80	7.2	7.7	7.3	6.6	1.8	1.2	2.1	3.6
		MF2019-8	81	7.2	7.7	7.3	6.6	1.8	1.2	2.1	3.6
2020	Arnafjord basin	MF2020-GC06	100								
	Indrefjord	MF2020-MC04	68								

Temp (°C) represents the average water temperature, Oxy (mg/l) represents the average available amount of oxygen in the fjord waterbody throughout the respective time horizon.

Table 6: Overview over the average LOI values and sedimentation rates for the different tributary fjord basins of the Sognefjord.

Sampling year	Fjord name	Core number	Water depth (m)	LOI (%) 2013-2019	LOI (%) 2001-2010	LOI (%) 1991-1999	LOI (%) 1978-1984	SR cm/y	Reference
2012	Sogndalsfjord	MF2012-7	260		10.7	10.6	10.0	0.067	Timmers (2014)
		MF2012-8	260		8.5	8.5	8.3	0.079	
		MF2012-9	260		8.1	8.3	7.8	0.069	
2013	Outer Barsnesfjord	MF2013-4	80		8.5	8.4	8.7	0.75	Bøthun et al. (2014)
		MF2013-6	80		8.9	9.3	6.5	0.75	
2014	Inner Barsnesfjord	MF2014-5	62	12.6	10.4	9.0	9.2	0.84	Tysnes et al. (2015)
	Outer Barsnesfjord	MF2014-7	79	8.4	8.9	8.0	7.0	0.75	
2015	Inner Nærøyfjord basin	MF2015-1	77	9.3	8.5	10.0	12.5	0.82	Dybo et al. (2016)
		MF2015-4	77	8.3	7.2	9.4	7.3	0.77	
2016	Inner Aurlandsfjord	MF2016-4	64	5.9				1.75	Midttømme et al. (2017)
		MF2016-9	37	6.0	5.9	5.5	6.3	0.19	
		MF2016-12	55	4.9	5.3	4.7	7.4	0.23	
2017	Fjærlandsfjord	HB17-211-01MC-A	108	2.8	2.4	2.4	2.1	0.40	Langeng & Slinning (2018)
		HB17-211-02MC-A	176	4.6	4.3	4.4	4.0	0.12	
2017	Inner Ikjefjord basin	MF2017-1	86	11.4	12.1	7.6	15.8	0.47	Van Rossum (2018)
		MF2017-2	82	11.3	12.7	8.4	15.8	0.44	
2019	Inner Barsnesfjord	MF2019-1	64	8.7	10.1	8.3	7.9	1.00	Kerbusch (2020)
		MF2019-3	61	9.1	8.0	6.0	8.0	1.00	
	Outer Barsnesfjord	MF2019-6	80	9.4	8.1	8.3	7.2	0.80	
		MF2019-8	81	5.7	9.3	6.8	7.9	0.80	
2020	Arnafjord basin	MF2020-GC06	100	4.0	4.1	4.1	4.0	0.105	Bucher (2020)
	Indrefjord	MF2020-MC04	68	3.9	3.8	3.7	3.9	0.136	

LOI (%) represents the average organic matter content in the sediments for each time horizon, SR (cm/year) represents the estimated sedimentation rate per year in the respective fjord basins. The sedimentation rate is ranging from relatively low (green) to high (red) values, as indicated by the colours.

Table 7: Overview over the meteorological factors and values of the different tributary fjord basins of the Sognefjord.

Sampling year	Fjord name	Core number	Water depth (m)	P (mm/y) 2013-2019	T (°C) 2013-2019	P (mm/y) 2001-2010	T (°C) 2001-2010	P (mm/y) 1991-1999	T (°C) 1991-1999	P (mm/y) 1978-1984	T (°C) 1978-1984
2012	Sogndalsfjord	MF2012-7	260	1744.4		1539.7		1561.2		1553.5	
		MF2012-8	260								
		MF2012-9	260								
2013	Outer Barsnesfjord	MF2013-4	80	1130.3		971.8		1102.1		1108.9	
		MF2013-6	80								
2014	Inner Barsnesfjord	MF2014-5	62	1130.3		971.8		1102.1		1108.9	
	Outer Barsnesfjord	MF2014-7	79								
2015	Inner Nærøyfjord basin	MF2015-1	77	2198.8		1839.9		1848.9		1879.1	
		MF2015-4	77								
2016	Inner Aurlandsfjord	MF2016-4	64	752.0		649.7		719.9		748.5	
		MF2016-9	37								
		MF2016-12	55								
2017	Fjærlandsfjord	HB17-211-01MC-A	108	1932.3	5.8	1750.6	5.5	1962.5	5.6	1976.2	4.8
		HB17-211-02MC-A	176								
2017	Inner Ikjefjord basin	MF2017-1	86	1928.9		1868.7		2173.9			
		MF2017-2	82								
2019	Inner Barsnesfjord	MF2019-1	64	1130.3		971.8		1102.1		1108.9	
		MF2019-3	61								
	Outer Barsnesfjord	MF2019-6	80								
		MF2019-8	81								
2020	Arnafjord basin	MF2020-GC06	100	1193.8		1055.4		1149.7		1122.4	
	Indrefjord	MF2020-MC04	68								

P (mm/y) represents the average annual precipitation, T (°C) represents the average air temperature for each time horizon at the nearest meteorological stations to the respective fjord basins.

Table 8: Overview over the hydropower and glacial influences as well as significant historical events on the different tributary fjord basins of the Sognefjord.

Sampling year	Fjord name	Core number	Water depth (m)	Hydropower start year	Glacial influence	Events
2012	Sogndalsfjord	MF2012-7	260	indirect influence from the Barsnesfjord	Fourth sedimentation basin	
		MF2012-8	260			
		MF2012-9	260			
2013	Outer Barsnesfjord	MF2013-4	80	1982	Third sedimentation basin	
		MF2013-6	80			
2014	Inner Barsnesfjord	MF2014-5	62	1982	Third sedimentation basin	
	Outer Barsnesfjord	MF2014-7	79			
2015	Inner Nærøyfjord basin	MF2015-1	77	indirect influence from the Aurlandsfjord	none	
		MF2015-4	77			
2016	Inner Aurlandsfjord	MF2016-4	64	1969	none	2014 century flood
		MF2016-9	37			
		MF2016-12	55			
2017	Fjærlandsfjord	HB17-211-01MC-A	108	2002	First sedimentation basin	
		HB17-211-02MC-A	176			
2017	Inner Ikjefjord basin	MF2017-1	86	1970	none	1983 natural overflow event
		MF2017-2	82			
2019	Inner Barsnesfjord	MF2019-1	64	1982	Third sedimentation basin	
		MF2019-3	61			
	Outer Barsnesfjord	MF2019-6	80			
		MF2019-8	81			
2020	Arnafjord basin	MF2020-GC06	100	1968	none	
	Indrefjord	MF2020-MC04	68			

Adjusting the available hydrographical raw data from Grieger (2021) for some of the tributary fjord basins required to sort the data in the first place into the selected time horizons. Afterwards, the average values for water temperature and oxygen were created by using the statistical function “arithmetic mean” within the respective time horizons. The same statistical function has been applied for the analysis of the meteorological data. Both the hydrographical and meteorological raw data are listed in Appendix IV and V.

It must be noted that the existing hydrological and the meteorological data do not provide overall consistent and exact fitting values to the LOI data. It happens that the water depth of the hydrological data measurements for oxygen and temperature in the particular fjord basins differ the water depth of the sediment core sampling. Regarding the available data on air temperature, only the meteorological station in Fjærland (*Figure 19*) provides a sufficient data input to get a climate change signal within the different time horizons. The two additionally picked meteorological stations are located in Vangsnes (*Figure 18*) and Takle (*Figure 17*). Some meteorological stations were replaced over the past four decades, that is why the station Fjærland – Skarestad operated until the year 2005, and the station Fjærland – Bremuseet has been in operation since then until today.

Also there was not always sufficient raw data available to create an average value for every time horizon, meaning that some averages do consider more raw data input than others and thus the starting point for creating the eventually used variables and factors has been different. These circumstances while executing the statistical analysis of the hydrographical and meteorological data can therefore lead to an undesirable possible source of inaccuracy.

With the earlier created graphs of the LOI content in the sediment cores, it was now possible to generate LOI averages for all time horizons at the specific locations. The sedimentation rate is required to date the sediments back to a certain time. Years can thus approximately be determined at a specific sediment depth in the cores. The following equation was used:

$$x\ cm = SR\frac{cm}{year} * n\ years$$

The outcome value x cm represents the sediment depth at a specific year, SR (cm/year) is the evaluated sedimentation rate and n years is the number of years applied for the considered time horizons.

For the sediment cores retrieved in 2012-2019 it was not possible to calculate the sediment depths for the complete latest time horizon (2013-2019), since the top layer of the respective sediment cores represents always the most recent year. Therefore, the average LOI value calculations for each time horizon, starting with the sediment cores in 2013, includes less estimated years than the calculation set up for the sediment cores in 2020. If it was not possible to calculate the year 2019, is it stated with “not available” (n.a.) in the data as shown in Appendix III.

After getting an approximate evaluation of which time horizon can be found between which sediment depths, the related average LOI value for these depths was compiled. It must be noted that this is only an approximation, since the data scale concerning sediment depth is only divided in certain cm steps and it was therefore not possible to consider the exact calculated values. This has been completed for all sediment cores, as far it was possible with regards to data availability. The data outcome of the average LOI values, as well as the utilized sedimentation rates for each tributary fjord basin and its reference can be found in *Table 6*.

Some fjord basins show data from several years of sampling with more than one sediment core, representing either the same area or different parts of the considered fjord basins. In a next step, it was needed to put the single sediment core data from the same locations together and summarize it to get an overall value for each time horizon. Therefore, at first, the average values for each time horizon out of all available sediment cores from each year and each fjord basin has been created by using the arithmetic mean. If there have been several years of sampling in some tributary fjords, again the arithmetic mean of these values before has been calculated. This statistical analysis has been performed for the LOI, as well as for the hydrology data (water temperature and oxygen) and meteorological data (air temperature and precipitation). The final average overall values for all considered factors are shown in Appendix VI.

The following subchapters outline the development of the LOI as well as the considered hydrographical factors (oxygen and water temperature).

All oxygen graphs mark the critical value for oxygen at 2 mg/l, which is the threshold value for the existence of marine life (Vaquer-Sunyer and Duarte, 2008). It can be also seen as the border from oxic to anoxic, which means that it can be assumed that no macroscopic life is possible anymore at lower oxygen concentrations than 2 mg/l. In advantage for the later following discussion and response to the objectives, significant anthropogenic or natural events with an impact on the environmental conditions are outlined in the graphs at its time of occurrence. The trend lines for each factor give a better view on the variations of the values over time.

3.2.1 LOI of the Fjærlandsfjord

Figure 29 shows the LOI progression in the Fjærlandsfjord within the selected time horizons. The LOI trend is tending to increase since the 1980s, turning from an average value of 3,1 % to 3,7% in the past 10 years. As an anthropogenic influence with possible implications on the environmental conditions in the Fjærlandsfjord, the hydropower production started in year 2002.

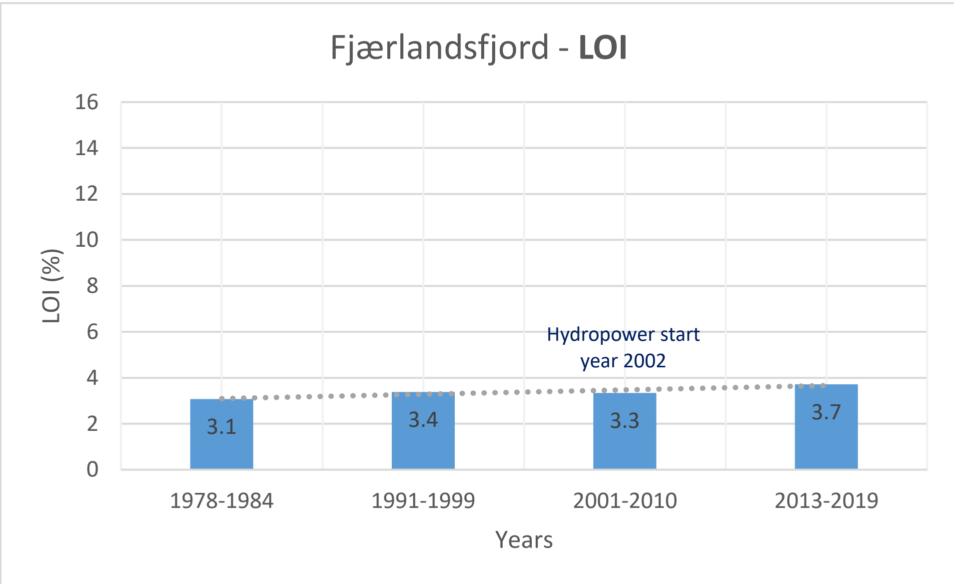

Figure 29: LOI trend in the Fjærlandsfjord.

3.2.2 LOI and hydrography of the Sogndalsfjord

Figure 30 shows the LOI progression the Sogndalsfjord basin at a water depth of 260 m. It can be seen that the LOI trend is tending to increase slightly since the 1980s, turning from an average value of 8,7% to 9,1% in the time period 2001-2010. It must be noted that it was not possible to retrieve LOI data for the most recent period (2013-2019).

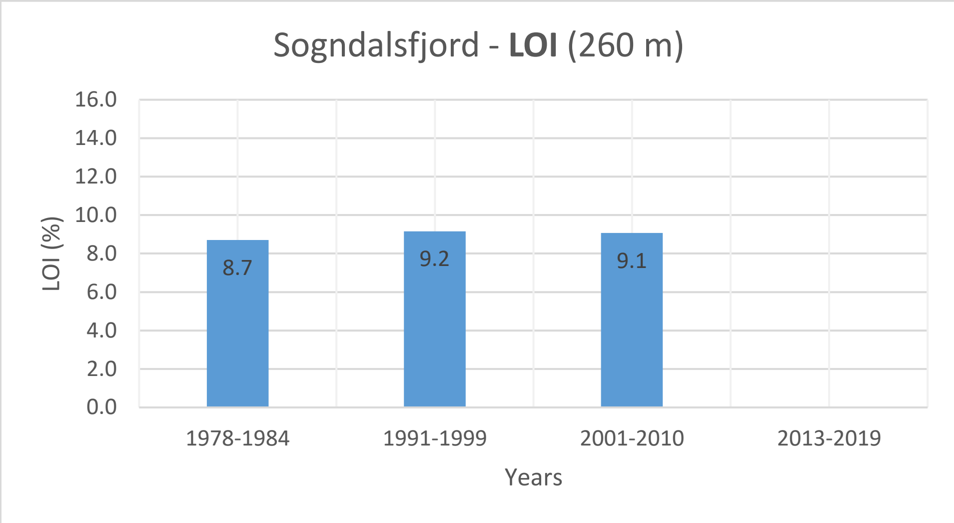

Figure 31: LOI trend in the Sogndalsfjord.

Figure 31 shows the progression of the oxygen conditions in the Sogndalsfjord basin, measured at a water depth of 200 m. Thus, the water depth of the hydrographical measurement differs from the water depth of the sediment core sampling. Coming from an average oxygen value of 6,1 mg/l in the 1980s, the oxygen is constantly decreasing over the years and reaching a minimum value of 3,6 mg/l in the time period 2001-2010. With this decline of the amount of oxygen in the waterbody, the Sogndalsfjord is tending to become less oxic within the past decades and therefore comes closer to the critical oxygen value of 2 mg/l.

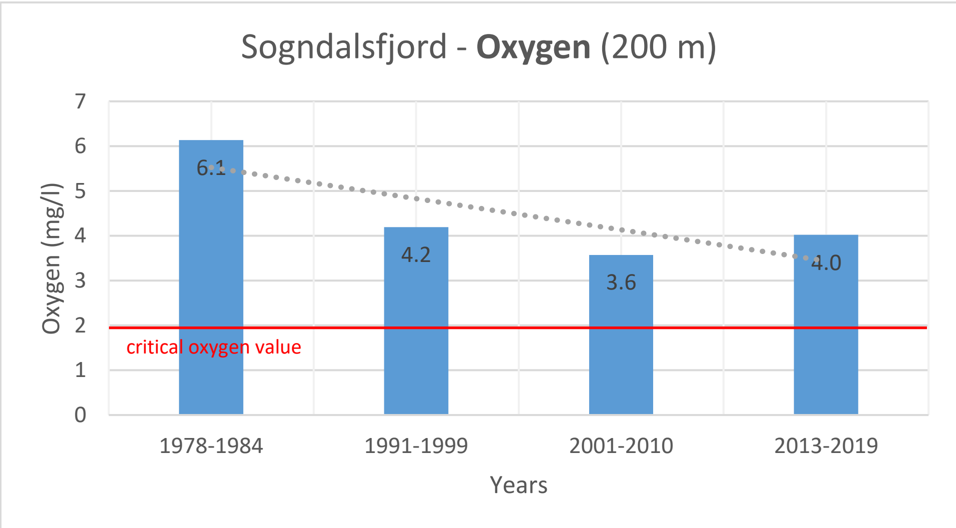

Figure 30: Oxygen trend in the Sogndalsfjord.

Figure 32 shows the progression of the water temperature in the Sogndalsfjord basin at a water depth of 200 m. The temperature measurement has been performed together with the hydrographical measurement of the oxygen conditions. It can be seen that the water temperature is constantly increasing over time since the period 1978-1984, with an average value of 7,4 °C turning into 8,3 °C as most recent. This corresponds to the increase of the air temperature measured at the meteorological station in Fjærland (*Figure 19*), showing a warming trend of 1°C within the considered time horizons.

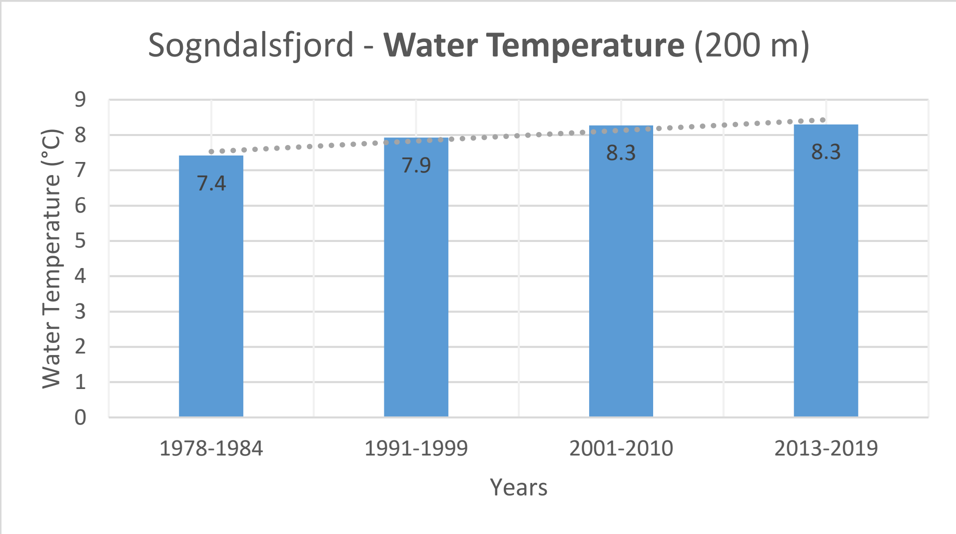

Figure 33: Water temperature trend in the Sogndalsfjord.

3.2.3 LOI and hydrography of the Barsnesfjord system

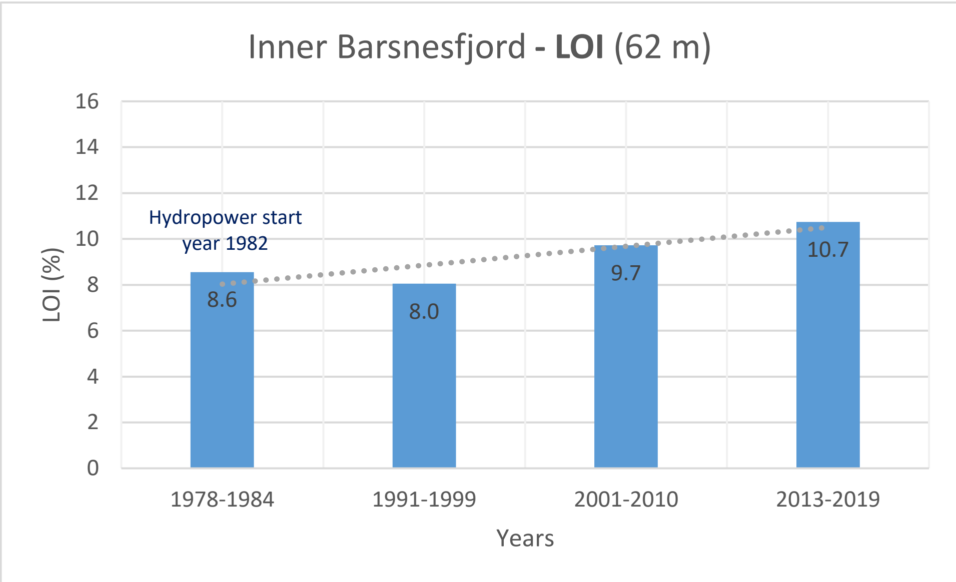

Figure 32: LOI trend in the Inner Barsnesfjord.

Figure 33 shows the progression of the LOI in the Inner Barsnesfjord basin at a water depth of 62 m. It can be seen that the trend of the LOI is increasing since the 1980s, coming from an average value of 8,6% to a maximum value of 10,7% in the time period 2013-2019. As an anthropogenic influence factor with possible implications on the environmental conditions in the Barsnesfjord, the hydropower start is displayed in year 1982.

Figure 34 shows the progression of the oxygen conditions in the Inner Barsnesfjord basin, measured at a water depth of 60 m. Thus, the water depth of the hydrographical measurement differs slightly from the water depth of the sediment core sampling. It must be noted that it was not possible to consider oxygen data from the time period 1978-1984. Overall, the oxygen values for all time horizons are below the critical oxygen value of 2 mg/l. This indicated anoxic conditions in the fjord basin. For the time period 1991-1999, the measurement shows no available oxygen for marine life. Although there happened an oxygen inflow event between 2001-2010, the oxygen conditions are still significantly low.

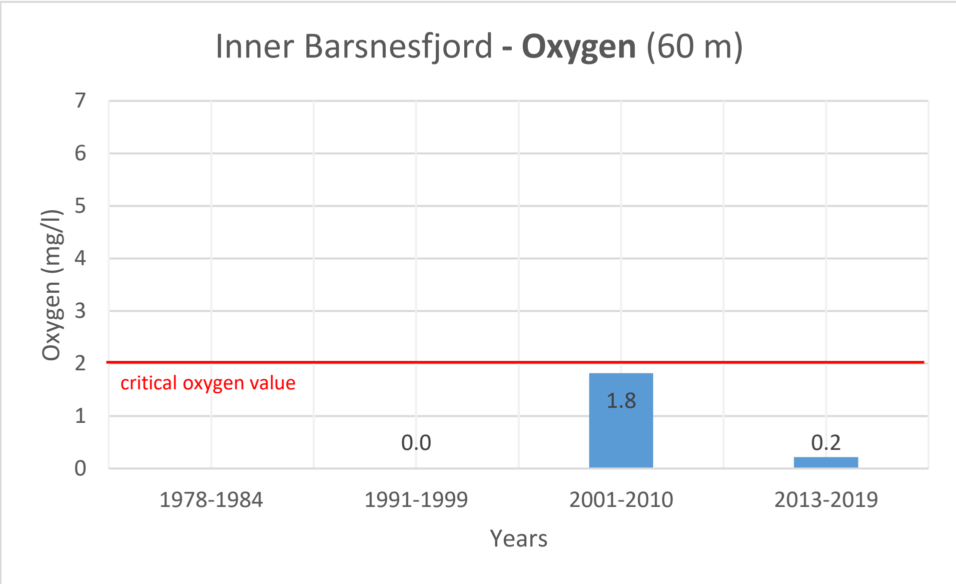

Figure 34: Oxygen trend in the Inner Barsnesfjord.

Figure 35 shows the progression of the water temperature in the Inner Barsnesfjord basin at a water depth of 60 m. The temperature measurement has been performed together with the hydrographical measurement of the oxygen conditions. It must be noted that it was not possible

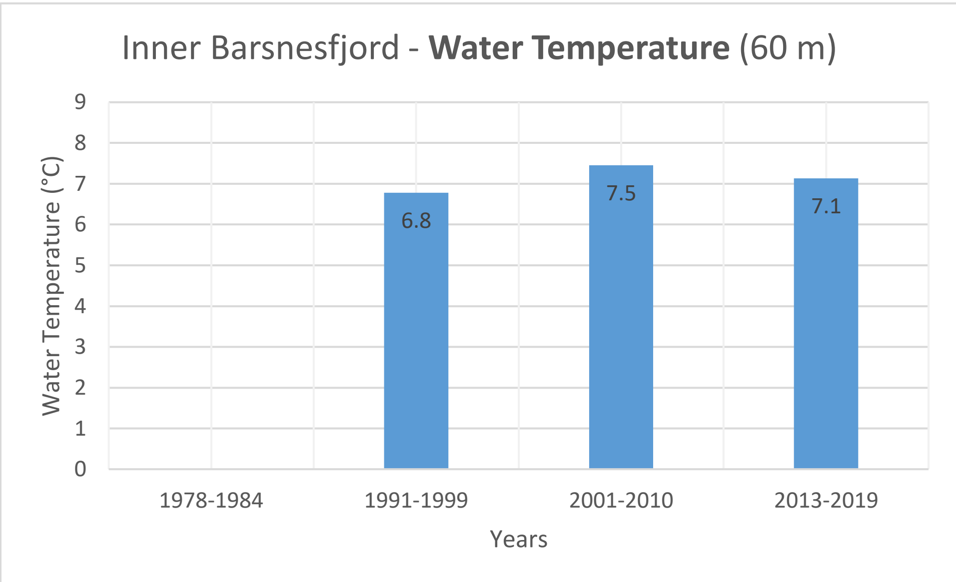

Figure 35: Water temperature trend in the Inner Barsnesfjord.

to consider data from the time period 1978-1984. The trend of the water temperature is increasing slightly since the past three decades, coming from an average value of 6,8°C to 7,1°C in the most recent period, even though the maximum water temperature in the fjord basin occurred between 2001-2010 with an average value of 7,5°C.

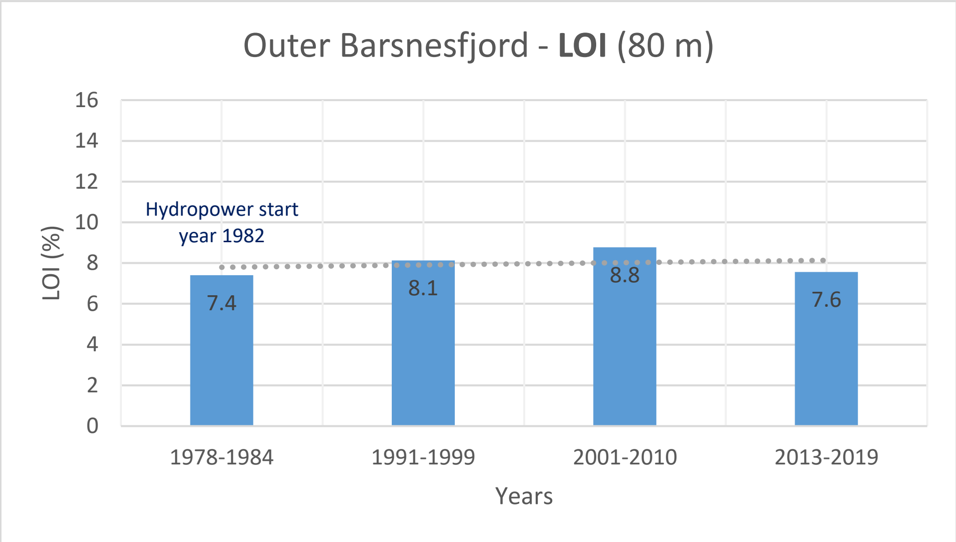

Figure 36: LOI trend in the Outer Barsnesfjord.

Figure 36 shows the progression of the LOI in the Outer Barsnesfjord basin at a water depth of 80 m. It can be seen that the trend has increased since the time period 1978-1984, starting from an average LOI value of 7,4% coming to a maximum LOI of 8,8% in 2001-2010 and then decreasing again to 8,0% in the most recent time period. As in the graph of the Inner Barsnesfjord, the Outer Barsnesfjord is influenced as well by hydropower activity started in year 1982.

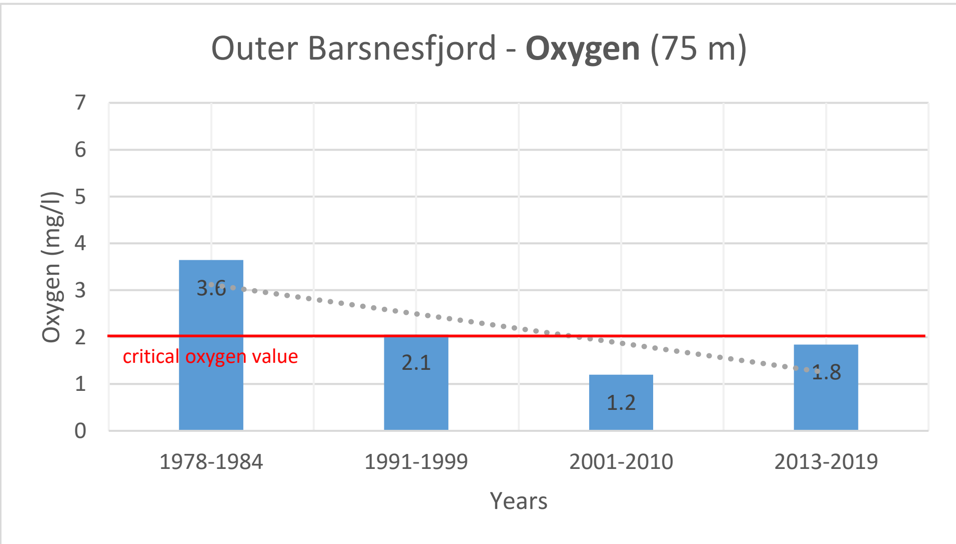

Figure 37: Oxygen trend in the Outer Barsnesfjord.

Figure 37 shows the progression of the oxygen conditions in the Outer Barsnesfjord basin, measured at a water depth of 75 m. Thus, the water depth of the hydrographical measurement differs slightly from the water depth of the sediment core sampling. It can be seen that there is a strong decline in the oxygen, starting with an average oxygen value of 3,6 mg/l in the basin waterbody, reaching the threshold for critical oxygen conditions in the time period 1991-1999 and continuing in a further decrease of 1,2 mg/l in 2001-2010. Although the average oxygen value is stated with 1,8 mg/l in the recent time period, it is still below the critical value und thus indicating anoxic conditions in the fjord basin. In general this means that the Outer Barsnesfjord went from low oxic to anoxic conditions in the waterbody.

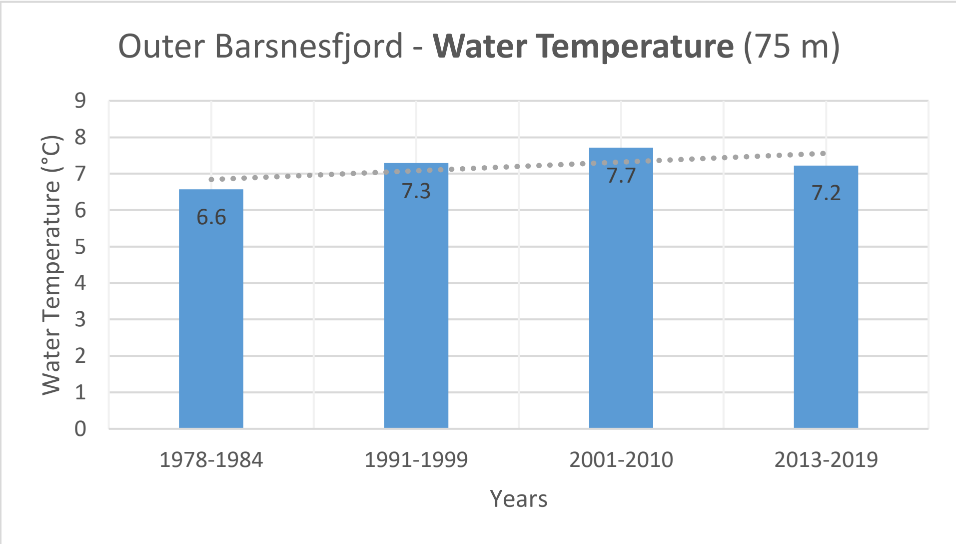

Figure 38: Water temperature trend in the Outer Barsnesfjord.

Figure 38 shows the progression of the water temperature in the Outer Barsnesfjord basin at a water depth of 75 m. The temperature measurement has been performed together with the hydrographical measurement of the oxygen conditions. It can be seen that the trend of the water temperature is increasing since the 1980s, coming from an average value of 6,6°C to a maximum value of 7,7°C in the time period 2001-2010. Afterwards there is a slight decrease again in 2013-2019 with an average water temperature of 7,2°C.

3.2.4 LOI and hydrography of the Inner Ikjefjord

Figure 39 shows the progression of the LOI in the Inner Ikjefjord basin at a water depth of 82 m. Starting with high average values of 15,8% in the time period 1978-1984, there has been a constant decrease until today with an average LOI of 11,4%. However, the minimum LOI happened in the time period 1991-1999 as stated in the graph with 8%. Hydropower activity with possible implications on the environmental conditions started in year 1970. In addition, a natural overflow occurred in 1983.

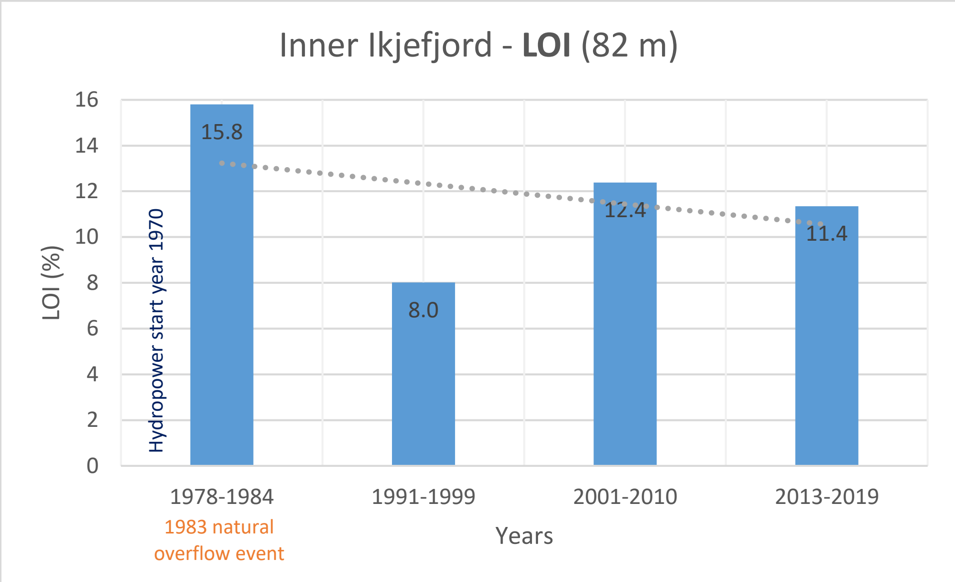

Figure 40: LOI trend in the Inner Ikjefjord.

Figure 40 shows the progression of the oxygen conditions in the Inner Ikjefjord basin, measured at a water depth of 75 m. Thus, the water depth of the hydrographical measurement differs slightly from the water depth of the sediment core sampling. It must be noted that it was only possible to consider oxygen data from the most recent time period 2013-2019 due to a lack of data for the remaining time horizons. However, the available oxygen data states an oxygen value below the critical point of 2 mg/l. With an average of 1,2 mg/l the fjord basin can recently be considered as anoxic.

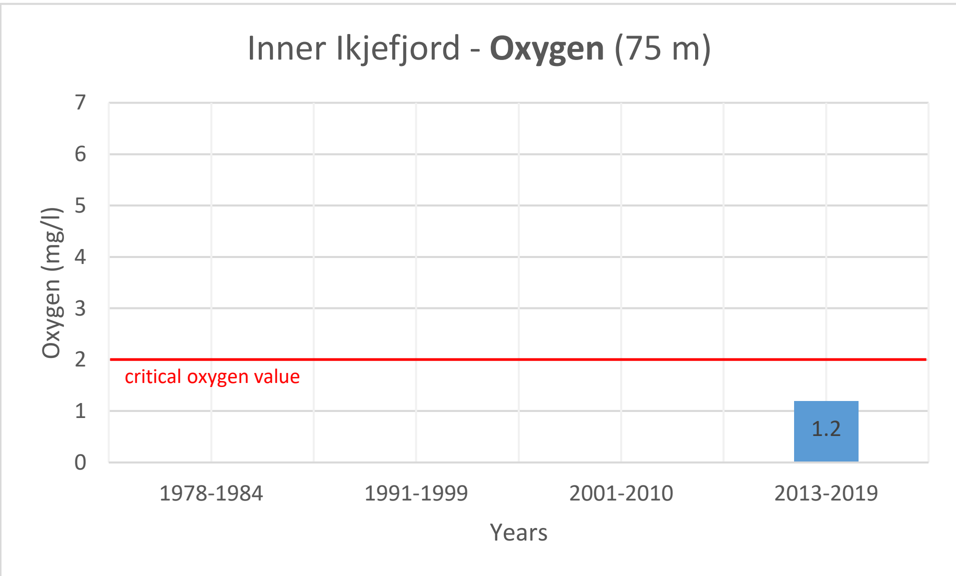

Figure 39: Oxygen trend in the Inner Ikjefjord.

Figure 41 shows the progression of the water temperature in the Inner Ikjefjord basin at a water depth of 75 m. The temperature measurement has been performed together with the hydrographical measurement of the oxygen conditions. That is why only water temperature

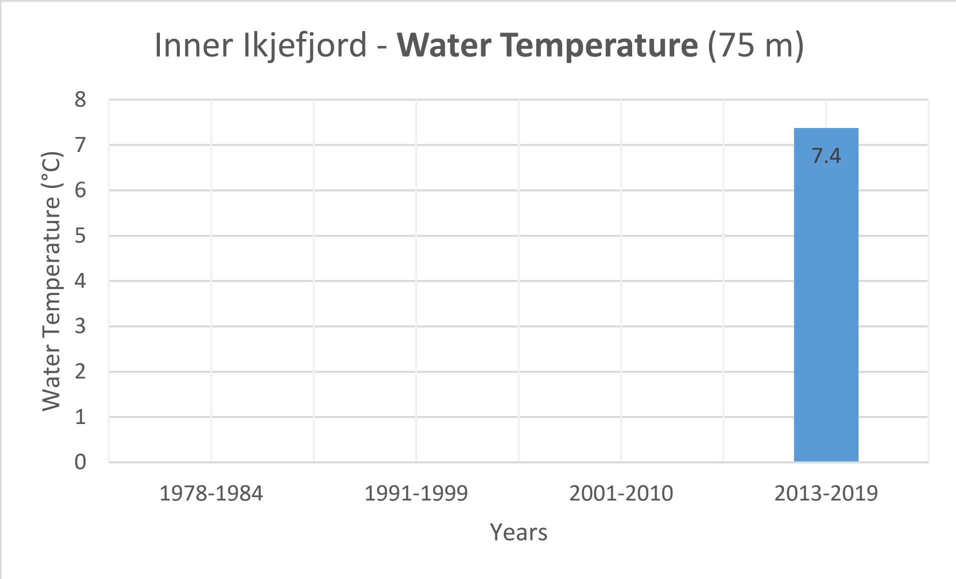

Figure 41: Water temperature trend in the Inner Ikjefjord.

data for the time period of 2013-2019 exists, respectively. The average temperature value in the fjord waterbody is therefore stated with 7,4°C.

3.2.5 LOI of the Arnafjord System

Figure 42 shows the progression of the LOI in the Arnafjord within the selected time horizons. The trend does not show a significant increase or decrease since the past four decades. The average LOI values remained stable at 3,9 or 4%, respectively. Hydropower production started to influence the fjord system in year 1968, as pictured in the graph.

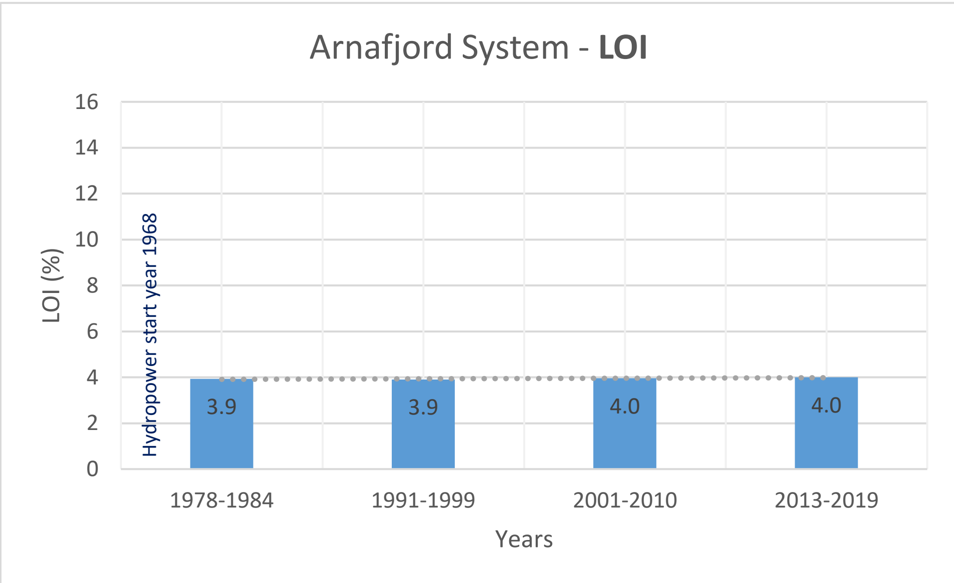

Figure 42: LOI trend in the Arnafjord System.

3.2.6 LOI and hydrography of the Inner Nærøyfjord

Figure 43 shows the progression of the LOI in the Inner Nærøyfjord basin at a water depth of 77m. It can be seen that the trend is decreasing since the past four decades. Starting with an average LOI value of 9,9% in 1978-1984, it reached a minimum in the time period 2001-2010 but increased again to 8,8% in the most recent time period. Looking at the trend line, an overall decrease from the 1980s until today can be detected. As an anthropogenic impact on the environmental conditions, the harbour construction around 1991 resulted in the natural delta loss and needs to be considered.

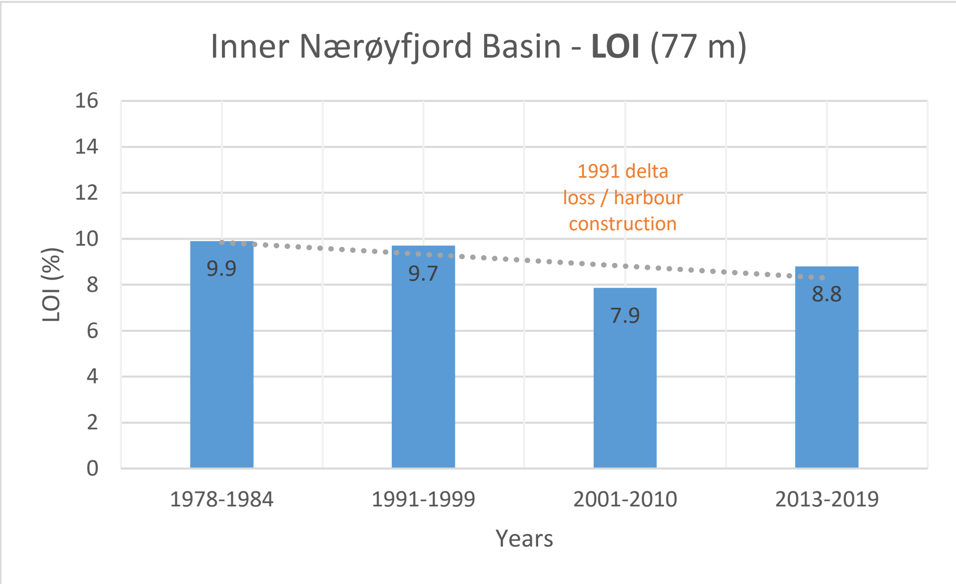

Figure 43: LOI trend in the Inner Nærøyfjord basin.

Figure 44 shows the progression of the oxygen conditions in the Inner Nærøyfjord basin, measured at a water depth of 70 m. Thus, the water depth of the hydrographical measurement differs slightly from the water depth of the sediment core sampling. It must be noted that it

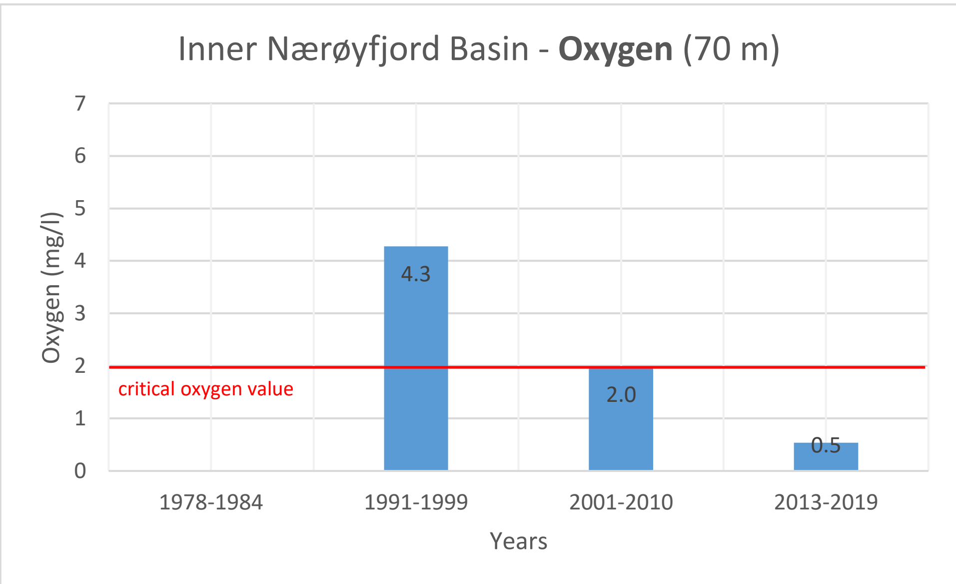

Figure 44: Oxygen trend in the Inner Nærøyfjord basin.

was not possible to consider oxygen data from the time period 1978-1984. A strong signal of oxygen decline within the fjord waterbody can be seen, coming from an average value of 4.3 mg/l in 1991-1999 to a minimum oxygen amount of 0,5 mg/l recently. In the time period 2001-2010, the threshold value of 2 mg/l has been reached. The oxygen conditions in the fjord basin therefore changed from oxic to anoxic since the 1990s until today.

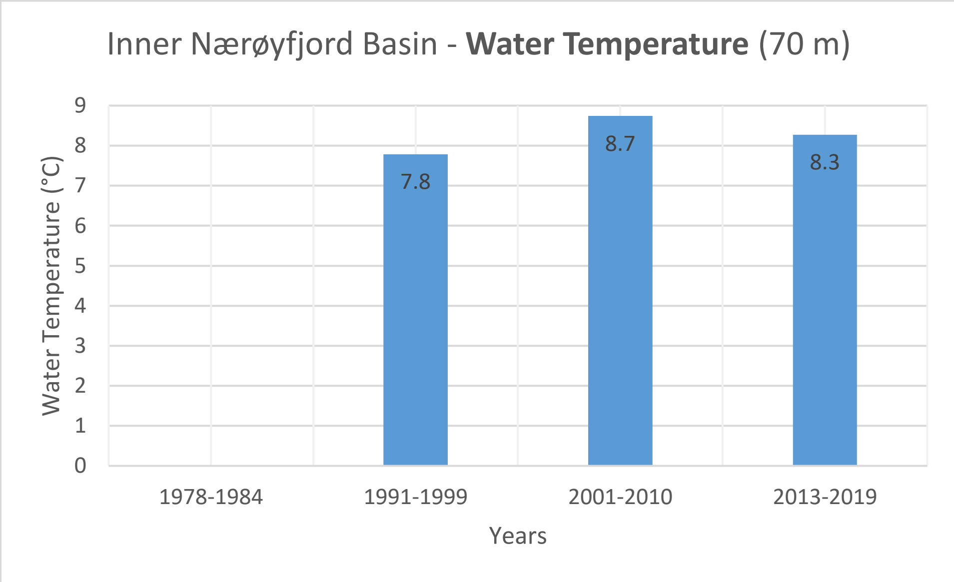

Figure 45: Water temperature trend in the Inner Nærøyfjord basin.

Figure 45 shows the progression of the water temperature in the Inner Nærøyfjord basin at a water depth of 70 m. The temperature measurement has been performed together with the hydrographical measurement of the oxygen conditions. This is why it was also not possible to consider water temperature data for the time period 1978-1984. It can be seen that the trend of the water temperature is increasing, starting with an average value of 7,8°C in 1991-1999 and reaching a maximum temperature in 2001-2010. A slight decrease happens within the most recent time period, as stated in an average value of 8,3°C in 2013-2019.

3.2.7 LOI of the Inner Aurlandsfjord

Figure 46 shows the progression of the LOI in the Inner Aurlandsfjord within the selected time horizons. It can be seen that the LOI trend is slightly decreasing since the past four decades. Starting with an average value of 6,8% in 1978-1984, the most recent average is stated with 5,6%. The minimum LOI value was found in the time period 1991-1999, as it is pictured in the graph. Hydropower activity started influencing the fjord in year 1969, and the flooding in 2014 was proposed to have an impact on the environmental conditions which needs to be considered.

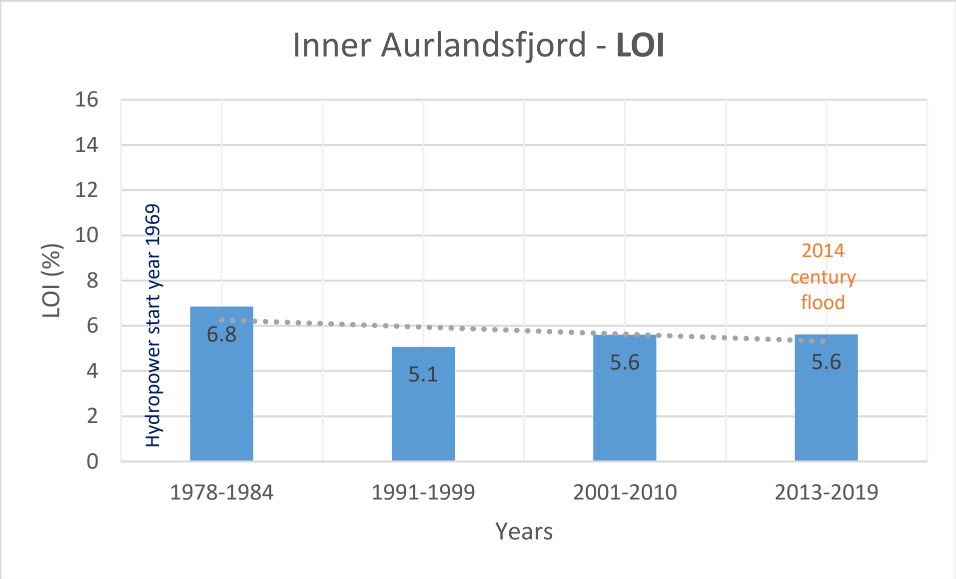

Figure 46: LOI trend in the Inner Aurlandsfjord.

4. Discussion

The three objectives stated at the beginning of this thesis, which were building the basis for the subsequent research including methods and results, are going to be answered and discussed in this chapter.

a) Are there spatial and temporal variations in the LOI content of the tributary fjord sediment samples of the Sognefjord?

The aim of this first objective was to gain insight about possible temporal and spatial variations in the LOI content of the different sediment cores from the tributary fjord basins of the Sognefjord. Therefore, all the available LOI data was gathered and summarized, as described in the applied methods for data analysis, in order to get an overall LOI value for the respective tributary fjord basins within the considered time horizons. The outcome of this analysis is summarized again in *Table 9* below.

Table 9: Overall average LOI values for the considered tributary fjord basins and time horizons.

Tributary fjord basin	Overall average LOI (%) values for the considered time horizons			
	1978-1984	1991-1999	2001-2010	2013-2019
Fjærlandsfjord	3.1	3.4	3.3	3.7
Sogndalsfjord	8.7	9.2	9.1	
Inner Barsnesfjord	8.6	8.0	9.7	10.7
Outer Barsnesfjord	7.4	8.1	8.8	8.0
Arnafjord System	3.9	3.9	4.0	4.0
Inner Ikjefjord	15.8	8.0	12.4	11.4
Inner Nærøyfjord	9.9	9.7	7.9	8.8
Inner Aurlandsfjord	6.8	5.1	5.6	5.6

Regarding the results of the temporal LOI development, it can be seen that almost all considered tributary fjord basins are showing a significant change, either stated in a decrease or increase of the average LOI values within the time horizons. For a better illustration, increasing values are indicated with a green colour, whereas decreasing values are indicted with a red colour. Yellow represents more or less stable LOI values without any significant trend.

The Fjærlandsfjord, the Sogndalsfjord and the Inner and Outer Barsnesfjord experienced an overall general increase of the average LOI from the earliest time horizon (1978-1984) until today (2013-2019). In contrast, the Inner Ikjefjord, the Inner Nærøyfjord and the Inner

Aurlandsfjord developed in the opposite direction, stating an overall decrease of the average LOI since 1978-1984. Besides, the Arnafjord System represents stable values throughout all considered time horizons. Despite the general LOI decrease for the Inner Ikjefjord, the Inner Nærøyfjord and the Inner Aurlandsfjord, some values in between the earliest und the latest time (2001-2010 and 1991-1999) are varying slightly around the overall decline.

What can be observed from *Table 9* as well is a first illustration of the spatial differences in the LOI content of the sediment samples from the tributary fjord basins of the Sognefjord. The shown increase and decrease, respectively, can be related to the northern and southern locations of the tributary fjord basins. The Fjærlandsfjord, the Sogndalsfjord and the Inner and Outer Barsnesfjord are northern tributary fjord basins of the Sognefjord and are stating an overall increase, whereas the Inner Ikjefjord, the Inner Nærøyfjord and the Inner Aurlandsfjord are considered southern tributaries of the Sognefjord, stating an overall decrease in LOI.

Concerning the individual LOI value quantity, no significance can be stated regarding the northern and southern tributary fjord distribution. The values seem to differ and range in an unpredictable order.

Further interpretations regarding the reason for the changing temporal progression, and their dependency on regional factors in terms of interpreting the spatial distribution are proposed by answering the next objective:

b) If so, is it possible to relate these LOI variations to environmental and climate change in the respective fjords?

After first determining that there are temporal and spatial variations in the LOI content of the tributary fjord basins of the Sognefjord, the question of interest would be why these changes do occur. For linking LOI changes to altering environmental conditions, additional values for the same time horizons were considered, observing the hydrographical and climatic state in the respective fjord areas.

In the following, an attempt is made to explain the observed LOI variations, in order to evaluate the influence of environmental and climate change on the LOI content in the tributary fjords. Therefore, the distribution in northern and southern location is representative.

Northern tributary fjords (Fjærlandsfjord, Sogndalsfjord, Barsnesfjord):

Generally, the source of the total organic matter measured in the sediment samples can either be marine or terrestrial (Bianchi et al., 2020). Since the simple LOI method is used for stating the total organic matter content (e.g. Bojko and Kabala, 2014), it is not possible to differentiate between these two sources. Observing increasing or decreasing organic matter trends in the fjord sediments can therefore be utilized to assess the balance between the input and output contributing to the organic matter supply system.

What can be derived from the analysis of the precipitation pattern in the Sognefjord area, is that there is an overall trend in annual precipitation is tending to increase. This leads to an increased runoff (e.g. Miller and Russell, 1992), meaning that potentially more organic matter from terrestrial sources can be transported into the river or lake systems, associated to the respective tributary fjord basins. In addition, the observed air temperature patterns for the Sognefjord area states a significant increase during the past 40 years as well (*Figure 17, 18, 19*). Rising temperatures are influencing the Jostedalsbreen glacier system and do result in an increased meltwater flux, what also adds to enhance the terrestrial runoff (e.g. Fellman et al., 2010). The increased precipitation and temperatures are furthermore having an impact on the productivity of the living environment (Ahmad et al., 2009), thus enhancing the growth of the biomass on land what in turn possibly could be terrestrial organic input to the fjord systems.

Regarding the marine organic matter supply, nutrients and solar radiation available for photosynthesis are the major distinctive factors (Bianchi et al., 2020). High availabilities of these two factors are resulting in enhanced primary productivity by microorganisms such as phytoplankton and macroalgae. Enhanced terrestrial runoff can also contribute to increased erosion (e.g. Ran et al., 2012) and weathering (e.g. Gislason et al., 2009) of soil and rocks. During these processes, nutrients out of mineralogical sources can be extracted (Velbel, 1988) and add to the increasing terrestrial nutrient flux into the fjord systems through the enhanced runoff.

Thus, the sources for marine and terrestrial organic matter supply are strongly influenced by the changing climatic conditions, resulting in increased air temperatures and precipitation and its implications on the runoff into the fjord systems. For earlier studies on the organic matter content in sediments of the Barsnesfjord, it is expected that the marine OM source is mainly responsible for the share in the overall increasing LOI trend since the 1980s in the northern tributary fjords of the Sognefjord. Paetzel and Schrader (1992) stated that over 90% of the existing organic matter can be considered from local marine origin.

Southern tributary fjords (Arnafjord System, Ikjefjord, Nærøyfjord, Aurlandsfjord):

In the southern tributary fjords of the Sognefjord, the same precipitation and temperature patterns, influenced by the changing climate, can be observed since their development accounts for the entire Sognefjord region. Therefore, the overall increasing air temperature and precipitation values do also influence the runoff and are thus responsible for an enhanced nutrient supply into the fjord systems. However, the southern fjords do not have a connection to the Jostedalsbreen glacier system, and thus no increasing meltwater flux is adding their share to the enhanced terrestrial runoff. The same accounts for the associated nutrient supply. Even though the total nutrient supply is proportionally less, an overall increase – although less extreme – in organic matter supply would still be expected to happen.

What can be observed is rather a development in the opposite direction, though. The measured LOI values in the Ikjefjord, the Nærøyfjord and the Aurlandsfjord are decreasing since the 1980s until today. Thus, there needs to be a superior factor which outweighs the possibly increasing nutrient supply for enhanced primary production of organic matter.

Extensive hydropower production in the areas around the southern tributary fjords could be an explanation for the overall decreasing LOI trend. Kaufmann (2014) stated that hydropower production in the respective fjord areas is influencing the seasonal runoff, leading to an increased freshwater supply in the winter seasons and a decreasing supply in summertime. As a result, the annual spring bloom of phytoplankton (Erga, 1984) mismatches the nutrient supply by the riverine discharge of freshwater inflow (e.g. Frigstad et al., 2020) into the fjord systems. Since nutrients and solar radiation are the limiting factors for the primary production (Bianchi et al., 2020), the non-available nutrients in the waterbody in spring lead to a decrease in primary production of organic material by marine microorganisms. In addition, for increasing the productivity of the hydropower plants, several rivers which once ensured the freshwater inflow into the fjord basins got either regulated or experienced a change in the direction of discharge (Appelgren and Ledje, 2016; Solbakken et al., 2011). This also leads to a lowering in nutrient supply by the decreased runoff into the fjord systems (Dårflot and Nævdal, 2020; Appelgren and Ledje, 2016; Schedel et al., 2015; Åtland et al., 1998). These significant changes and their associated altering of the environmental conditions, resulting in an overall decrease of organic matter availability in the fjord basin sediments, can be seen as the major implication of hydropower production in the areas around the southern tributary fjords.

It must be noted that even if there is hydropower activity in the northern tributary fjords of the Sognefjord as well, the extent of impacting the surrounding environment is not as significant as for the southern tributary fjords (see *Figure 15*). Here, the hydrographical implications are tremendous regarding the freshwater discharge due to several redirections of the inflowing rivers, whereas the overall hydrographical impact on runoff of the northern tributary fjord basins remains negligible.

c) Do such LOI controlling factors account for the entire Sognefjord region, or do they depend on the uniqueness of each tributary fjord?

In addition to the general precipitation and air temperature pattern of the entire Sognefjord region, stating the climatic development during the last four decades, the available oxygen and water temperature variables were considered to gain insight about the unique hydrographical conditions in each tributary fjord basin.

Whether a fjord basin has oxic or anoxic features is impacting the organic matter, or simplified as carbon, preservation potential (e.g., Smith et al., 2015; Syvitski et al., 1987). Therefore, it must be distinguished between a "real" net change in LOI values, where organic matter actually accumulated in the sediments, and only a change in the overall LOI flux. Usually, the supply on organic matter in not constant, which means that the flux of what deposits in the sediments and what gets decomposed varies naturally (Arndt et al., 2013). Enhanced accumulation can only take place if there is no or little decomposition in the sediments, which can be related to oxygen depletion in the water body (Arndt et al., 2013).

From the development of the hydrographical variables can be seen that the Inner and Outer Barsnesfjord do show anoxic features (see *Figure 34* and *Figure 37*), as well as the Inner Ikjefjord (see *Figure 40*) and the Inner Nærøyfjord (see *Figure 44*). The trend of all fjord basins getting more depleted in oxygen throughout the time can also be related to the increasing water temperatures in the fjord basin waterbodies. The anoxic environmental conditions in the Barsnesfjord system would therefore support the increasing trend in the LOI values, indicated by the preserving circumstances for the supplied organic matter through the anoxia in the fjord basin water.

However, the preserving circumstances would also apply for the anoxic considered fjord basins of the Inner Nærøyfjord and the Inner Ikjefjord. But in fact, the overall trend for the organic matter in these sediments is tending to decrease since the 1980s. A complete comparison between the observed LOI trend in all tributary fjord basins and the organic matter preserving potential, as indicated with the oxygen conditions in the waterbody, is shown in *Table 10*.

Table 10: Comparison between the overall LOI trend in the tributary fjord basins of the Sognefjord and the oxygen conditions.

	Tributary fjord basin	Overall LOI trend	Oxygen conditions	OM preserving potential
NORTH	Fjærlandsfjord	Increasing	Oxic	Low
	Sogndalsfjord	Increasing	Oxic	Low
	Inner Barsnesfjord	Increasing	Anoxic	High
	Outer Barsnesfjord	Increasing	Suboxic/Anoxic	High
SOUTH	Arnafjord System	Stable	Oxic	Low
	Inner Ikjefjord	Decreasing	Anoxic	High
	Inner Nærøyfjord	Decreasing	Anoxic	High
	Inner Aurlandsfjord	Decreasing	Oxic	Low

As a result, by comparing the fjord features in terms of hydrographical factors with the observed LOI trend throughout the last four decades, it can be shown that the unique environmental conditions in the respective fjord basins are not the major controlling factor for the observed trend. Rather the local influence of the northern and southern location outweighs the intended uniqueness of each tributary fjord basin of the Sognefjord.

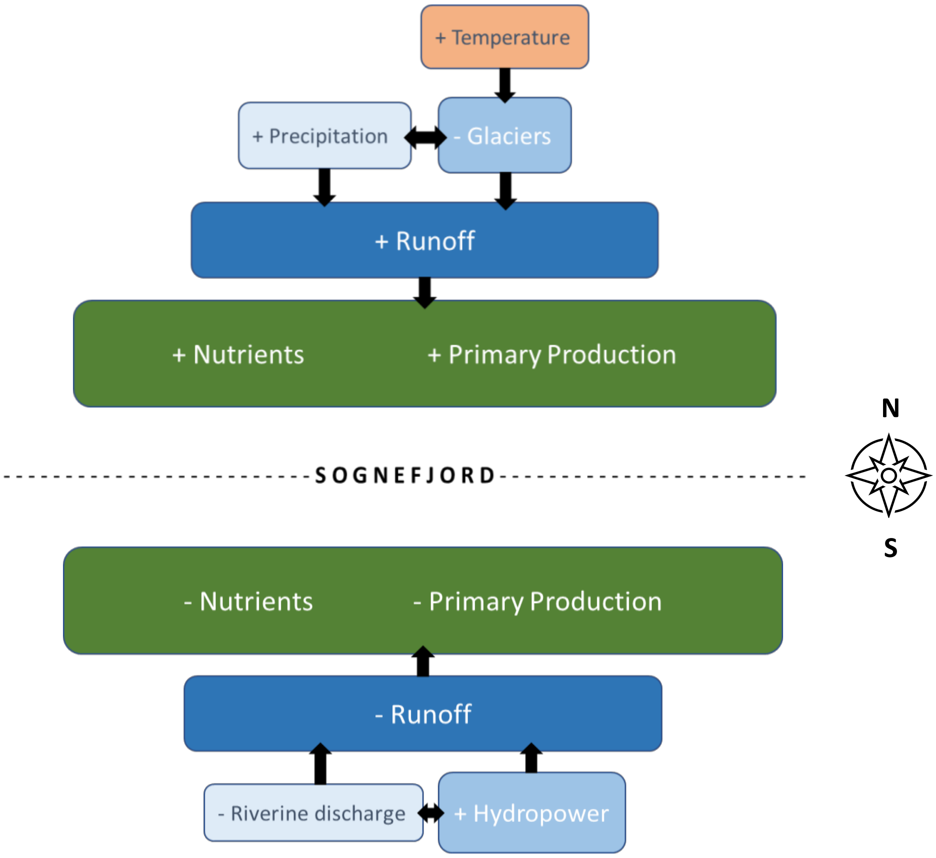

Figure 47: Schematic illustration of the processes and factors controlling the organic matter supply into the northern and southern tributary fjord systems of the Sognefjord.

Figure 47 is summarizing the above mentioned controlling factors for the organic matter supply into the tributary fjord systems with using a simplified box model. Hydropower influence is considered as the major process in the southern tributaries, whereas climate change induced precipitation and temperature control is the happening process in the northern tributaries.

5. Conclusion

Spatial and temporal variations in the LOI content of the sediment samples of the tributary fjord basins of the Sognefjord do occur. The overall trend states an increase in LOI concentrations since the 1980s until today for the north-located tributary fjords, whereas the southern tributary fjord basins experience an overall decrease in the LOI development.

The variations can be mainly explained by the link to climate change and glacial impact on the northern side of the Sognefjord, and the link to human-induced environmental change through hydropower on the southern side of the Sognefjord.

Unique local fjord features, resulting in an oxic or anoxic environment, are not the major controlling factor for the observed trend. The regional influence of the northern and southern location outweighs the intended individuality of each tributary fjord basin of the Sognefjord.

References

Aksnes, D. L., Aure, J., Johansen, P. O., Johnsen, G. H., & Salvanes, A. G. V. (2019). Multi-decadal warming of Atlantic water and associated decline of dissolved oxygen in a deep fjord. *Estuarine, Coastal and Shelf Science*, *228*, 106392.

Åtland, Å., Bjerknes, V., Barlaup, B., Kvellestad, A., Raddum, G. G., & Sundt, R. (1998). Undersøkelse av regulerte vassdrag med anadrome fiskebestander i Høyanger kommmune, Sogn og Fjordane. *Rapport LNR 3812.*

Andreassen, L. M., Nagy, T., Kjøllmoen, B., & Leigh, J. R. (2022). An inventory of Norway's glaciers and ice-marginal lakes from 2018–19 Sentinel-2 data. *Journal of Glaciology*, 1-22.

Appelgren, L., & Ledje, U.P. (2016). Overføring av Langavatnet, Vik kommune – virkninger for miljø og naturressurser. *Ecofact Report 504.*

Arndt, S., Jørgensen, B. B., LaRowe, D. E., Middelburg, J. J., Pancost, R. D., & Regnier, P. (2013). Quantifying the degradation of organic matter in marine sediments: a review and synthesis. *Earth-science reviews*, *123*, 53-86.

Askheim, S. (2020). Arnafjorden. *Store Norske Leksikon.* https://snl.no/Arnafjorden, 24.05.2022, 11:18.

Askheim, S. (2020). Fjærlandsfjorden. *Store Norske Leksikon.* https://snl.no/Fj%C3%A6rlandsfjorden, 24.05.2022, 10:38.

Askheim, S. (2020). Sogndalsfjorden. *Store Norske Leksikon.* https://snl.no/Sogndalsfjorden, 24.05.2022, 10:51.

Berg, A. S., Fauskanger, L., Muggerud, K., & Arhus, R. H. (2017). Vannkraft – Naturens pris. Effekter på hydrografisk og økologiske forhold i Sognefjorden (Unpublished thesis). *Høgskulen på Vestlandet.*

Bianchi, T. S., Arndt, S., Austin, W. E. N., Benn, D. I., Bertrand, S., Cui, X., Faust, J. C., Koziorowska-Makuch, K., Moy, C. M., Savage, C., Smeaton, C., Smith, R. W., & Syvitski, J. (2020). Fjords as aquatic critical zones (ACZs). *Earth-Science Reviews*, *203*, 103145.

Bojko, O., & Kabała, C. (2014). Loss-on-ignition as an estimate of total organic carbon in the mountain soils. *Polish Journal of Soil Science*, *47*(2).

Bøthun, M., Mørch, E. O., & Brochmann, K. E. (2014). Innflytelse av endringer i hydrografi på avsetning av organisk karbon i Barsnesfjorden, Vest-Norge (Unpublished thesis). *Høgskulen på Vestlandet*.

Bucher, A. (2020). Recent environmental change as recorded in sediments from the Arnafjord system, Western Norway (Unpublished thesis). *Høgskulen på Vestlandet*.

Carrivick, J. L., Andreassen, L. M., Nesje, A., & Yde, J. C. (2022). A reconstruction of Jostedalsbreen during the Little Ice Age and geometric changes to outlet glaciers since then. *Quaternary Science Reviews*, *284*, 107501.

Dale, T., & Hovgaard, P. (1993). En undersøkelse av resipientforholdene i Sogndalsfjorden, Barsnesfjorden og Kaupangerbukten i perioden 1991–1993. *Sogn og Fjordane Distriktshøgskule*.

Dårflot, I., & Nævdal, T. B. (2020). Vilkårsrevisjon Arnafjord Vikvassdraga. *Revisjonsdokument.*

Dean, W. E. (1974). Determination of carbonate and organic matter in calcareous sediments and sedimentary rocks by loss on ignition; comparison with other methods. *Journal of Sedimentary Research*, *44*(1), 242-248.

Doney, S. C., Ruckelshaus, M., Emmett Duffy, J., Barry, J. P., Chan, F., English, C. A., Galindo, H. M., Grebmeier, J. M., Hollowed, A. B., Knowlton, N., Polovina, J., Rabalais, N. N., Sydeman, W. J., & Talley, L. D. (2012). Climate change impacts on marine ecosystems. *Annual review of marine science*, *4*, 11-37.

Doney, S. C., Fabry, V. J., Feely, R. A., & Kleypas, J. A. (2009). Ocean acidification: the other CO2 problem. Annual review of marine science, 1, 169-192.

Dybo, M. H., Sundheim, M. L., & Søgnesand, A. M. (2016). Analyse av resente sedimentkjerner i den anoksiske Nærøyfjorden, Vest-Norge (Unpublished thesis). *Høgskulen på Vestlandet*.

Erga, S. R. (1989). Ecological studies on the phytoplankton of Boknafjorden, Western Norway. 1. The effect of water exchange processes and environmental factors on temporal and vertical variability of biomass. *Sarsia*, *74*(3), 161-176.

Erga, S. R., & Heimdal, B. R. (1984). Ecological studies on the phytoplankton of Korsfjorden, western Norway. The dynamics of a spring bloom seen in relation to hydrographical conditions and light regime. *Journal of Plankton Research*, *6*(1), 67-90.

Faust, J. C., Scheiber, T., Fabian, K., Vogt, C., & Knies, J. (2017). Geochemical characterisation of northern Norwegian fjord surface sediments: A baseline for further paleo-environmental investigations. *Continental Shelf Research, 148,* 104-115.

Faust, J. C., Fabian, K., Milzer, G., Giraudeau, J., & Knies, J. (2016). Norwegian fjord sediments reveal NAO related winter temperature and precipitation changes of the past 2800 years. *Earth and Planetary Science Letters*, *435*, 84-93.

Fellman, J. B., Spencer, R. G., Hernes, P. J., Edwards, R. T., D'Amore, D. V., & Hood, E. (2010). The impact of glacier runoff on the biodegradability and biochemical composition of terrigenous dissolved organic matter in near-shore marine ecosystems. *Marine Chemistry*, *121*(1-4), 112-122.

Frigstad, H., Kaste, Ø., Deininger, A., Kvalsund, K., Christensen, G., Bellerby, R. G., Sørensen, K., Norli, M. & King, A. L. (2020). Influence of riverine input on Norwegian coastal systems. *Frontiers in Marine Science*, *7*, 332.

Gislason, S. R., Oelkers, E. H., Eiriksdottir, E. S., Kardjilov, M. I., Gisladottir, G., Sigfusson, B., Snorasson, A., Elefsen, S., Hardardottir, J., Torssander, B. & Oskarsson, N. (2009). Direct evidence of the feedback between climate and weathering. *Earth and Planetary Science Letters*, *277*(1-2), 213-222.

Grieger, J. (2021). Hydrographical History of 7 Fjord Basins Along the Norwegian Sognefjorden with Emphasis on Oxygen Conditions (Unpublished thesis). *Høgskulen på Vestlandet*.

Hanssen-Bauer, I., Førland, E. J., Haddeland, I., Hisdal, H., Lawrence, D., Mayer, S., Nesje, A., Nilsen, J. E. Ø., Sandven, S., Sandø, A. B., Sorteberg, A., & Ådlandsvik, B. (2017). Climate in Norway 2100 – a knowledge base for climate adaptation. *Norwegian Environment Agency (Miljødirektoratet), Oslo, Rapport nr. 1/2017.*

Heiri, O., Lotter, A. F., & Lemcke, G. (2001). Loss on ignition as a method for estimating organic and carbonate content in sediments: reproducibility and comparability of results. *Journal of paleolimnology*, *25*(1), 101-110.

Holtedahl, H. (1967). Notes on the formation of fjords and fjord-valleys. *Geografiska Annaler: Series A, Physical Geography*, *49*(2-4), 188-203.

Howe, J. A., Austin, W. E., Forwick, M., Paetzel, M., Harland, R. E. X., & Cage, A. G. (2010). Fjord systems and archives: a review. *Geological Society, London, Special Publications, 344(1),* 5-15.

Inall, M. E., & Gillibrand, P. A. (2010). The physics of mid-latitude fjords: a review. *Geological Society, London, Special Publications*, *344*(1), 17-33.

IPCC (2021): Summary for Policymakers. In: *Climate Change 2021: The Physical Science Basis. Contribution of Working Group I to the Sixth Assessment Report of the Intergovernmental Panel on Climate Change* [Masson-Delmotte, V., P. Zhai, A. Pirani, S.L. Connors, C. Péan, S. Berger, N. Caud, Y. Chen, L. Goldfarb, M.I. Gomis, M. Huang, K. Leitzell, E. Lonnoy, J.B.R. Matthews, T.K. Maycock, T. Waterfield, O. Yelekçi, R. Yu, and B. Zhou (eds.)]. Cambridge University Press, Cambridge, United Kingdom and New York, NY, USA, pp. 3−32, doi:10.1017/9781009157896.001.

Johannesen, P. J., & Lønning, T. M. (1988) Resipientundersøkelser i Aurland kommune. *Rapp. Nr. 71-1988.*

Kaufmann, S. (2014). A 100 year hydrographical record of the Barsnesfjord, Western Norway and its environmental application (Unpublished thesis). *Høgskulen på Vestlandet.*

Keeling, R. F., Körtzinger, A., & Gruber, N. (2010). Ocean deoxygenation in a warming world. *Annual review of marine science*, *2*, 199-229.

Kerbusch, S. (2020). The Barsnesfjord holistic science approach: Implications on the application of the EU Water Framework Directive (Unpublished thesis). *Høgskulen på Vestlandet.*

Klamer, T. (2017). *River Deltas of the Inner Sognefjord (Inner Sogn Region): Consequences of Anthropogenic Change* (Unpublished thesis). *Høgskulen på Vestlandet.*

Koek, A., & Van Doorn, M. (2018). Investigating environmental change in the micro-organism distribution of anoxic Ikjefjord sediments since the 1960s, Western Norway (Unpublished thesis). *Høgskulen på Vestlandet.*

Kuliński, K., Kędra, M., Legeżyńska, J., Gluchowska, M., & Zaborska, A. (2014). Particulate organic matter sinks and sources in high Arctic fjord. *Journal of Marine Systems*, *139*, 27-37.

Langeng, T., & Slinning, A. (2018). Sedimenthistorie fra Fjærlandsfjorden, Vest-Norge, de siste 400 år (Unpublished thesis). *Høgskulen på Vestlandet.*

Manzetti, S., & Stenersen, J. H. V. (2010). A critical view of the environmental condition of the Sognefjord. *Marine pollution bulletin*, *60*(12), 2167-2174.

Massnes, A. (2016). Endringar i Ikjefjord og Massnes 1950 – 2015. *n.p.*

Midttømme, M., Thiem, E. R., Haga, O. N. (2017). Avsetninger fra historiske hendelser i Indre Aurlandsfjorden, Vest-Norge, over de siste 40 år – del I. De sedimentologiske signaler (Unpublished thesis). *Høgskulen på Vestlandet.*

Miller, J. R., & Russell, G. L. (1992). The impact of global warming on river runoff. *Journal of Geophysical Research: Atmospheres*, *97*(D3), 2757-2764.

Molina-Navarro, E., Andersen, H. E., Nielsen, A., Thodsen, H., & Trolle, D. (2018). Quantifying the combined effects of land use and climate changes on stream flow and nutrient loads: A modelling approach in the Odense Fjord catchment (Denmark). *Science of the Total Environment*, *621*, 253-264.

Monsen, S. (2017). Multi corer. *University of Bergen.* https://www.uib.no/en/geo/111820/multi-corer, 24.05.2022, 12:55.

Nesje, A., Bakke, J., Dahl, S. O., Lie, Ø., & Matthews, J. A. (2008). Norwegian mountain glaciers in the past, present and future. *Global and Planetary Change*, *60*(1-2), 10-27.

Nesje, A., & Dahl, S. O. (2003). The 'little ice age'–only temperature?. *The Holocene*, *13*(1), 139-145.

Nesje, A., Matthews, J. A., Dahl, S. O., Berrisford, M. S., & Andersson, C. (2001). Holocene glacier fluctuations of Flatebreen and winter-precipitation changes in the Jostedalsbreen region, western Norvay, based on glaciolacustrine sediment records. *The Holocene*, *11*(3), 267-280.

Nesje, A., & Whillans, I. M. (1994). Erosion of Sognefjord, Norway. *Geomorphology, 9*(1), 33-45.

Niemistö, L. (1974). A gravity corer for studies of soft sediments. *Merentutkimuslait. Julk./Havsforskningsinst. Skr. 238,* 33-38.

Nussbaumer, S. U., Nesje, A., & Zumbühl, H. J. (2011). Historical glacier fluctuations of Jostedalsbreen and Folgefonna (southern Norway) reassessed by new pictorial and written evidence. *The Holocene*, *21*(3), 455-471.

Paetzel, M., & Dale, T. (2010). Climate proxies for recent fjord sediments in the inner Sognefjord region, western Norway. *Geological Society, London, Special Publications*, *344*(1), 271-288.

Paetzel, M., & Schrader, H. (1992). Recent environmental changes recorded in anoxic Barsnesfjord sediments: Western Norway. *Marine geology*, *105*(1-4), 23-36.

Paetzel, M., & Schrader, H. (1991). Heavy metal (Zn, Cu, Pb) accumulation in the Barsnesfjord: Western Norway. *Norsk geologisk tidsskrift*, *71*(2), 65-73.

Ramberg, I. B. (Ed.). (2008). The making of a land: geology of Norway. *Geological Society of London.*

Ran, Q., Su, D., Li, P., & He, Z. (2012). Experimental study of the impact of rainfall characteristics on runoff generation and soil erosion. *Journal of Hydrology*, *424*, 99-111.

Ress, T. (2015). Some hydrographical changes in the Sognefjord and its tributaries, the Sogndalsfjord and the Barsnesfjord (Western Norway), the last century (Unpublished thesis). *Høgskulen på Vestlandet.*

SAIV A/S (n.d.). CTD profiler Model SD204. https://saiv.no/sd204-ctd-profiler, 24.05.2022, 12:42.

Santisteban, J. I., Mediavilla, R., Lopez-Pamo, E., Dabrio, C. J., Zapata, M., Garcia, M. J. G., Castano, S., & Martínez-Alfaro, P. E. (2004). Loss on ignition: a qualitative or quantitative method for organic matter and carbonate mineral content in sediments?. *Journal of Paleolimnology*, *32*(3), 287-299.

Schedel, J. B., Heibo, E., & Hanssen, K. (2015). Ungfiskregistreringar i regulerte elvar frå 2009 til 2014 i Sogn og Fjordane.

Selland, S.-G. (2021). Aurlandsfjorden. *Store Norske Leksikon.* https://snl.no/Aurlandsfjorden, 24.05.2022, 11:33.

Smith, R. W., Bianchi, T. S., Allison, M., Savage, C., & Galy, V. (2015). High rates of organic carbon burial in fjord sediments globally. *Nature Geoscience*, *8*(6), 450-453.

Solbakken, R., Henriksen, K., Reitan, K. I., Arff, J., Ellingsen, I. H., Hindar, K., Fiske, P., Robertsen, G., Finstad, B., Aas, Ø., & Johnsen, B. O. (2011). Innsamling og sammenstilling av relevant kunnskap om Sognefjorden. *Trondheim, SINTEF Fiskeri og havbruk AS.*

Syvitski, J. P. M., Burrell, D. C., & Skei, J. M. (1987). Fjords: processes and products. *Springer-Verlag New York Inc.*

Thorsnæs, G. (2021). Nærøyfjorden. *Store Norske Leksikon.* https://snl.no/N%C3%A6r%C3%B8yfjorden, 24.05.2022, 11:24.

Timmers, T. (2014). Sediment response to post-Little Ice Age climate change in the Sogndalsfjord, Western Norway (Unpublished thesis). *Høgskulen på Vestlandet.*

Tysnes, A., Bøen, M. R., & Rongved, J. A. S. (2015). Endringer i sammensetningen av sedimenter i Barsnesfjorden, Vest-Norge, over de siste 50 år (Unpublished thesis). *Høgskulen på Vestlandet.*

Van Rossum, M. J. H. (2018). Environmental change recorded in sediments of the anoxic Ikjefjord, Western-Norway, over the last 50 years (Unpublished thesis). *Høgskulen på Vestlandet.*

Vangsnes, T. H. (1981). Maringeologiske Undersøkelser I Indre Fjærlandsfjord, Sogn. *Universitetet i Bergen.*

Vaquer-Sunyer, R., & Duarte, C. M. (2008). Thresholds of hypoxia for marine biodiversity. *Proceedings of the National Academy of Sciences*, *105*(40), 15452-15457.

Velbel, M. A. (1988). Weathering and soil-forming processes. In *Forest hydrology and ecology at Coweeta* (pp. 93-102). Springer, New York, NY.

Vitousek, P. M. (1992). Global environmental change: an introduction. *Annual review of Ecology and Systematics*, *23*(1), 1-14.

Appendix

Appendix I: LOI raw data

The raw data is sorted by year of sediment core sampling (2012-2020).

Location: **Sogndalsfjord**
Core ID: **MF2012-7**

Sample number	Tara [g]	before oven [g]	after oven [g]	Loss on ignition	depth (cm)	LOI (%)		Sample number	Tara [g]	before oven [g]	after oven [g]	Loss on ignition	depth (cm)	LOI (%)
1	40.0758	41.1132	41.0025	0.1067	0.5	10.67091		31	18.7596	20.6986	20.5465	0.0784	30.5	7.84425
2	40.5859	41.4662	41.3725	0.1064	1.5	10.64410		32	16.3133	18.3164	18.1388	0.0887	31.5	8.86626
3	40.3010	41.5885	41.4601	0.0997	2.5	9.97282		33	15.6838	18.0151	17.7970	0.0936	32.5	9.35530
4	40.5001	42.1644	42.0113	0.0920	3.5	9.19906		34	17.7893	19.4174	19.2705	0.0902	33.5	9.02279
5	40.6130	42.0473	41.9122	0.0942	4.5	9.41923		35	17.8302	20.0080	19.8492	0.0729	34.5	7.29176
6	40.1810	41.3937	41.2801	0.0937	5.5	9.36753		36	22.5307	24.4744	24.3345	0.0720	35.5	7.19761
7	38.4046	39.4349	39.3382	0.0939	6.5	9.38562		37	19.1971	21.4158	21.2617	0.0695	36.5	6.94551
8	40.6676	41.7132	41.6151	0.0938	7.5	9.38217		38	17.2843	19.4670	19.3217	0.0666	37.5	6.65689
9	41.1084	42.4680	42.3330	0.0993	8.5	9.92939		39	23.8460	25.6592	25.5155	0.0793	38.5	7.92522
10	41.2343	42.3545	42.2494	0.0938	9.5	9.38225		40	40.6186	42.4378	42.2754	0.0893	39.5	8.92700
11	40.4011	41.6957	41.5790	0.0901	10.5	9.01437		41	39.3313	41.0223	40.8709	0.0895	40.5	8.95328
12	40.3407	41.7695	41.6482	0.0849	11.5	8.48964		42	40.2530	42.0937	41.9321	0.0878	41.5	8.77927
13	38.5981	40.1016	39.9739	0.0849	12.5	8.49352		43	39.8136	41.5763	41.4174	0.0901	42.5	9.01458
14	40.7822	42.1210	42.0018	0.0890	13.5	8.90350		44	40.2354	42.4613	42.2693	0.0863	43.5	8.62572
15	41.2826	43.0406	42.8880	0.0868	14.5	8.68032		45	39.7164	41.6814	41.4905	0.0972	44.5	9.71501
16	40.9676	42.4143	42.2880	0.0873	15.5	8.73021		46	38.9253	40.9688	40.7898	0.0876	45.5	8.75948
17	40.9786	42.4453	42.3222	0.0839	16.5	8.39299		47	40.9369	42.9057	42.7144	0.0972	46.5	9.71658
18	40.6404	41.7491	41.6550	0.0849	17.5	8.48742		48	38.7200	40.3328	40.1700	0.1009	47.5	10.09425
19	40.6612	42.3217	42.1867	0.0813	18.5	8.13008		49	39.2913	41.0885	40.9220	0.0926	48.5	9.26441
20	40.2181	41.6037	41.4888	0.0829	19.5	8.29244								
21	39.8508	41.5035	41.3734	0.0787	20.5	7.87197								
22	40.5712	42.0298	41.9247	0.0721	21.5	7.20554								
23	40.2373	42.4144	42.2587	0.0715	22.5	7.15172								
24	39.8222	41.4411	41.3182	0.0759	23.5	7.59157								
25	16.6272	18.6882	18.5363	0.0737	24.5	7.37021								
26	17.5435	19.4715	19.3440	0.0661	25.5	6.61307								
27	23.6532	25.6520	25.5170	0.0675	26.5	6.75405								
28	16.7658	18.5293	18.4271	0.0580	27.5	5.79529								
29	23.9511	25.9224	25.8404	0.0416	28.5	4.15969								
30	17.6501	19.5283	19.4208	0.0572	29.5	5.72357								

Location: **Sogndalsfjord**
Core ID: **MF2012-8**

Sample number	Tara [g]	before oven [g]	after oven [g]	Loss on ignition	depth (cm)	LOI (%)
1	40.0736	42.064	41.895	0.0849	0.5	8.49076
2	40.5853	43.002	42.797	0.0848	1.5	8.48264
3	40.2996	42.032	41.888	0.0831	2.5	8.31217
4	40.4987	41.92	41.86	0.0422	3.5	
5	40.5952	42.13	42.008	0.0795	4.5	7.94892
6	40.1807	41.92	41.762	0.0908	5.5	9.08411
7	38.405	40.03	39.896	0.0825	6.5	8.24615
8	40.6677	42.46	42.317	0.0798	7.5	7.97858
9	41.1081	43.18	43.014	0.0801	8.5	8.01197
10	41.2332	43.47	43.293	0.0791	9.5	7.91309
11	40.4004	42.16	42.018	0.0807	10.5	8.07002
12	40.3709	42.16	42.021	0.0777	11.5	7.76927
13	38.598	40.89	40.719	0.0746	12.5	7.46073
14	40.781	42.49	42.364	0.0737	13.5	7.37273
15	41.2811	43.15	43.016	0.0717	14.5	7.16999
16	40.9668	42.81	42.662	0.0803	15.5	8.02951
17	40.9779	43	42.849	0.0747	16.5	7.46748
18	40.6403	43.09	42.905	0.0755	17.5	7.55195
19	40.6598	42.77	42.617	0.0725	18.5	7.25050
20	40.2177	42.98	42.779	0.0728	19.5	7.27654
21	39.8495	42.56	42.361	0.0734	20.5	7.34182
22	40.5703	43.69	43.472	0.0699	21.5	6.98785
23	40.2365	43.12	42.918	0.0701	22.5	7.00538
24	39.822	41.81	41.674	0.0684	23.5	6.84105
25	19.1978	21.7	21.535	0.0659	24.5	6.59420
26	18.5106	21.39	21.197	0.0670	25.5	6.70279
27	17.5432	19.87	19.709	0.0692	26.5	6.91937
28	16.3125	18.72	18.557	0.0677	27.5	6.77051
29	16.2323	19.54	19.324	0.0653	28.5	6.53022
30	16.1935	18.69	18.525	0.0661	29.5	6.60925
31	23.6506	25.54	25.41	0.0688	30.5	6.88049
32	16.653	18.33	18.203	0.0757	31.5	7.57305
33	18.0183	20.42	20.249	0.0712	32.5	7.11996
34	23.9517	26.83	26.618	0.0737	33.5	7.36546
35	16.7663	19.76	19.532	0.0762	34.5	7.61599
36	16.7289	19.28	19.086	0.0760	35.5	7.60456
37	22.5313	25.12	24.91	0.0811	36.5	8.11218
38	15.6841	18.07	17.877	0.0809	37.5	8.08919
39	19.0458	21.08	20.897	0.0900	38.5	8.99617
40	23.8457	26.45	26.23	0.0845	39.5	8.44757
41	39.3309	41.83	41.64	0.0760	40.5	7.60274

Location: **Sogndalsfjord**
Core ID: **MF2012-9**

Sample number	Tara [g]	before oven [g]	after oven [g]	Loss on ignition	depth (cm)	LOI (%)		Sample number	Tara [g]	before oven [g]	after oven [g]	Loss on ignition	depth (cm)	LOI (%)
1	40.0698	42.9173	42.6880	0.0805	0.5	8.05268		31	18.7597	21.1449	20.9569	0.0788	30.5	7.88194
2	40.5819	42.1654	42.0336	0.0832	1.5	8.32333		32	16.3133	18.9215	18.7539	0.0643	31.5	6.42589
3	40.2977	42.3489	42.1881	0.0784	2.5	7.83931		33	15.6844	18.7313	18.4697	0.0859	32.5	8.58578
4	40.4961	42.6923	42.5147	0.0809	3.5	8.08670		34	17.7897	20.8190	20.5634	0.0844	33.5	8.43759
5	40.5928	42.6656	42.4972	0.0812	4.5	8.12428		35	17.8304	21.3631	21.0784	0.0806	34.5	8.05899
6	40.1782	42.2242	42.0600	0.0803	5.5	8.02542		36	22.5315	25.8365	25.5181	0.0963	35.5	9.63389
7	38.4013	40.3126	40.1602	0.0797	6.5	7.97363		37	19.1975	22.4143	22.1557	0.0804	36.5	8.03905
8	40.6657	42.5672	42.4179	0.0785	7.5	7.85170		38	17.2848	19.7682	19.5695	0.0800	37.5	8.00113
9	41.1066	42.8368	42.7010	0.0785	8.5	7.84880		39	23.8459	26.9999	26.7313	0.0852	38.5	8.51617
10	41.2322	43.4173	43.2496	0.0767	9.5	7.67471		40	40.6201	44.0523	43.7520	0.0875	39.5	8.74949
11	40.3987	42.1451	42.0124	0.0760	10.5	7.59849		41	39.3328	42.7438	42.4585	0.0836	40.5	8.36412
12	40.3388	42.8529	42.6683	0.0734	11.5	7.34259		42	40.2546	43.3519	43.0921	0.0839	41.5	8.38795
13	38.5968	40.6692	43.3871		12.5	6.91951		43	39.8149	42.0961	41.9071	0.0829	42.5	8.28511
14	40.7807	43.1445	42.9794	0.0698	13.5	6.98452								
15	41.2817	43.5439	40.5258		14.5	6.93131								
16	40.9664	43.1218	42.9110	0.0978	15.5	9.78009								
17	40.9775	42.8995	42.7150	0.0960	16.5	9.59938								
18	40.6405	42.9913	42.7831	0.0886	17.5	8.85656								
19	40.6600	42.8280	42.6401	0.0867	18.5	8.66697								
20	40.2174	43.1307	42.8994	0.0794	19.5	7.93945								
21	39.8500	42.2673	42.0713	0.0811	20.5	8.10822								
22	40.5699	43.1574	42.9605	0.0761	21.5	7.60966								
23	40.2364	42.8957	42.6991	0.0739	22.5	7.39292								
24	39.8217	42.7029	42.4932	0.0728	23.5	7.27822								
25	16.6270	19.5101	19.3094	0.0696	24.5	6.96126								
26	17.5437	20.0091	19.8426	0.0675	25.5	6.75347								
27	23.6519	26.6589	26.4572	0.0671	26.5	6.70768								
28	16.7657	20.0060	19.7857	0.0680	27.5	6.79875								
29	23.9510	26.5554	26.3812	0.0669	28.5	6.68868								
30	17.6492	20.0663	19.9061	0.0663	29.5	6.62778								

Location: **Outer Barsnesfjord**
Core ID: **MF2013-4**

Sample number	Tara [g]	before oven [g]	after oven [g]	Loss on ignition	depth (cm)	LOI (%)
1	41.1619	41.9276	41.8715	0.0733	0.5	7.32663
2	39.7672	40.5064	40.448	0.0790	1.5	7.90043
3	38.9241	39.3122	39.278	0.0881	2.5	8.81216
4	40.1814	40.4493	40.4252	0.0900	3.5	8.99589
5	40.6414	41.4667	41.3927	0.0897	4.5	8.96644
6	41.2335	42.0125	41.9522	0.0774	5.5	7.74069
7	40.5973	41.5039	41.4345	0.0765	6.5	7.65497
8	38.5977	38.8601	38.8372	0.0873	7.5	8.72713
9	40.9428	41.4365	41.3877	0.0988	8.5	9.88455
10	40.9788	41.4772	41.4298	0.0951	9.5	9.51043
11	40.3403	40.7642	40.7226	0.0981	10.5	9.81364
12	40.3011	40.6141	40.5828	0.1000	11.5	10.00000
13	38.4041	38.7262	38.6966	0.0919	12.5	9.18969
14	39.7162	41.1403	41.0225	0.0827	13.5	8.27189
15	16.9004	17.3937	17.3547	0.0791	14.5	7.90594
16	17.5697	18.6517	18.5749	0.0710	15.5	7.09797
17	18.0175	19.1985	19.1203	0.0662	16.5	6.62151
18	18.0176	19.0809	19.015	0.0620	17.5	6.19769
19	17.9139	18.6381	18.5991	0.0539	18.5	5.38525
20	17.5431	18.4577	18.4093	0.0529	19.5	5.29193
21	18.0685	18.884	18.8136	0.0863	20.5	8.63274
22	18.5105	18.972	18.9315	0.0878	21.5	8.77573
23	17.2811	18.0416	17.9776	0.0842	22.5	8.41552
24	18.1872	18.5462	18.5143	0.0889	23.5	8.88579
25	17.6691	18.2848	18.2315	0.0866	24.5	8.65681
26	17.2135	17.6617	17.6215	0.0897	25.5	8.96921
27	19.1971	19.7369	19.6918	0.0835	26.5	8.35495
28	17.4156	18.0086	17.9592	0.0833	27.5	8.33052
29	18.3799	18.7631	18.7306	0.0848	28.5	8.48121

Location: **Outer Barsnesfjord**
Core ID: **MF2013-6**

Sample number	Tara [g]	before oven [g]	after oven [g]	Loss on ignition	depth (cm)	LOI (%)
1	40.4991	41.4946	41.4219	0.0730	0.9	7.30286
2	40.0747	42.7513	42.5787	0.0645	2.7	6.44848
3	40.9675	42.5668	42.4463	0.0753	4.5	7.53455
4	40.6191	41.3643	41.2805	0.1125	6.3	11.24530
5	41.2826	42.1507	42.059	0.1056	8.1	10.56330
6	40.2187	42.168	42.0588	0.0560	9.9	5.60201
7	40.4018	41.9599	41.8006	0.1022	11.7	10.22399
8	40.9362	42.5909	42.4154	0.1061	13.5	10.60615
10	40.2351	41.721	41.5715	0.1006	15.3	10.06124
11	40.2553	41.8089	41.6518	0.1011	17.1	10.11200
12	40.2995	41.8508	41.7113	0.0899	18.9	8.99246
13	39.8224	41.718	41.5815	0.0720	20.7	7.20089
14	39.2914	43.2924	43.1228	0.0424	22.5	4.23894
15	40.6611	42.2356	42.1096	0.0800	24.3	8.00254

Location: **Inner Barsnesfjord**
Core ID: **MF2014-5**

Sample number	Tara [g]	before oven [g]	after oven [g]	Loss on ignition	depth (cm)	LOI (%)		Sample number	Tara [g]	before oven [g]	after oven [g]	Loss on ignition	depth (cm)	LOI (%)
28	16.8304	17.0979	17.0618	0.1350	0.25	13.49533		108	41.1958	41.6613	41.6221	0.0842	15.25	8.42105
29	19.6464	19.9174	19.8858	0.1166	0.75	11.66052		109	40.6968	41.2453	41.1999	0.0828	15.75	8.27712
32	19.1005	19.3147	19.2835	0.1457	1.25	14.56583		110	41.01	41.4774			16.25	
33	19.1602	19.3724	19.3468	0.1206	1.75	12.06409		17	18.2674	18.776	18.7251	0.1001	16.75	10.00786
48	18.039	18.3716	18.3365	0.1055	2.25	10.55322		65	16.645	17.1778	17.121	0.1066	17.25	10.66066
72	16.5058	16.815	16.7807	0.1109	2.75	11.09314		111	40.2134	40.7376	40.6917	0.0876	17.75	8.75620
30	21.9504	22.2892	22.2576	0.0933	3.25	9.32704		26	17.0777	17.548	17.4988	0.1046	18.25	10.46141
34	22.0305	22.4733	22.4246	0.1100	3.75	10.99819		112	39.3221	39.7884	39.7549	0.0718	18.75	7.18422
31	18.8671	19.235	19.1931	0.1139	4.25	11.38896		113	40.3749	40.8905	40.8465	0.0853	19.25	8.53375
58	17.688	18.0712	18.0273	0.1146	4.75	11.45616		3	16.2512	16.9116	16.8493	0.0943	19.75	9.43368
90	40.9743	41.5088	41.4641	0.0836	5.25	8.36296		45	37.0883	37.5654	37.5162	0.1031	20.25	10.31230
106	22.5543	22.9406	22.8923	0.1250	5.75	12.50324		15	40.3866	40.853	40.8068	0.0991	20.75	9.90566
91	38.9556	39.4528	39.4108	0.0845	6.25	8.44730		114	39.8548	40.3922	40.346	0.0860	21.25	8.59695
92	39.8432	40.694	40.6152	0.0926	6.75	9.26187		46	40.3106	40.9095	40.8527	0.0948	21.75	9.48405
93	40.3325	40.8808	40.835	0.0835	7.25	8.35309		47	37.8514	38.2653	38.2271	0.0923	22.25	9.22928
117	23.6891	24.0977	24.0338	0.1564	7.75	15.63877		73	38.3391	38.7124	38.6815	0.0828	22.75	8.27752
8	16.3241	16.75	16.7045	0.1068	8.25	10.68326		53	37.4878	37.8332	37.8025	0.0889	23.25	8.88825
59	23.9842	24.4679	24.4115	0.1166	8.75	11.66012		50	39.9994	40.6173	40.5635	0.0871	23.75	8.70691
94	39.7983	40.1996	40.1648	0.0867	9.25	8.67182		35	38.4669	38.8246	38.7798	0.1252	24.25	12.52446
95	40.675	41.2076	41.1641	0.0817	9.75	8.16748		36	37.7835	38.286	38.2403	0.0909	24.75	9.09453
96	40.8125	41.6663			10.25			37	38.4742	38.8585	38.824	0.0898	25.25	8.97736
61	23.9753	24.3641	24.322	0.1083	10.75	10.82819		38	38.779	39.3588	39.2995	0.1023	25.75	10.22766
25	17.8571	18.1715	18.1318	0.1263	11.25	12.62723		39	40.5157	41.0706	41.1067		26.25	
97	40.628	41.383	41.3156	0.0893	11.75	8.92715		40	37.806	38.2911	38.2493	0.0862	26.75	8.61678
98	41.1393	40.7886	41.7301		12.25			42	38.333	39.0061	38.9472	0.0875	27.25	8.75056
99	39.3616	40.0278			12.75			41	40.565	40.9759	40.9361	0.0969	27.75	9.68606
103	40.6162	41.2434	41.1901	0.0850	13.25	8.49809		44	38.0538	38.7581	38.6985	0.0846	28.25	8.46230
104	38.4334	38.8073	38.7801	0.0727	13.75	7.27467		43	36.6769	37.1872	37.143	0.0866	28.75	8.66157
22	17.8092	18.2295	18.1853	0.1052	14.25	10.51630		118	17.2937	17.7791	17.7359	0.0890	29.25	8.89988
107	40.2666	40.8036			14.75			158	18.0864	18.3372	18.313	0.0965	29.75	9.64912

Table continues on the next page.

Location: **Inner Barsnesfjord**
Core ID: **MF2014-5**

Sample number	Tara [g]	before oven [g]	after oven [g]	Loss on ignition	depth (cm)	LOI (%)		Sample number	Tara [g]	before oven [g]	after oven [g]	Loss on ignition	depth (cm)	LOI (%)
139	17.4376	17.7645	17.7325	0.0979	30.25	9.78893		12	17.9348	19.0549	18.9534	0.0906	45.25	9.06169
184	17.6897	18.0459	18.0164	0.0828	30.75	8.28186		18	16.9193	17.9532	17.8579	0.0922	45.75	9.21753
126	41.042	41.353	41.3107	0.1360	31.25	13.60129		52	17.2351	18.1526	18.065	0.0955	46.25	9.54768
174	40.354	40.7094	40.6715	0.1066	31.75	10.66404		23	18.4079	19.3591	19.2646	0.0993	46.75	9.93482
120	41.2842	41.6072	41.5762	0.0960	32.25	9.59752		19	19.2155	20.1203	20.0242	0.1062	47.25	10.62113
185	40.6324	41.1993	41.1493	0.0882	32.75	8.81990		24	18.3977	19.4698	19.358	0.1043	47.75	10.42813
131	38.6457	39.3894	39.3316	0.0777	33.25	7.77195		4	17.196	18.0455	17.9534	0.1084	48.25	10.84167
124	39.8691	40.2427	40.2038	0.1041	33.75	10.41221		105	23.678	24.6615	24.5554	0.1079	48.75	10.78800
169	38.97	39.5208	39.4739	0.0851	34.25	8.51489		116	18.7823	19.487	19.4086	0.1113	49.25	11.12530
145	39.3385	39.868	39.83	0.0718	34.75	7.17658		2	16.7488	18.0555	17.8918	0.1253	49.75	12.52774
141	39.8585	40.4844	40.4378	0.0745	35.25	7.44528		49	17.6758	18.287	18.218	0.1129	50.25	11.28927
123	40.2827	40.9793	40.9293	0.0718	35.75	7.17772		1	16.7919	17.212	17.1647	0.1126	50.75	11.25922
100	41.1512	41.9197	41.8687	0.0664	36.25	6.63630		7	17.5891	18.3435	18.2702	0.0972	51.25	9.71633
64	41.2145	41.8757	41.8298	0.0694	36.75	6.94192								
60	40.2267	41.154	41.094	0.0647	37.25	6.47040								
163	38.4469	39.028	38.9862	0.0719	37.75	7.19325								
70	39.3754	40.1769	40.1208	0.0700	38.25	6.99938								
102	39.8135	40.3055	40.2697	0.0728	38.75	7.27642								
115	40.8268	41.7039	41.6376	0.0756	39.25	7.55900								
51	40.6462	41.3973	41.3305	0.0889	39.75	8.89362								
101	40.693	41.5976	41.5282	0.0767	40.25	7.67190								
148	40.9953	41.872	41.8032	0.0785	40.75	7.84761								
66	40.7135	41.5206	41.4683	0.0648	41.25	6.47999								
6	18.2115	19.74	19.6281	0.0732	41.75	7.32090								
71	17.6695	18.6037	18.5295	0.0794	42.25	7.94262								
5	18.0396	19.043	18.9678	0.0749	42.75	7.49452								
9	18.0395	19.1646	19.078	0.0770	43.25	7.69709								
10	18.5329	19.4545	19.3793	0.0816	43.75	8.15972								
21	16.6714	17.4314	17.3683	0.0830	44.25	8.30263								
16	17.5659	18.5651	18.481	0.0842	44.75	8.41673								

Location: **Outer Barsnesfjord**
Core ID: **MF2014-7**

Sample number	Tara [g]	before oven [g]	after oven [g]	Loss on ignition	depth (cm)	LOI (%)	Sample number	Tara [g]	before oven [g]	after oven [g]	Loss on ignition	depth (cm)	LOI (%)
1	17.5891	18.0702	18.0257	0.092496363	0	9.24964	31	17.6775	18.4996	18.4299	0.084782873	15	8.47829
2	18.0839	18.6447	18.6018	0.07649786	0.5	7.64979	32	16.7885	18.2356	18.124	0.077119757	15.5	7.71198
3	17.6886	18.5913	18.5186	0.080536169	1	8.05362	33	16.2468	17.0917	17.0244	0.079654397	16	7.96544
4	16.9202	17.158	17.133	0.105130362	1.5	10.51304	34	22.556	23.9454	23.8293	0.083561249	16.5	8.35612
5	18.0413	18.2055	18.1867	0.114494519	2	11.44945	35	39.8071	40.9566	40.8721	0.073510222	17	7.35102
6	16.6735	16.9195	16.8925	0.109756098	2.5	10.97561	36	40.6262	41.5073	41.4458	0.069799115	17.5	6.97991
7	17.5675	18.3064	18.2389	0.09135201	3	9.13520	37	40.9842	42.3667	42.2682	0.07124774	18	7.12477
8	18.533	19.1674	19.1089	0.092213115	3.5	9.22131	38	40.223	41.1254	41.0514	0.082003546	18.5	8.20035
9	17.437	18.258	18.1935	0.078562728	4	7.85627	39	38.4437	39.7943	39.7004	0.069524656	19	6.95247
10	17.2914	18.0959	18.0193	0.095214419	4.5	9.52144	40	40.6388	41.9957	41.8938	0.075097649	19.5	7.50976
11	19.2172	19.8369	19.7827	0.087461675	5	8.74617	41	39.8536	40.5286	40.475	0.079407407	20	7.94074
12	18.2095	18.703	18.6567	0.093819656	5.5	9.38197	42	40.7077	41.6595	41.5889	0.074175247	20.5	7.41752
13	18.0403	18.621	18.5691	0.089374892	6	8.93749	43	40.385	41.4065	41.3324	0.072540382	21	7.25404
14	18.4086	19.1967	19.1274	0.087933003	6.5	8.79330	44	41.1524	42.2731	42.1864	0.077362363	21.5	7.73624
15	17.2365	18.0908	18.0179	0.085333021	7	8.53330	45	39.331	40.4738	40.3892	0.074028701	22	7.40287
16	17.9369	18.2312	18.2062	0.084947333	7.5	8.49473	46	41.2083	42.0441	41.9894	0.065446279	22.5	6.54463
17	18.3976	19.2996	19.2212	0.08691796	8	8.69180	47	40.342	42.0087	41.8913	0.070438591	23	7.04386
18	18.2673	19.2055	19.1214	0.089639736	8.5	8.96397	48	38.9656	39.4022	39.3723	0.068483738	23.5	6.84837
19	16.7513	17.6346	17.5537	0.091588362	9	9.15884	49	39.8667	40.9213	40.8482	0.06931538	24	6.93154
20	23.6774	24.5659	24.4835	0.092740574	9.5	9.27406	50	40.6847	42.0057	41.9164	0.067600303	24.5	6.76003
21	17.6712	18.9258	18.8162	0.087358521	10	8.73585	51	41.0204	42.1182	42.0357	0.075150301	25	7.51503
22	18.785	19.096	19.0469	0.157877814	10.5		52	39.3706	40.6832	40.5882	0.072375438	25.5	7.23754
23	16.6477	17.5477	17.4678	0.088777778	11	8.87778	53	40.2773	41.3478	41.2693	0.07333022	26	7.33302
24	17.196	18.0692	18.0027	0.076156665	11.5	7.61567	54	40.8226	42.0059	41.9211	0.071663991	26.5	7.16640
25	17.6705	18.8029	18.7143	0.078240904	12	7.82409	55	23.6758	24.6086	24.5424	0.070969125	27	7.09691
26	16.3239	17.4666	17.3771	0.078323269	12.5	7.83233	56	18.2671	19.8113	19.7038	0.069615335	27.5	6.96153
27	17.849	18.7939	18.7128	0.085829188	13	8.58292	57	17.0774	18.0135	17.9445	0.073710074	28	7.37101
28	17.6883	19.0256	18.9257	0.074702759	13.5	7.47028	58	17.8485	19.6034	19.4819	0.069234714	28.5	6.92347
29	17.0783	18.0748	17.9911	0.083993979	14	8.39940	59	17.6705	18.9178	18.8291	0.071113605	29	7.11136
30	19.0642	20.3909	20.2913	0.075073491	14.5	7.50735	60	16.6458	17.6291	17.5591	0.071188854	29.5	7.11889

Table continues on the next page.

Location: **Outer Barsnesfjord**
Core ID: **MF2014-7**

Sample number	Tara [g]	before oven [g]	after oven [g]	Loss on ignition	depth (cm)	LOI (%)		Sample number	Tara [g]	before oven [g]	after oven [g]	Loss on ignition	depth (cm)	LOI (%)
61	22.5565	23.9531	23.8602	0.066518688	30	6.65187								
62	17.6754	18.8713	18.7933	0.065222845	30.5	6.52228								
63	18.7811	20.3021	20.204	0.064497041	31	6.44970								
64	16.7494	18.1299	18.0397	0.065338645	31.5	6.53386								
65	17.2895	18.3781	18.3096	0.062924858	32	6.29249								
66	17.5879	18.973	18.8875	0.061728395	32.5	6.17284								
67	18.0383	19.977	19.8602	0.060246557	33	6.02466								
68	16.6707	18.0243	17.9406	0.061835106	33.5	6.18351								
69	18.2095	19.2288	19.1622	0.065338958	34	6.53390								
70	19.2184	20.9185	20.8144	0.061231692	34.5	6.12317								
71	18.0859	19.7514	19.6503	0.060702492	35	6.07025								
72	18.5346	19.869	19.7898	0.059352518	35.5	5.93525								
73	17.5674	18.9478	18.8661	0.059185743	36	5.91857								
74	17.2362	18.4751	18.4036	0.057712487	36.5	5.77125								
75	18.3996	19.7157	19.639	0.058278246	37	5.82782								
76	18.4102	19.5538	19.4854	0.059811123	37.5	5.98111								
77	17.4369	18.9891	18.8994	0.057788945	38	5.77889								
78	16.9205	18.9124	18.795	0.058938702	38.5	5.89387								
79	18.0412	19.5077	19.4193	0.060279577	39	6.02796								
80	19.9366	19.6858	19.583		39.5									
81	17.6894	19.3232	19.2246	0.060350104	40	6.03501								
82	17.6713	19.0821	18.9941	0.062375957	40.5	6.23760								
83	16.3258	18.4167	18.2866	0.06222201	41	6.22220								
84	17.6892	19.9354	19.7953	0.062372006	41.5	6.23720								
85	16.7875	18.6946	18.5712	0.064705574	42	6.47056								
86	17.1965	19.0861	18.9628	0.065251905	42.5	6.52519								
87	19.0669	20.597	20.4992	0.063917391	43	6.39174								
88	16.2488	17.342	17.2698	0.06604464	43.5	6.60446								
89	39.8577	41.3708	41.2799	0.060075342	44	6.00753								
90	40.6305	42.7451	42.6301	0.054383808	44.5	5.43838								

Location: **Inner Nærøyfjord basin**
Core ID: **2015-1**

Sample number	Tara [g]	before oven [g]	after oven [g]	Loss on ignition	depth (cm)	LOI (%)		Sample number	Tara [g]	before oven [g]	after oven [g]	Loss on ignition	depth (cm)	LOI (%)
18	40.2406	40.5214	40.4963	0.0894	0.5	8.93875		35	39.3825	39.8164	39.7751	0.0952	15.5	9.51832
46	38.9855	39.2314	39.2083	0.0939	1	9.39406		35	39.3872	39.6732	39.6445	0.1003	16	10.03497
1	40.8395	41.0834	41.0602	0.0951	1.5	9.51210		12	41.2966	41.7119	41.676	0.0864	16.5	8.64435
2	40.5531	40.754	40.7381	0.0791	2	7.91439		33	40.7173	41.1602	41.1129	0.1068	17	10.67961
4	39.903	40.1871	40.1592	0.0982	2.5	9.82049		4	39.9053	40.3321	40.2842	0.1122	17.5	11.22306
45	41.0336	41.3415	41.3168	0.0802	3	8.02209		14	39.8647	40.1643	40.1283	0.1202	18	12.01602
10	40.8724	41.3665	41.3174	0.0994	3.5	9.93726		51	40.6731	40.9194	40.8873	0.1303	18.5	13.03289
3	38.6529	38.9031	38.8757	0.1095	4	10.95124		11	39.8815	40.228	40.1917	0.1048	19	10.47619
35	39.3884	39.7122	39.6871	0.0775	4.5	7.75170		42	40.306	40.5323	40.5027	0.1308	19.5	13.07998
69	41.2224	41.5731	41.5433	0.0850	5	8.49729		13	39.8269	40.1158	40.0821	0.1166	20	11.66494
100	40.9984	41.3493	41.322	0.0778	5.5	7.77999		15	40.73	40.9753	40.9448	0.1243	20.5	12.43375
40	41.0359	41.318	41.2961	0.0776	6	7.76320		38	39.771	40.1234	40.0859	0.1064	21	10.64132
13	39.8213	40.098	40.0765	0.0777	6.5	7.77015		3	38.6514	39.0354	38.9944	0.1068	21.5	10.67708
14	39.8664	40.1872	40.1543	0.1026	7	10.25561		19	40.3655	40.7017	40.6589	0.1273	22	12.73052
90	40.3617	40.7237	40.6953	0.0785	7.5	7.84530		18	40.2991	40.6335	40.5845	0.1465	22.5	14.65311
38	39.7703	40.1674	40.1361	0.0788	8	7.88215		9	38.4636	38.6842	38.6634	0.0943	23	9.42883
9	38.4523	38.8538	38.8186	0.0877	8.5	8.76712		18	40.2424	40.5296	40.4983	0.1090	23.5	10.89833
33	40.7161	41.1206	41.0848	0.0885	9	8.85043		74	40.6603	41.0132	40.9727	0.1148	24	11.47634
51	40.676	40.8695	40.8545	0.0775	9.5	7.75194		90	40.3636	40.6266	40.5948	0.1209	24.5	12.09125
74	40.6535	41.0452	41.0135	0.0809	10	8.09293		10	40.8743	41.1445	41.108	0.1351	25	13.50851
78	40.2992	40.6408	40.6083	0.0951	10.5	9.51405		49	39.342	39.7475	39.6892	0.1438	25.5	14.37731
17	40.3967	40.875	40.8359	0.0817	11	8.17479		100	41.0044	41.2734	41.2383	0.1305	26	13.04833
20	40.1369	40.5476	40.5108	0.0896	11.5	8.96031		20	40.1413	40.4179	40.3822	0.1291	26.5	12.90672
16	41.1639	41.4415	41.4181	0.0843	12	8.42939		40	41.0384	41.3062	41.2761	0.1124	27	11.23973
19	40.3547	40.8018	40.7605	0.0924	12.5	9.23731		24	40.6394	40.9567	40.924	0.1031	27.5	10.30570
12	41.2893	41.6676	41.6317	0.0949	13	9.48982		46	38.983	39.2856	39.2514	0.1130	28	11.30205
42	40.3048	40.7235	40.6884	0.0838	13.5	8.38309		69	41.2215	41.5899	41.5442	0.1240	28.5	12.40499
11	39.8763	40.4357	40.3943	0.0740	14	7.40079		17	40.4	40.7142	40.6729	0.1314	29	13.14449
15	40.7246	41.0912	41.0607	0.0832	14.5	8.31969		2	40.554	40.8633	40.8272	0.1167	29.5	11.67152
49	39.342	39.7652	39.7351	0.0711	15	7.11248		16	41.1665	41.4866	41.4474	0.1225	30	12.24617

Table continues on the next page.

Location: **Inner Nærøyfjord basin**
Core ID: **2015-1**

Sample number	Tara [g]	before oven [g]	after oven [g]	Loss on ignition	depth (cm)	LOI (%)		Sample number	Tara [g]	before oven [g]	after oven [g]	Loss on ignition	depth (cm)	LOI (%)
42	40.304	40.5737	40.5333	0.1498	30.5	14.97961								
3	38.6514	38.9479	38.908	0.1346	31	13.45700								
14	39.866	40.2366	40.1845	0.1406	31.5	14.05828								
11	39.8769	40.1905	40.1505	0.1276	32	12.75510								
4	39.9046	40.1582	40.1232	0.1380	32.5	13.80126								
19	40.3576	40.7499	40.7021	0.1218	33	12.18455								
1	40.8382	41.205	41.1572	0.1303	33.5	13.03162								
35	39.3943	39.7026	39.6631	0.1281	34	12.81220								
13	39.8234	40.1597	40.1151	0.1326	34.5	13.26197								
15	40.7295	41.1142	41.0618	0.1362	35	13.62100								
38	39.7692	40.0908	40.0519	0.1210	35.5	12.09577								
12	41.2887	41.6967	41.6517	0.1103	36	11.02941								
18	40.2927	40.933	40.886	0.0734	36.5	7.34031								
45	41.042	41.5413	41.5048	0.0731	37	7.31023								
51	40.6696	40.9785	40.9424	0.1169	37.5	11.68663								
17	40.399	40.819	40.7666	0.1248	38	12.47619								
40	41.0353	41.4177	41.3703	0.1240	38.5	12.39540								
24	40.6353	40.9738	40.9182	0.1643	39	16.42541								
9	38.452	38.7373	38.6909	0.1626	39.5	16.26358								
10	40.8717	41.169	41.1256	0.1460	40	14.59805								

Location: **Inner Nærøyfjord basin** Core ID: **2015-4**														
Sample number	Tara [g]	before oven [g]	after oven [g]	Loss on ignition	depth (cm)	LOI (%)		Sample number	Tara [g]	before oven [g]	after oven [g]	Loss on ignition	depth (cm)	LOI (%)
49	39.3399	39.6603	39.6317	0.0893	0.5	8.92634		10	40.8733	41.425	41.3868	0.0692	15.5	6.92405
18	40.2352	40.5067	40.4818	0.0917	1	9.17127		90	40.6351	40.8845	40.8467	0.1516	16	15.15638
100	40.9959	41.4451	41.4145	0.0681	1.5	6.81211		49	39.3454	39.7247	39.6854	0.1036	16.5	10.36119
69	41.2186	41.837	41.8137	0.0377	2	3.76779		40	41.0381	41.453	41.4169	0.0870	17	8.70089
90	40.3652	40.6866	40.6609	0.0800	2.5	7.99627		100	41.0044	41.5117	41.4693	0.0836	17.5	8.35797
16	41.1635	41.4413	41.4147	0.0958	3	9.57523		2	40.5546	41.0839	41.0396	0.0837	18	8.36954
14	40.6541	41.0009	40.9684	0.0937	3.5	9.37140		14	40.6565	41.3015	41.2513	0.0778	18.5	7.78295
2	40.5514	41.0437	41.0187	0.0508	4	5.07820		17	40.398	40.9875	40.9535	0.0577	19	5.76760
20	40.1365	40.9842	40.955	0.0344	4.5	3.44461		24	40.643	41.1788	41.1312	0.0888	19.5	8.88391
46	38.9775	39.6737	39.6523	0.0307	5	3.07383		20	40.1402	40.4979	40.4654	0.0909	20	9.08583
45	41.0323	41.3381	41.3145	0.0772	5.5	7.71746		18	40.2921	40.7779	40.7466	0.0644	20.5	6.44298
11	39.8762	40.1003	40.0831	0.0768	6	7.67515		38	39.7642	40.3309	40.2891	0.0738	21	7.37604
1	40.8403	41.1206	41.0944	0.0935	6.5	9.34713		3	38.649	39.3103	39.2634	0.0709	21.5	7.09209
3	38.6512	38.9047	38.8862	0.0730	7	7.29783		14	39.8753	40.6882	40.6434	0.0551	22	5.51113
4	39.9011	40.1631	40.1391	0.0916	7.5	9.16031		4	39.9095	40.962	40.9282	0.0321	22.5	3.21140
51	40.6704	41.0773	41.0525	0.0609	8	6.09486		1	40.8393	41.7283	41.7142	0.0159	23	
13	39.8198	40.1039	40.0763	0.0971	8.5	9.71489		51	40.6723	41.3209	41.2898	0.0479	23.5	4.79494
15	40.7244	41.0367	41.0098	0.0861	9	8.61351		11	39.8746	40.3467	40.3068	0.0845	24	8.45160
42	40.3047	40.6742	40.6462	0.0758	9.5	7.57781		13	39.829	40.2913	40.2528	0.0833	24.5	8.32793
19	40.3554	40.7059	40.6796	0.0750	10	7.50357		45	41.0377	41.5228	41.4959	0.0555	25	5.54525
12	41.289	41.5503	41.528	0.0853	10.5	8.53425		15	40.7251	41.4608	41.4228	0.0517	25.5	5.16515
35	39.3841	39.6916	39.664	0.0898	11	8.97561		42	40.3036	40.9058	40.874	0.0528	26	5.28064
14	39.865	40.1289	40.1061	0.0864	11.5	8.63964		12	41.2886	41.7444	41.7099	0.0757	26.5	7.56911
18	40.2933	40.6909	40.6692	0.0546	12	5.45775		19	40.3539	40.7388	40.6974	0.1076	27	10.75604
38	39.7639	40.3532	40.3177	0.0602	12.5	6.02410								
46	38.99	39.2863	39.2494	0.1245	13	12.45359								
16	41.1649	41.5203	41.4778	0.1196	13.5	11.95836								
18	40.2406	40.6157	40.5814	0.0914	14	9.14423								
69	41.2211	41.5583	41.5219	0.1079	14.5	10.79478								
9	38.4543	38.9375	38.905	0.0673	15	6.72599								

Location: **Inner Aurlandsfjord**
Core ID: **MF2016-4**

Sample number	Tara [g]	before oven [g]	after oven [g]	Loss on ignition	depth (cm)	LOI (%)
1	40.7755	46.6002	46.2301	0.0635	0.5	6.35398
3	38.5885	43.51	43.087	0.0859	1	8.59494
4	39.8375	45.1565	44.6943	0.0869	1.5	8.68960
5	40.6118	44.4983	44.3072	0.0492	2	4.91702
9	38.3922	42.3496	42.1447	0.0518	2.5	5.17764
10	40.807	45.2309	44.9897	0.0545	3	5.45220
11	39.8121	43.7331	43.5717	0.0412	3.5	4.11630
12	41.2236	45.2183	45.0103	0.0521	4	5.20690
13	39.7584	44.8145	44.5151	0.0592	4.5	5.92156
14	39.8034	43.3741	43.1939	0.0505	5	5.04663
15	40.6606	44.7734	44.5683	0.0499	5.5	4.98687
16	41.0995	45.4212	45.2159	0.0475	6	4.75045
17	40.3327	42.5308	42.4307	0.0455	6.5	4.55393
18	40.2291	43.0161	42.878	0.0496	7	4.95515
19	40.2919	45.8442	45.5222	0.0580	7.5	5.79940
24	40.5734	45.5873	45.0057	0.1160	8	11.59975

Location: **Inner Aurlandsfjord**
Core ID: **MF2016-9**

Sample number	Tara [g]	before oven [g]	after oven [g]	Loss on ignition	depth (cm)	LOI (%)
71	18.7612	21.6628	21.4877	0.0603	0.5	6.03460
72	16.7361	19.6475	19.4818	0.0569	1	5.69142
73	16.6334	19.8468	19.6276	0.0682	1.5	6.82144
74	23.9534	27.5492	27.3284	0.0614	2	6.14050
75	17.6518	21.1237	20.9767	0.0423	2.5	4.23399
76	17.792	21.1415	20.9144	0.0678	3	6.78012
77	23.6515	26.2408	26.0853	0.0601	3.5	6.00548
78	17.1765	21.2727	21.0307	0.0591	4	5.90791
79	16.3103	19.4701	19.3022	0.0531	4.5	5.31363
80	22.537	26.1862	26.0149	0.0469	5	4.69418
81	16.2291	20.5701	20.3398	0.0531	5.5	5.30523
82	17.832	23.4191	22.9046	0.0921	6	9.20871
83	17.6604	20.7397	20.5244	0.0699	6.5	6.99185
84	23.234	27.3821	27.1916	0.0459	7	4.59246
85	23.9502	27.7015	27.5408	0.0428	7.5	4.28385
1	40.7674	45.0076	44.8149	0.0454	8	4.54460
3	38.5796	42.9222	42.7342	0.0433	8.5	4.32920
4	39.8274	43.9925	43.7983	0.0466	9	4.66255
5	40.6029	45.4234	45.2024	0.0458	9.5	4.58459
9	38.3826	42.7386	42.5126	0.0519	10	5.18825
10	40.7982	48.6979	48.057	0.0811	10.5	8.11297
11	39.8028	44.4312	44.1881	0.0525	11	5.25236
12	41.2156	44.8211	44.641	0.0500	11.5	4.99515
13	39.7509	44.1512	43.9402	0.0480	12	4.79513
14	39.7947	43.1654	42.991	0.0517	12.5	5.17400
15	40.6498	44.0695	43.8825	0.0547	13	5.46832
16	41.0904	44.511	44.3223	0.0552	13.5	5.51658
17	40.3273	47.8823	47.1658	0.0948	14	9.48379

Location: **Inner Aurlandsfjord**
Core ID: **2016-12**

Sample number	Tara [g]	before oven [g]	after oven [g]	Loss on ignition	depth (cm)	LOI (%)
71	23.9479	26.0393	25.9369	0.0490	0.5	4.89624
72	23.952	26.7983	26.6512	0.0517	1	5.16811
73	16.3088	19.2362	19.0801	0.0533	1.5	5.33238
74	17.8297	20.8019	20.6474	0.0520	2	5.19817
75	23.2304	26.2019	26.0397	0.0546	2.5	5.45852
76	17.7903	20.6496	20.4993	0.0526	3	5.25653
77	16.7328	20.0673	19.8979	0.0508	3.5	5.08022
78	22.5345	25.927	25.7621	0.0486	4	4.86072
79	17.6522	21.2113	21.0394	0.0483	4.5	4.82987
80	18.76	22.5113	22.3466	0.0439	5	4.39048
81	23.6498	26.9643	26.8143	0.0453	5.5	4.52557
82	17.1754	21.2247	21.0332	0.0473	6	4.72921
83	16.227	19.7342	19.5676	0.0475	6.5	4.75023
84	17.657	21.3726	21.1873	0.0499	7	4.98708
85	16.6315	20.3619	20.1869	0.0469	7.5	4.69119
18	40.2157	43.6463	43.4394	0.0603	8	6.03101
19	40.2802	44.582	44.1455	0.1015	8.5	10.14692
24	40.5428	44.6672	44.3036	0.0882	9	8.81583
38	39.6947	43.4238	43.1064	0.0851	9.5	8.51144
45	40.9612	45.123	44.5145	0.1462	10	14.62108
49	39.2758	43.3123	42.7441	0.1408	10.5	14.07655
69	41.1487	45.2895	45.0361	0.0612	11	6.11959
94	40.5821	44.1369	43.9188	0.0614	11.5	6.13537
98	40.167	44.8226	44.1619	0.1419	12	14.19151
100	40.9284	47.015	46.19	0.1355	12.5	13.55437

Sample number	Tara [g]	before oven [g]	after oven [g]	Loss on ignition	depth (cm)	LOI (%)

Location: **Fjærlandsfjord**
Core ID: **HB17-211-01MC-A**

Sample number	Tara [g]	before oven [g]	after oven [g]	Loss on ignition	depth (cm)	LOI (%)		Sample number	Tara [g]	before oven [g]	after oven [g]	Loss on ignition	depth (cm)	LOI (%)
205	37.5316	39.4253	39.3651	0.0318	0	3.17896								
4	39.9005	41.9938	41.9373	0.0270	1	2.69909								
219	35.2501	37.3435	37.2878	0.0266	2	2.66074								
203	33.9539	35.9705	35.9207	0.0247	3	2.46950								
217	36.7308	38.7989	38.7465	0.0253	4	2.53373								
12	41.2826	43.618	43.5645	0.0229	5	2.29083								
207	35.494	37.6594	37.6105	0.0226	6	2.25824								
215	36.1305	38.2675	38.2203	0.0221	7	2.20870								
210	37.0933	39.1517	39.0969	0.0266	8	2.66226								
213	38.9997	41.1635	41.1134	0.0232	9	2.31537								
218	36.0048	38.0557	38.0097	0.0224	10	2.24292								
212	36.3252	38.3775	38.3242	0.0260	11	2.59709								
205	37.5353	39.558	39.51	0.0237	12	2.37307								
209	36.7056	38.887	38.8369	0.0230	13	2.29669								
208	35.1998	37.6833	37.649	0.0138	14	1.38112								
2	40.5486	42.8472	42.8012	0.0200	15	2.00122								
220	36.6817	38.5781	38.5244	0.0283	16	2.83168								
220	36.6842	38.6895	38.6463	0.0215	17	2.15429								
211	34.4662	36.4595	36.4145	0.0226	18	2.25756								
214	35.868	37.8329	37.7867	0.0235	19	2.35126								
200	37.613	39.6502	39.5984	0.0254	20	2.54271								
216	36.2303	38.1684	38.1227	0.0236	21	2.35798								
33	40.713	42.7284	42.6855	0.0213	22	2.12861								
201	36.2682	38.3006	38.2552	0.0223	23	2.23381								
217	36.7263	38.7297	38.6818	0.0239	24	2.39094								
210	37.0923	39.0614	39.0124	0.0249	25	2.48845								
219	35.2442	37.3099	37.259	0.0246	26	2.46406								
213	38.998	41.1663	41.1207	0.0210	27	2.10303								
203	33.9495	36.1238	36.0798	0.0202	28	2.02364								

Location: **Fjærlandsfjord**
Core ID: **HB17-211-02MC-A**

Sample number	Tara [g]	before oven [g]	after oven [g]	Loss on ignition	depth (cm)	LOI (%)		Sample number	Tara [g]	before oven [g]	after oven [g]	Loss on ignition	depth (cm)	LOI (%)
208	35.1958	36.6235	36.5579	0.0459	0	4.59480		207	35.4918	37.1854	37.1249	0.0357	30	3.57227
218	36.002	37.5675	37.5014	0.0422	1	4.22229		206	33.6941	35.612	35.5447	0.0351	31	3.50905
207	35.4903	37.077	37.0079	0.0435	2	4.35495		215	36.1309	37.895	37.8345	0.0343	32	3.42951
201	36.2674	37.9826	37.9066	0.0443	3	4.43097		219	35.2482	37.0007	36.9405	0.0344	33	3.43509
215	36.13	37.7204	37.6557	0.0407	4	4.06816		208	35.1981	36.9462	36.8912	0.0315	34	3.14627
214	35.8653	37.4761	37.4118	0.0399	5	3.99181		2	40.5497	42.2985	42.2455	0.0303	35	3.03065
206	33.6928	35.3091	35.2455	0.0393	6	3.93491		4	39.9014	41.6545	41.6023	0.0298	36	2.97758
211	34.4643	36.1473	36.0821	0.0387	7	3.87403		33	40.7128	42.6114	42.5578	0.0282	37	2.82313
209	36.6998	38.4531	38.3865	0.0380	8	3.79855		51	40.6686	42.3379	42.2878	0.0300	38	3.00126
216	36.2282	37.9203	37.8571	0.0374	9	3.73500		12	41.285	43.0279	42.9776	0.0289	39	2.88599
200	37.6105	39.2792	39.2165	0.0376	10	3.75742		203	33.9543	35.7577	35.7161	0.0231	40	2.30675
12	41.2838	42.8866	42.8207	0.0411	11	4.11155		216	36.2295	37.9429	37.9028	0.0234	41	2.34038
2	40.5462	42.1645	42.1012	0.0391	12	3.91151		214	35.8656	37.5401	37.4987	0.0247	42	2.47238
33	40.7117	42.4909	42.4231	0.0381	13	3.81070		207	35.4911	37.2439	37.2057	0.0218	43	2.17937
51	40.6655	42.3698	42.3049	0.0381	14	3.80802		208	35.1968	37.2141	37.1671	0.0233	44	2.32985
4	39.8978	41.5614	41.4997	0.0371	15	3.70882		200	37.6094	39.5665	39.5195	0.0240	45	2.40151
217	36.7295	38.3354	38.275	0.0376	16	3.76113								
203	33.9532	35.6685	35.6056	0.0367	17	3.66700								
212	36.3257	37.9725	37.9114	0.0371	18	3.71023								
209	36.7026	38.345	38.2826	0.0380	19	3.79932								
211	34.4657	36.0868	36.028	0.0363	20	3.62717								
205	37.5337	39.1866	39.1233	0.0383	21	3.82963								
214	35.8667	37.6369	37.5742	0.0354	22	3.54197								
213	38.9978	40.7781	40.7181	0.0337	23	3.37022								
200	37.6103	39.5151	39.4464	0.0361	24	3.60668								
210	37.0934	38.8408	38.779	0.0354	25	3.53668								
220	36.682	38.4032	38.3442	0.0343	26	3.42784								
216	36.2303	38.0207	37.9556	0.0364	27	3.63606								
201	36.2667	38.1235	38.0598	0.0343	28	3.43063								
218	36.0034	37.6613	37.6028	0.0353	29	3.52856								

Location: **Inner Ikjefjord** Core ID: **MF2017-1**						
Sample number	Tara [g]	before oven [g]	after oven [g]	Loss on ignition	depth (cm)	LOI (%)
					0	8.5000
					1	14.7000
					2	10.9000
					3	15.2000
					4	15.5000
					5	13.1000
					6	10.3000
					7	9.8000
					8	8.4000
					9	9.2000
					10	8.2000
					11	7.6000
					12	4.5000
					13	
					14	9.0000
					15	15.6000
					16	16.2000
					17	15.5000
					18	15.6000
					19	15.9000
					20	16.1000
					21	11.2000
					22	15.0000
					23	16.5000
					24	16.1000
					25	14.5000
					26	14.8000
					27	14.9000
					28	14.8000

Location: **Inner Ikjefjord** Core ID: **MF2017-2**						
Sample number	Tara [g]	before oven [g]	after oven [g]	Loss on ignition	depth (cm)	LOI (%)
	41.778	44.0237	43.8233	0.0892	0	8.92372
	40.3302	41.507	41.3346	0.1465	1	14.64990
	46.8782	48.1609	48.0268	0.1045	2	10.45451
	45.4986	46.7214	46.536	0.1516	3	15.16192
	43.0918	44.2207	44.047	0.1539	4	15.38666
	44.2848	45.556	45.3878	0.1323	5	13.23159
	40.6102	42.6016	42.397	0.1027	6	10.27418
	45.9639	48.3537	48.124	0.0961	7	9.61168
	45.853	48.626	48.3895	0.0853	8	8.52867
	39.703	42.3566	42.1142	0.0913	9	9.13476
	41.0985	43.7612	43.5334	0.0856	10	8.55523
	42.3696	45.341	45.1163	0.0756	11	7.56209
	44.4697	48.741	48.5708	0.0398	12	3.98474
	40.171	47.5428	47.4722	0.0096	13	
	39.8372	42.2683	42.052	0.0890	14	8.89721
	40.9674	42.7087	42.4385	0.1552	15	15.51714
	40.6814	42.4086	42.1252	0.1641	16	16.40806
	44.0125	46.3082	45.9507	0.1557	17	15.57259
	42.3313	43.76	43.5357	0.1570	18	15.69959
	45.9509	48.3264	47.9472	0.1596	19	15.96296
	38.392	40.1614	39.8762	0.1612	20	16.11846
	39.7568	41.4097	41.2263	0.1110	21	11.09565
	45.7708	47.1797	46.9685	0.1499	22	14.99042
	44.2477	45.8403	45.5759	0.1660	23	16.60178
	40.5709	42.3699	42.0825	0.1598	24	15.97554
	40.2885	42.5663	42.2421	0.1423	25	14.23303
	43.1641	44.5703	44.3644	0.1464	26	14.64230
	46.0792	48.1452	47.8406	0.1474	27	14.74347
	40.8043	41.8863	41.7285	0.1458	28	14.58410

Location: **Inner Barsnesfjord**
Core ID: **MF2019-1**

Sample number	Tara [g]	before oven [g]	after oven [g]	Loss on ignition	depth (cm)	LOI (%)		Sample number	Tara [g]	before oven [g]	after oven [g]	Loss on ignition	depth (cm)	LOI (%)
35	39.325	41.198	41.029	0.0902	1	9.02296		211	34.355	35.255	35.174	0.0900	31	9.00000
15	40.654	42.552	42.125	0.2250	2			12	41.234	43.187	43.035	0.0778	32	7.78290
119	46.109	49.089	48.878	0.0708	3	7.08054		103	45.798	47.571	47.463	0.0609	33	6.09137
16	41.101	43.278	43.07	0.0955	4	9.55443		104	45.988	47.778	47.644	0.0749	34	7.48603
51	40.608	43.022	42.827	0.0808	5	8.07788		18	40.188	41.924	41.807	0.0674	35	6.73963
220	36.671	38.615	38.422	0.0993	6	9.92798		38	39.706	41.589	41.451	0.0733	36	7.32873
19	40.294	42.123	41.939	0.1006	7	10.06014		9	38.396	40.899	40.741	0.0631	37	6.31243
20	40.073	41.919	41.715	0.1105	8	11.05092		106	44.499	46.299	46.126	0.0961	38	9.61111
11	39.817	41.981	41.787	0.0896	9	8.96488		69	41.162	43.088	42.961	0.0659	39	6.59398
200	37.593	38.813	38.664	0.1221	10	12.21311		209	36.254	38.593	38.402	0.0817	40	8.16588
108	41.804	42.759	42.65	0.1141	11	11.41361		112	42.37	43.879	43.72	0.1054	41	10.53678
219	35.248	36.265	36.164	0.0993	12	9.93117		46	38.923	40.902	40.765	0.0692	42	6.92269
222	37.491	38.371	38.28	0.1034	13	10.34091		110	43.106	45.126	44.987	0.0688	43	6.88119
208	36.723	37.808	37.694	0.1051	14	10.50691		109	45.888	48.013	47.806	0.0974	44	9.74118
14	40.585	42.762	42.566	0.0900	15	9.00322		1118	33.93	35.639	35.506	0.0778	45	7.78233
42	40.241	41.373	41.239	0.1184	16	11.83746		2	40.503	42.586	42.52	0.0317	46	3.16851
24	40.576	43.081	42.877	0.0814	17	8.14371		113	43.197	47.171	46.882	0.0727	47	7.27227
214	35.842	37.636	37.478	0.0881	18	8.80713								
116	46.896	48.793	48.625	0.0886	19	8.85609								
33	40.668	42.788	42.606	0.0858	20	8.58491								
3	38.594	40.158	40.028	0.0831	21	8.31202								
115	45.522	47.754	47.596	0.0708	22	7.07885								
118x2	42.391	44.54	44.338	0.0940	23	9.39972								
4	39.839	41.45	41.303	0.0912	24	9.12477								
17	40.349	42.718	42.52	0.0836	25	8.35796								
117	44.322	45.762	45.642	0.0833	26	8.33333								
49	39.282	41.399	41.234	0.0779	27	7.79405								
107	45.988	47.78	47.648	0.0737	28	7.36607								
218	35.993	37.907	37.76	0.0768	29	7.68025								
1	35.455	38.163	37.975	0.0694	30	6.94239								

Location: **Inner Barsnesfjord**
Core ID: **MF2019-3**

Sample number	Tara [g]	before oven [g]	after oven [g]	Loss on ignition	depth (cm)	LOI (%)
1	35.452	37.634	37.42	0.0981	1	9.80752
2	40.49	44.342	44.007	0.0870	2	8.69678
3	38.592	41.707	41.412	0.0947	3	9.47030
4	39.84	42.307	42.073	0.0949	4	9.48520
9	38.396	42.185	41.864	0.0847	5	8.47189
11	39.818	42.484	42.254	0.0863	6	8.62716
12	41.226	44.721	44.432	0.0827	7	8.26896
13	39.758	42.539	42.313	0.0813	8	8.12657
14	40.585	43.664	43.412	0.0818	9	8.18448
15	40.658	43.194	42.953	0.0950	10	9.50315
16	41.103	44.768	44.475	0.0799	11	7.99454
17	40.342	43.912	43.605	0.0860	12	8.59944
18	40.175	43.935	43.639	0.0787	13	7.87234
19	40.292	43.95	43.644	0.0837	14	8.36523
20	40.082	43.641	43.343	0.0837	15	8.37314
24	40.577	43.794	43.555	0.0743	16	7.42928
33	40.655	44.339	44.094	0.0665	17	6.65038
35	39.328	43.32	43.029	0.0729	18	7.28958
38	39.708	43.977	43.685	0.0684	19	6.84001
42	40.242	44.827	44.542	0.0622	20	6.21592
46	38.914	42.911	42.664	0.0618	21	6.17963
49	39.282	41.554	41.416	0.0607	22	6.07394
51	40.622	44.467	44.226	0.0627	23	6.26788
69	41.151	44.664	44.465	0.0566	24	5.66467
100	40.917	45.076	44.829	0.0594	25	5.93893
103	45.805	49.36	49.165	0.0549	26	5.48523
104	45.982	48.226	48.082	0.0642	27	6.41711
106	44.49	48.734	48.493	0.0568	28	5.67861
107	45.975	50.539	50.257	0.0618	29	6.17879
108	41.794	45.698	45.432	0.0681	30	6.81352

Sample number	Tara [g]	before oven [g]	after oven [g]	Loss on ignition	depth (cm)	LOI (%)
110	43.123	46.904	46.626	0.0735	31	7.35255
109	45.87	49.791	49.478	0.0798	32	7.98266
111	40.696	43.561	43.349	0.0740	33	7.39965
112	42.36	46.553	46.27	0.0675	34	6.74934
113	43.183	46.497	46.302	0.0588	35	5.88413
115	45.511	48.465	48.268	0.0667	36	6.66892
116	46.894	49.905	49.655	0.0830	37	8.30289
117	44.312	46.645	46.446	0.0853	38	8.52979
118 x2	42.397	45.073	44.841	0.0867	39	8.66966
119	46.107	48.576	48.352	0.0907	40	9.07250
200	37.576	41.488	41.146	0.0874	41	8.74233
208	36.694	40.352	40.02	0.0908	42	9.07600
209	36.246	38.276	38.095	0.0892	43	8.91626
211	34.436	35.698	35.58	0.0935	44	9.35024
214	35.835	37.854	37.661	0.0956	45	9.55919
218	35.97	38.051	37.871	0.0865	46	8.64969
219	35.223	37.605	37.416	0.0793	47	7.93451
220	36.658	38.825	38.654	0.0789	48	7.89109
222	37.493	40.819	40.636	0.0550	49	5.50210
1118	33.919	38.27	38.065	0.0471	50	4.71156
18	18.76	23.847	23.611	0.0464	51	4.63928
93	23.954	28.47	28.175	0.0653	52	6.53233
94	23.949	27.231	27.026	0.0625	53	6.24619

Location: **Outer Barsnesfjord**
Core ID: **MF2019-6**

Sample number	Tara [g]	before oven [g]	after oven [g]	Loss on ignition	depth (cm)	LOI (%)		Sample number	Tara [g]	before oven [g]	after oven [g]	Loss on ignition	depth (cm)	LOI (%)
1	35.455	37.058	36.88	0.1110	1	11.10418		109	45.868	48.222	48.132	0.0382	31	3.82328
2	40.489	42.461	42.292	0.0857	2	8.56998		110	43.1	44.512	44.349	0.1154	32	11.54391
3	38.591	40.559	40.41	0.0757	3	7.57114		111	40.7	43.856	43.675	0.0574	33	5.73511
4	39.84	41.029	40.909	0.1009	4	10.09251		112	42.356	45.883	45.674	0.0593	34	5.92572
9	38.393	39.459	39.356	0.0966	5	9.66229		113	43.184	47.57	47.354	0.0492	35	4.92476
11	39.813	41.274	41.139	0.0924	6	9.24025		115	45.51	49.875	49.696	0.0410	36	4.10080
12	41.22	44.031	43.789	0.0861	7	8.60904		116	46.892	51.863	51.674	0.0380	37	3.80205
13	39.756	41.027	40.917	0.0865	8	8.65460		117	44.308	50.124	49.961	0.0280	38	2.80261
14	40.583	42.211	42.072	0.0854	9	8.53808		118 x2	42.386	45.746	45.556	0.0565	39	5.65476
15	40.655	42.368	42.224	0.0841	10	8.40630		208	36.707	38.888	38.766	0.0559	40	5.59376
16	41.101	42.648	42.538	0.0711	11	7.11054		209	36.246	39.26	39.087	0.0574	41	5.73988
17	40.338	42.79	42.603	0.0763	12	7.62643		211	34.441	38.051	37.836	0.0596	42	5.95568
18	40.175	42.514	42.338	0.0752	13	7.52458		214	35.85	40.361	40.111	0.0554	43	5.54201
19	40.303	42.189	42.03	0.0843	14	8.43054								
20	40.088	41.684	41.534	0.0940	15	9.39850								
24	40.586	42.198	42.057	0.0875	16	8.74690								
33	40.664	42.336	42.184	0.0909	17	9.09091								
35	39.335	40.639	40.525	0.0874	18	8.74233								
38	39.715	41.12	41.043	0.0548	19	5.48043								
42	40.252	41.965	41.812	0.0893	20	8.93170								
46	38.923	41.244	41.038	0.0888	21	8.87548								
49	39.29	41.061	40.917	0.0813	22	8.13100								
51	40.619	42.107	42.059	0.0323	23	3.22581								
69	41.159	42.647	42.518	0.0867	24	8.66935								
100	40.923	42.705	42.557	0.0831	25	8.30527								
103	45.799	48.103	47.93	0.0751	26	7.50868								
104	45.987	47.749	47.602	0.0834	27	8.34279								
106	44.449	46.417	46.26	0.0798	28	7.97764								
107	45.983	48.14	47.982	0.0732	29	7.32499								
108	41.803	44.014	43.86	0.0697	30	6.96517								

Location: **Outer Barsnesfjord**
Core ID: **MF2019-8**

Sample number	Tara [g]	before oven [g]	after oven [g]	Loss on ignition	depth (cm)	LOI (%)		Sample number	Tara [g]	before oven [g]	after oven [g]	Loss on ignition	depth (cm)	LOI (%)
1	35.467	37.633	37.417	0.0997	0.5	9.97230		104	45.982	48.065	47.894	0.0821	30.5	8.20931
3	38.59	43.664	43.51	0.0304	1.5	3.03508		106	44.488	46.518	46.352	0.0818	31.5	8.17734
4	39.838	43.869	43.718	0.0375	2.5	3.74597		107	45.977	48.128	47.961	0.0776	32.5	7.76383
9	38.395	44.778	44.568	0.0329	3.5	3.28999		108	41.795	44.681	44.464	0.0752	33.5	7.51906
11	39.813	41.778	41.609	0.0860	4.5	8.60051		109	45.878	48.438	48.257	0.0707	34.5	7.07031
12	41.221	44.596	44.365	0.0684	5.5	6.84444		110	43.113	45.498	45.328	0.0713	35.5	7.12788
13	39.757	46.357	46.147	0.0318	6.5	3.18182		111	40.704	42.88	42.722	0.0726	36.5	7.26103
14	40.585	43.507	43.31	0.0674	7.5	6.74196		112	43.36	45.746	45.536	0.0880	37.5	8.80134
15	40.659	42.792	42.594	0.0928	8.5	9.28270		113	43.183	47.014	46.769	0.0640	38.5	6.39520
16	41.102	43.133	42.918	0.1059	9.5	10.58592		115	45.509	47.838	47.684	0.0661	39.5	6.61228
17	40.336	42.931	42.668	0.1013	10.5	10.13487		116	46.894	50.62	50.387	0.0625	40.5	6.25335
18	40.175	42.569	42.353	0.0902	11.5	9.02256								
19	40.292	42.05	41.875	0.0995	12.5	9.95449								
24	40.575	43.405	43.162	0.0859	13.5	8.58657								
35	39.323	41.29	41.096	0.0986	14.5	9.86274								
38	39.703	41.724	41.535	0.0935	15.5	9.35181								
42	40.239	42.148	41.969	0.0938	16.5	9.37664								
46	38.913	41.369	41.163	0.0839	17.5	8.38762								
49	39.279	41.574	41.402	0.0749	18.5	7.49455								
51	40.609	44.584	44.39	0.0488	19.5	4.88050								
69	41.152	44.148	44.053	0.0317	20.5	3.17089								
71	17.651	20.388	20.234	0.0563	21.5	5.62660								
72	17.669	19.938	19.749	0.0833	22.5	8.32966								
74	16.227	17.997	17.84	0.0887	23.5	8.87006								
75	16.732	19.343	19.129	0.0820	24.5	8.19609								
76	17.063	19.029	18.87	0.0809	25.5	8.08749								
91	22.535	24.364	24.199	0.0902	26.5	9.02132								
92	23.23	25.482	25.292	0.0844	27.5	8.43694								
100	40.908	43.173	42.995	0.0786	28.5	7.85872								
103	45.782	48.19	47.998	0.0797	29.5	7.97342								

Location: **Arnafjord basin**
Core ID: **MF2020-GC06**

Sample number	Tara [g]	before oven [g]	after oven [g]	Loss on ignition	depth (cm)	LOI (%)
A1	23.6861	25.4603	25.3886	0.0404	1	4.04126
A3	16.3345	18.148	18.0733	0.0412	3	4.11911
A4	16.3348	18.4791	18.3968	0.0384	5	3.83808
A5	17.6964	19.5147	19.4406	0.0408	7	4.07524
A7	17.6797	19.8997	19.8018	0.0441	9	4.40991
A9	16.253	18.6648	18.5634	0.0420	11	4.20433
A10	22.5693	25.1847	25.0861	0.0377	13	3.76998
A12	23.2681	25.1952	25.1247	0.0366	15	3.65835
A13	19.0757	21.4137	21.3303	0.0357	17	3.56715
A18	15.7018	17.8865	17.8122	0.0340	21	3.40092
A21	23.9836	26.9122	26.8054	0.0365	25	3.64679
A22	16.6567	19.3846	19.3004	0.0309	29	3.08662

Location: **Indrefjord**
Core ID: **MF2020-MC04**

Sample number	Tara [g]	before oven [g]	after oven [g]	Loss on ignition	depth (cm)	LOI (%)
A23	17.2043	18.3318	18.2873	0.0395	1	3.94678
A25	23.9911	25.5202	25.4636	0.0370	3	3.70152
A24	16.7574	18.1297	18.0765	0.0388	5	3.87670
A27	18.7916	20.6261	20.5412	0.0463	7	4.62796
A30	16.2115	17.5491	17.484	0.0487	15	4.86693
13	17.6835	18.9468	18.8856	0.0484	21	4.84445

Appendix II: LOI graphs

The graphs are sorted by the sediment core sampling location (northern-southern).

Fjærlandsfjord

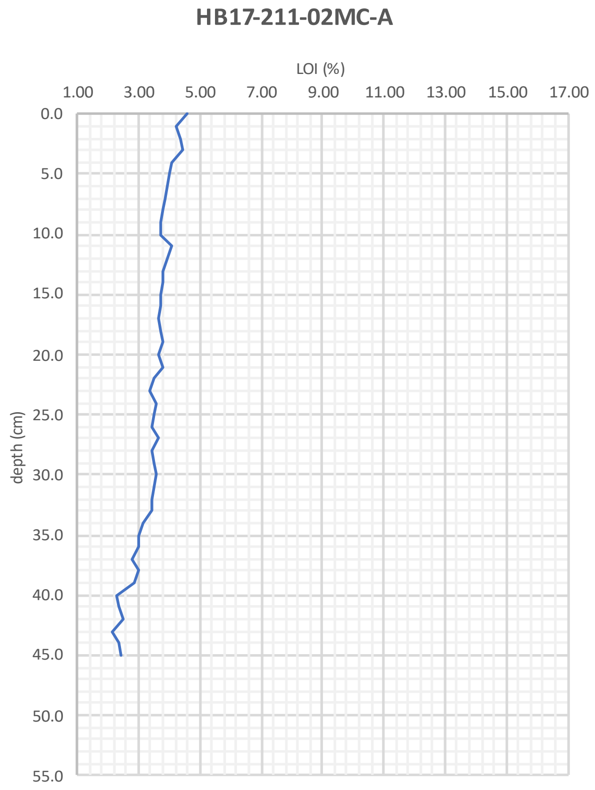

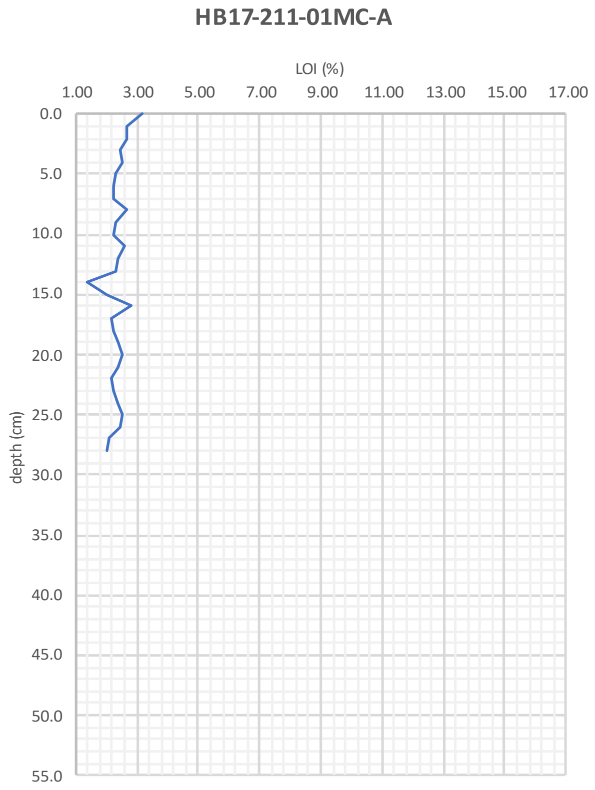

Sogndalsfjord

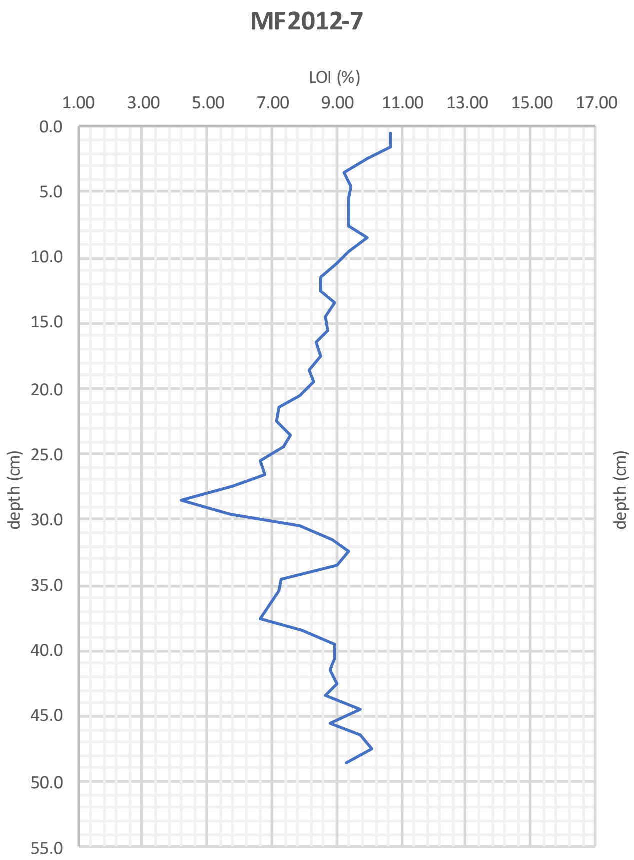

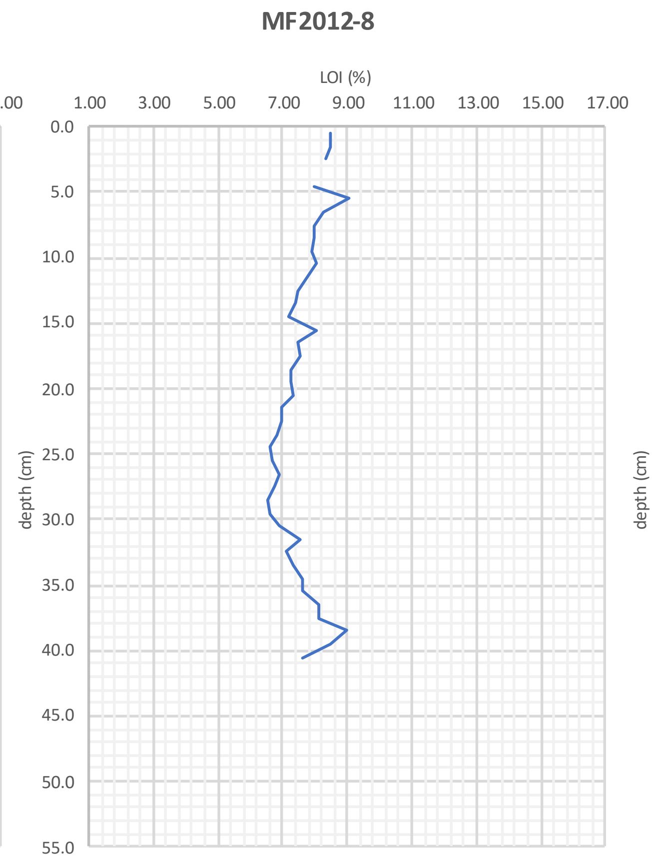

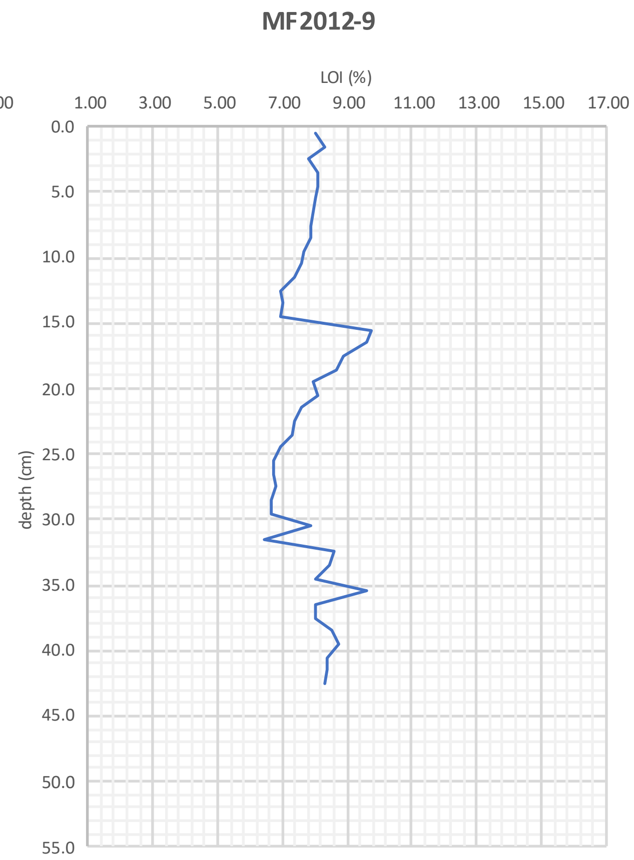

Outer Barsnesfjord

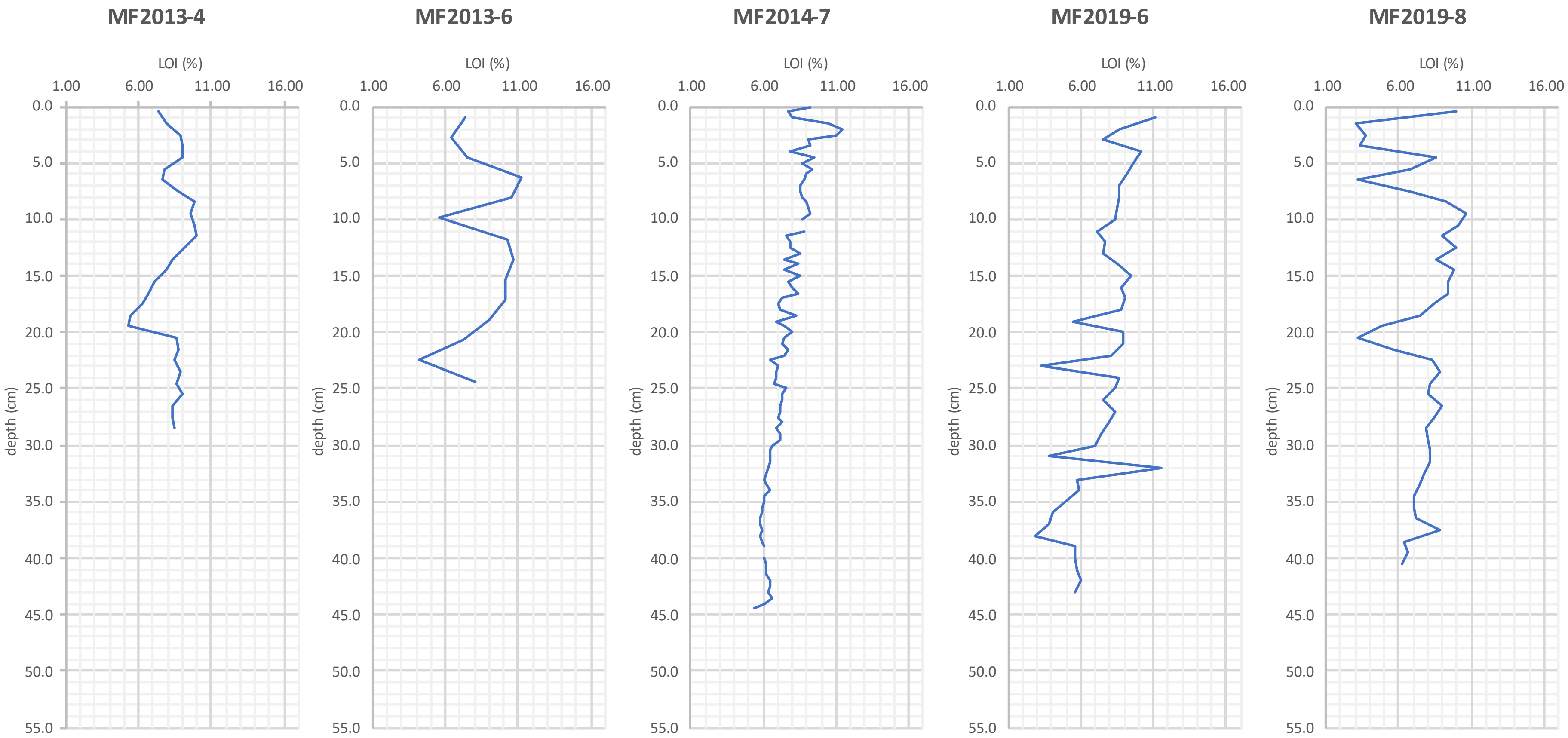

Inner Barsnesfjord

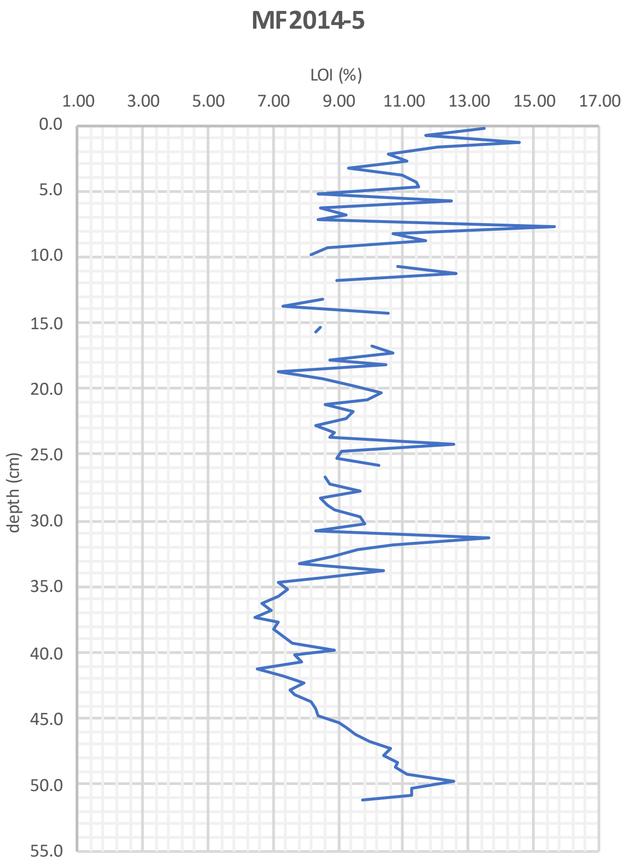

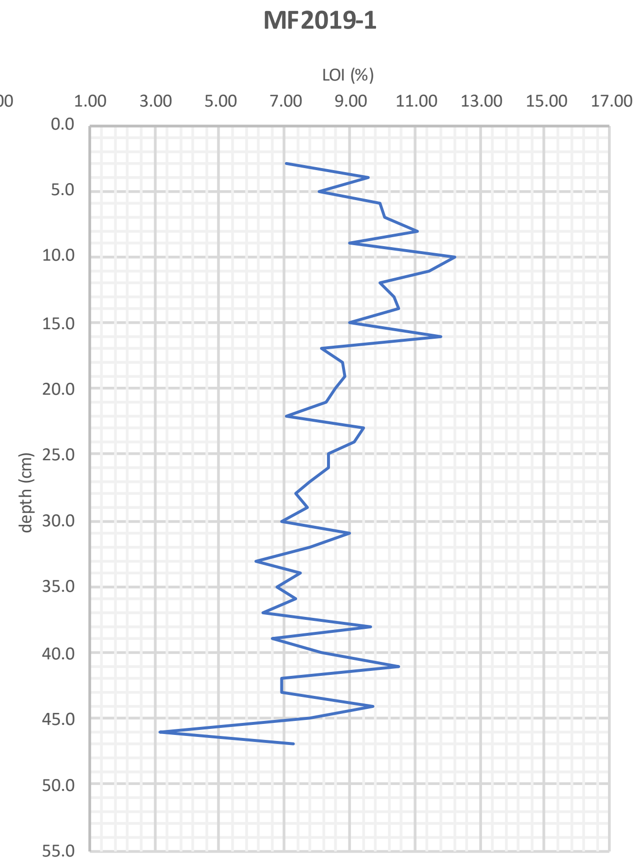

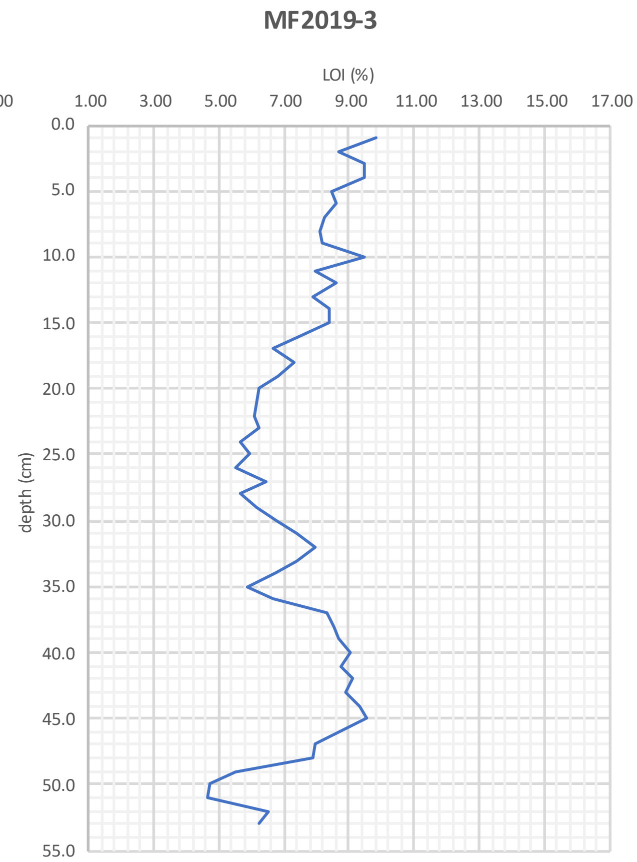

Inner Ikjefjord

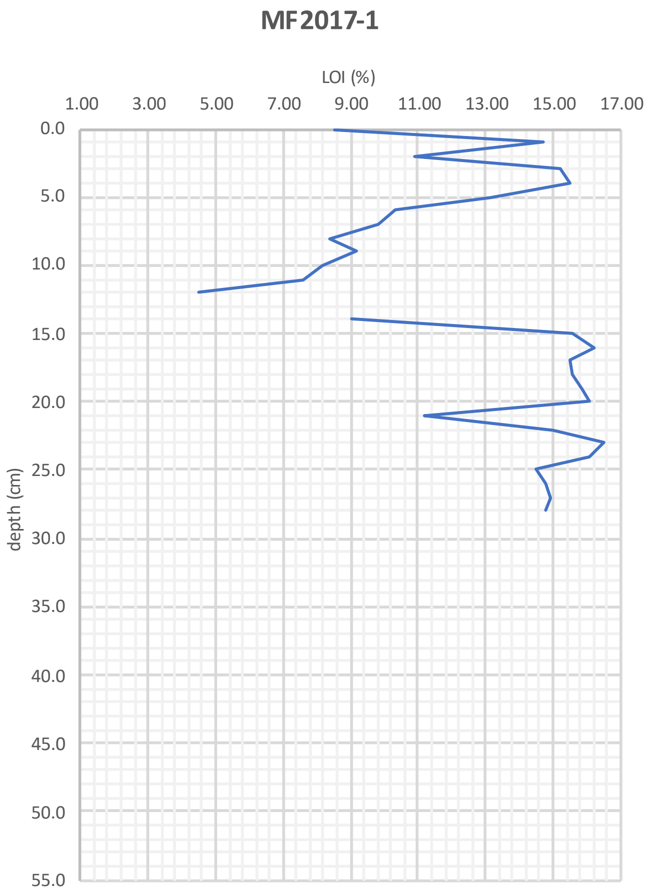

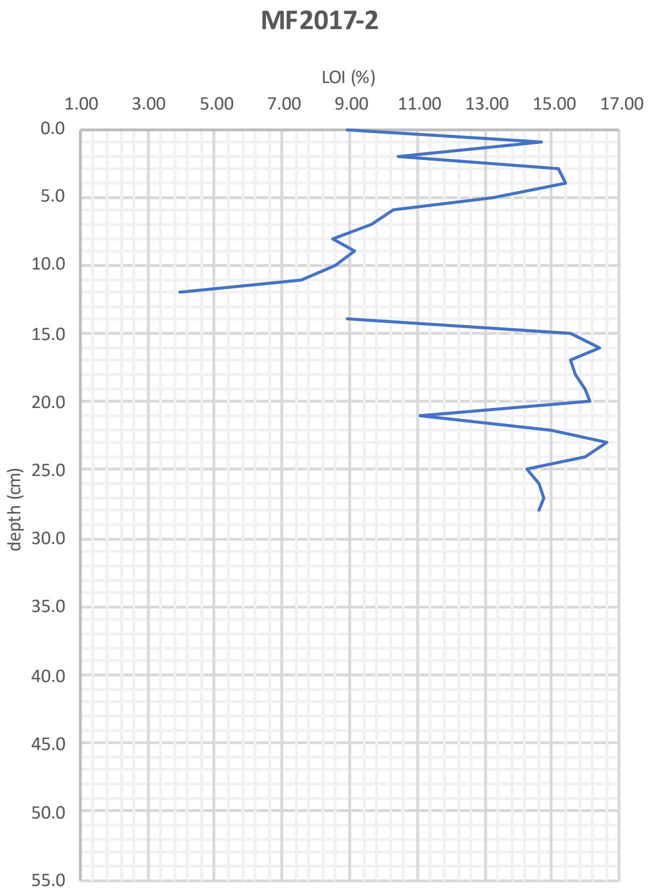

Arnafjord and Indrefjord

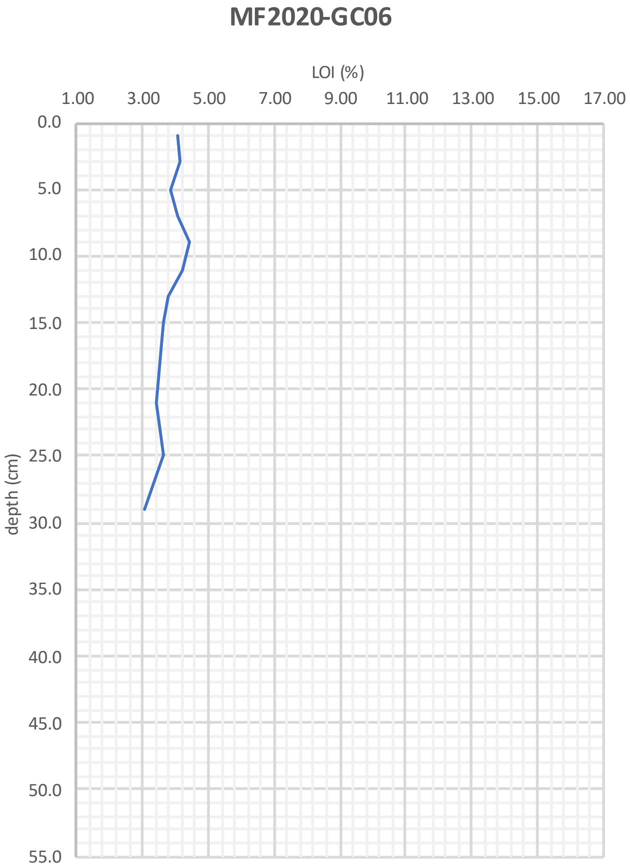

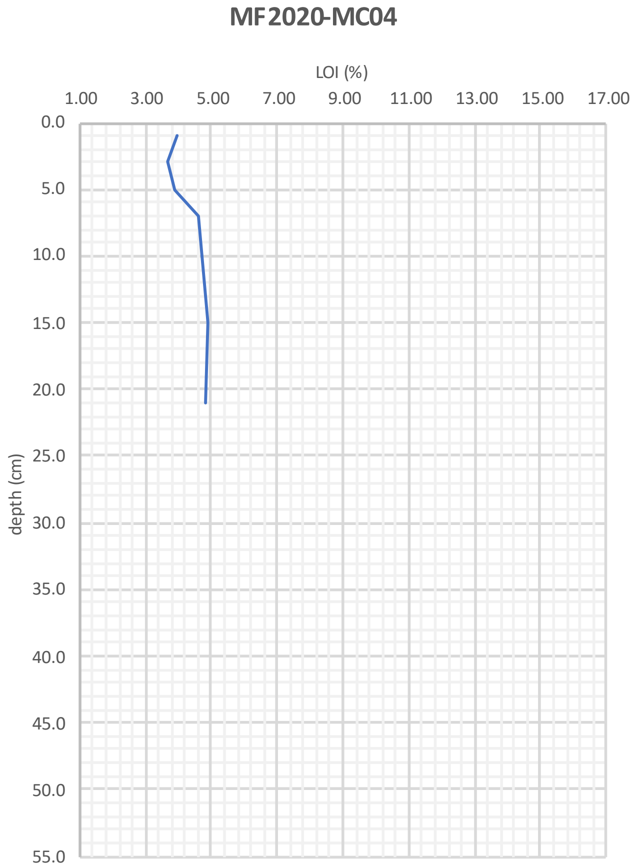

Inner Nærøyfjord

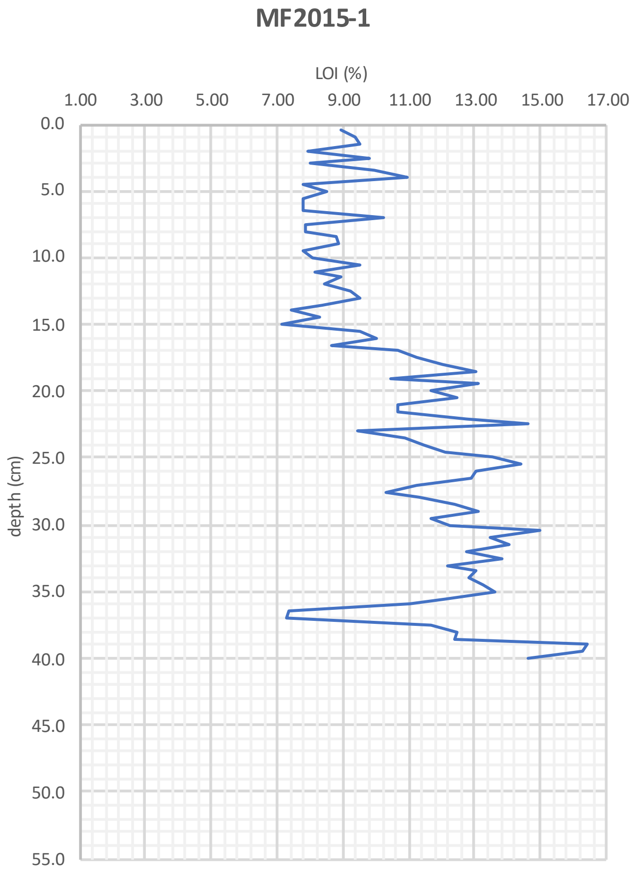

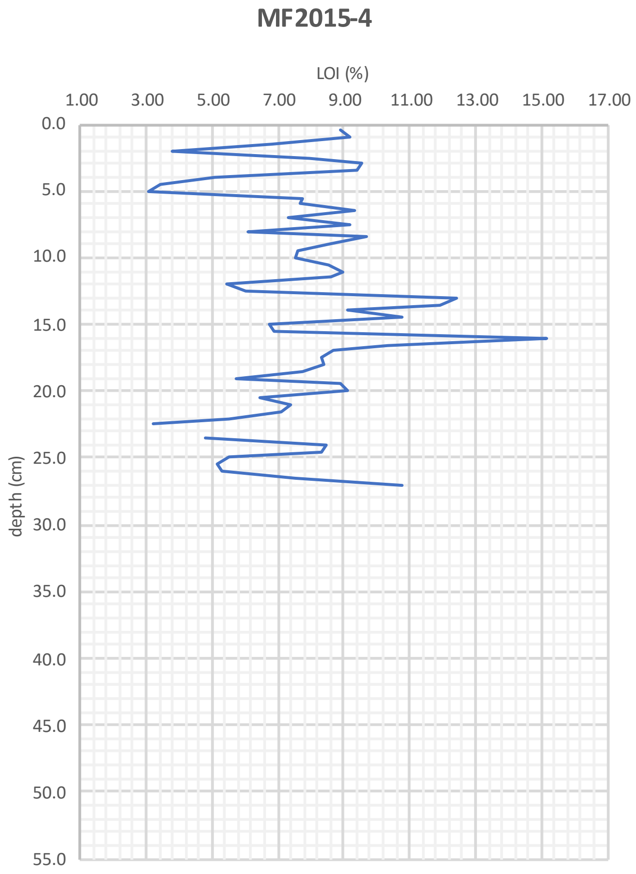

Inner Aurlandsfjord

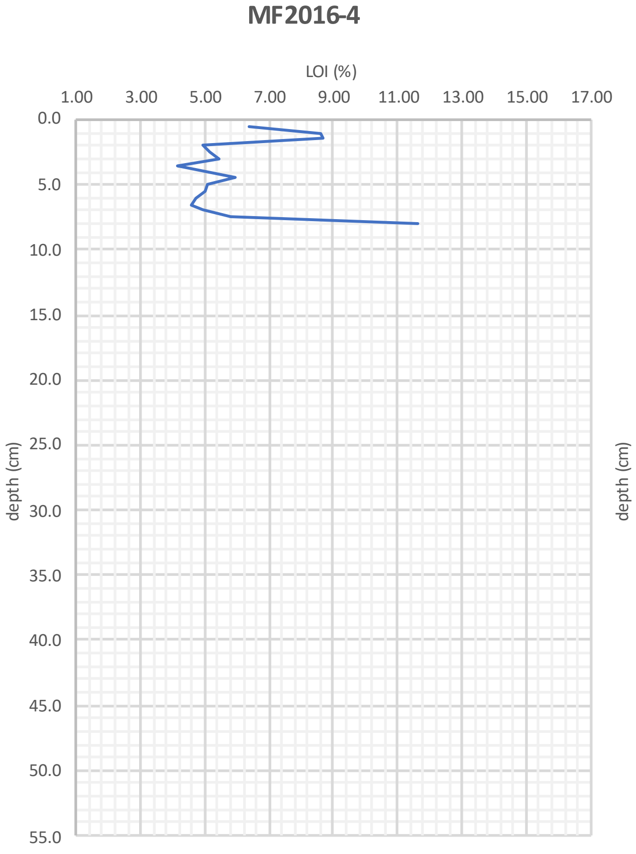

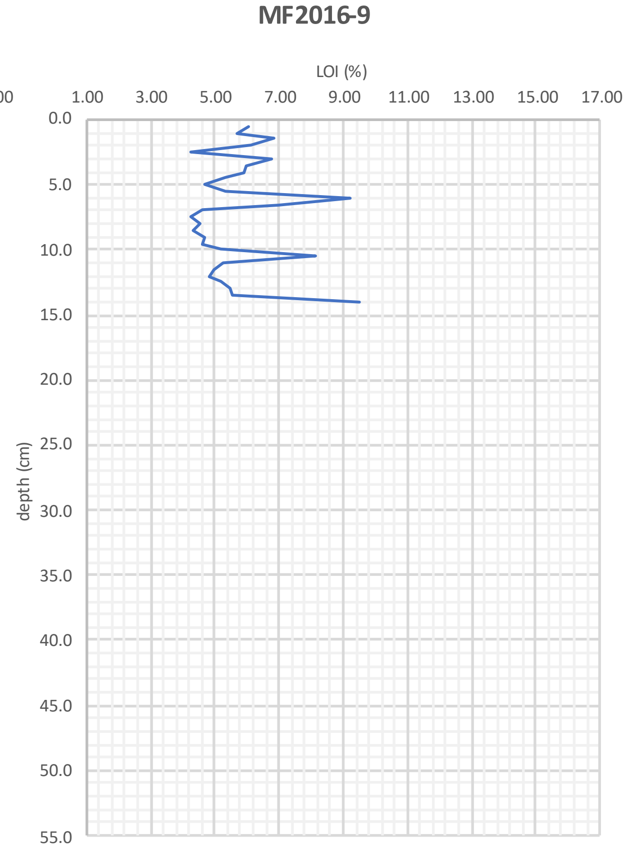

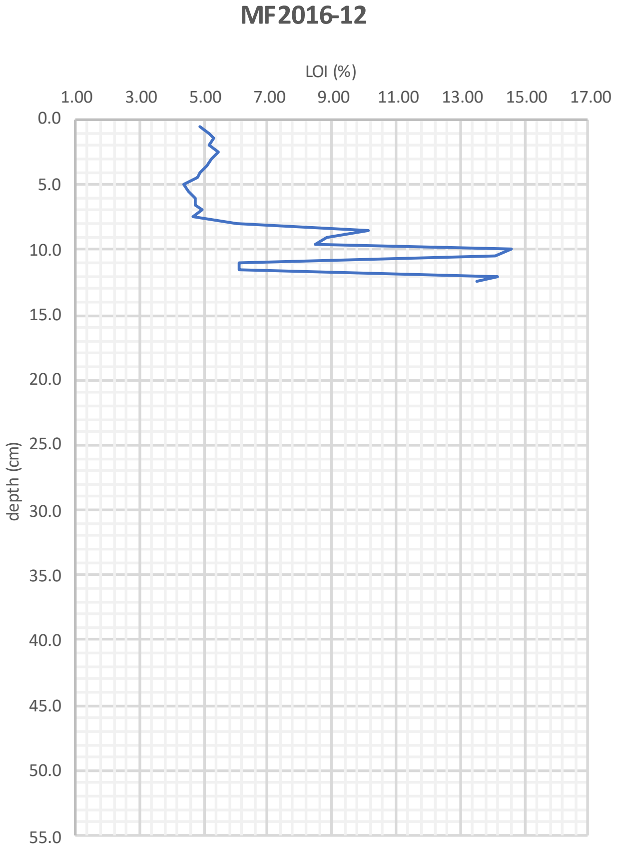

Appendix III: Average LOI calculation for the respective time horizons

Sediment Core ID	SR (mm/year)	CALC	2019	2013	2010	2001	1999	1991	1984	1978
		Sediment depth (cm)	n.a.	n.a.	0.134	0.737	0.871	1.407	1.876	2.278
MF2012-7	0.067	Mean LOI (%)	n.a.	n.a.	10.67091		10.64410		9.97282	
		Sediment depth (cm)	n.a.	n.a.	0.158	0.869	1.027	1.659	2.212	2.686
MF2012-8	0.079	Mean LOI (%)	n.a.	n.a.	8.49076		8.48264		8.31217	
		Sediment depth (cm)	n.a.	n.a.	0.138	0.759	0.897	1.449	1.932	2.346
MF2012-9	0.069	Mean LOI (%)	n.a.	n.a.	8.05268		8.32333		7.83931	
		Sediment depth (cm)	n.a.	n.a.	2.25	9	10.5	16.5	21.75	26.25
MF2013-4	0.75	Mean LOI (%)	n.a.	n.a.	8.48288		8.41438		8.67634	
		Sediment depth (cm)	n.a.	n.a.	2.25	9	10.5	16.5	21.75	26.25
MF2013-6	0.75	Mean LOI (%)	n.a.	n.a.	8.94791		9.32108		6.48079	
		Sediment depth (cm)	n.a.	0.84	3.36	10.92	12.6	19.32	25.2	30.24
MF2014-5	0.84	Mean LOI (%)	12.57792		10.38323		8.96285		9.17202	
		Sediment depth (cm)	n.a.	0.75	3	9.75	11.25	17.25	22.5	27
MF2014-7	0.75	Mean LOI (%)	8.44971		8.90785		7.99790		7.04773	
		Sediment depth (cm)	n.a.	1.64	4.1	11.48	13.12	19.68	25.42	30.34
MF2015-1	0.82	Mean LOI (%)	9.28163		8.53801		9.95795		12.51151	
		Sediment depth (cm)	n.a.	1.54	3.85	10.78	12.32	18.48	23.87	28.49
MF2015-4	0.77	Mean LOI (%)	8.30324		7.20239		9.44262		7.29939	
		Sediment depth (cm)		5.25	10.5	26.25	n.a.	n.a.	n.a.	n.a.
MF2016-4	1.75	Mean LOI (%)	5.94768		n.a.		n.a.		n.a.	
		Sediment depth (cm)	n.a.	0.57	1.14	2.85	3.23	4.75	6.08	7.22
MF2016-9	0.19	Mean LOI	6.03460		5.93349		5.48030		6.26922	
		Sediment depth (cm)	n.a.	0.69	1.38	3.45	3.91	5.75	7.36	8.74
MF2016-12	0.23	Mean LOI (%)	4.89624		5.26516		4.66717		7.42124	
		Sediment depth (cm)	n.a.	1.6	2.8	6.4	7.2	10.4	13.2	15.6
HB17-211-01MC-A	0.4	Mean LOI (%)	2.84626		2.38808		2.35731		2.12768	
		Sediment depth (cm)	n.a.	0.48	0.84	1.92	2.16	3.12	3.96	4.68
HB17-211-02MC-A	0.12	Mean LOI (%)	4.59480		4.28862		4.39296		4.02998	
		Sediment depth (cm)	n.a.	1.88	3.29	7.52	8.46	12.22	15.51	18.33
MF2017-1	0.47	Mean LOI (%)	11.3667		12.0500		7.5800		15.7667	
		Sediment depth (cm)	n.a.	1.76	3.08	7.04	7.92	11.44	14.52	17.16
MF2017-2	0.44	Mean LOI (%)	11.34271		12.73321		8.44519		15.83260	
		Sediment depth (cm)	n.a.	6	9	18	20	28	35	41
MF2019-1	1	Mean LOI (%)	8.73276		10.11621		8.26130		7.89836	
		Sediment depth (cm)	n.a.	6	9	18	20	28	35	41

MF2019-3	1	Mean LOI (%)	9.09314		8.02616		5.99133		7.98146	
MF2019-6	0.8	Sediment depth (cm)	n.a.	4.8	7.2	14.4	16	22.4	28	32.8
		Mean LOI (%)	9.40002		8.11251		8.28554		7.22835	
MF2019-8	0.8	Sediment depth (cm)	n.a.	4.8	7.2	14.4	16	22.4	28	32.8
		Mean LOI (%)	5.72877		9.27148		6.75235		7.91695	
MF2020-GC06	0.105	Sediment depth (cm)	0.105	0.735	1.05	1.995	2.205	3.045	3.78	4.41
		Mean LOI (%)	4.04126		4.08018		4.11911		3.97859	
MF2020-MC04	0.136	Sediment depth (cm)	0.136	0.952	1.36	2.584	2.856	3.944	4.896	5.712
		Mean LOI (%)	3.94678		3.82415		3.70152		3.87670	

Appendix IV: Hydrographical raw data

SOGNDALSFJORD (200 m)			
Date	Temperature (°C)	Date	Oxygen (mg/l)
27.08.2019	8.399	27.08.2019	4.38
05.09.2018	8.394	05.09.2018	4.6
02.09.2014	8.1855	02.09.2014	3.299
Mean 2019-2013	8.303375	Mean 2019-2013	4.01975
02.09.2010	8.21	02.09.2010	5.9
03.09.2009	8.353	03.09.2009	4.57
11.08.2009	8.356	11.08.2009	4.35
11.03.2009	8.429		
09.10.2008	8.412	09.10.2008	2.46
25.08.2008	8.412	25.08.2008	2.56
02.10.2007	8.313	02.10.2007	2.8
13.06.2007	8.303	13.06.2007	3.06
24.08.2006	8.298	24.08.2006	3.52
01.09.2004	8.093		
12.09.2003	8.069	12.09.2003	2.95
27.08.2003	8.066		
Mean 2010-2001	8.276166667	Mean 2010-2001	3.574444444
12.10.1999	7.8	12.10.1999	2.74
20.04.1993	8.1	20.04.1993	3.9
27.02.1993	8	27.02.1993	3.6
17.12.1991	8	17.12.1991	5.7
22.10.1991	8	22.10.1991	5.6
21.09.1991	8	21.09.1991	5.5
27.08.1991	8.1	27.08.1991	5.7
25.05.1991	7.8	25.05.1991	3.7
24.04.1991	7.9	24.04.1991	3.4
20.03.1991	7.8	20.03.1991	3.4
27.02.1991	8		
29.01.1991	7.6	29.01.1991	3.6
26.01.1991	8	26.01.1991	3.5
Mean 1999-1991	7.930769231	Mean 1999-1991	4.195
19.11.1984	7.2	19.11.1984	6.2
09.10.1984	7.1	09.10.1984	7.2
18.06.1984	7.3		
02.05.1984	7.8	02.05.1984	5

INNER IKJEFJORD (75 m)			
Date	Temperature (°C)	Date	Oxygen (mg/l)
21.02.2019	7.862	21.02.2019	2.15793651
18.10.2017	7.295	18.10.2017	0.68102041
29.08.2017	7.30278065	29.08.2017	0.97406452
24.06.2017	7.3215	24.06.2017	1.173375
31.05.2015	7.08946774	31.05.2015	0.99064516
Mean 2019-2013	7.374149677	Mean 2019-2013	1.195408319

22.03.1984	7.8		
10.01.1984	7.3		
Mean 1984-1978	7.416666667	Mean 1984-1978	6.133333333

INNER BARSNESFJORD (60 m)			
Date	**Temperature (°C)**	**Date**	**Oxygen (mg/l)**
03.09.2013	7.13	03.09.2013	0.22
Mean 2019-2013	7.13	Mean 2019-2013	0.22
18.05.2010	6.928	31.08.2010	5.66
31.08.2010	6.964		
01.09.2009	8.18	31.08.2009	0.12
25.08.2008	8.098	01.09.2008	0.05
24.08.2006	7.821	23.08.2006	2.39
		24.08.2005	0.02
01.09.2004	6.903	25.08.2004	0.05
		01.09.2003	3.98571429
27.08.2001	7.28	27.08.2001	3.99
Mean 2010-2001	7.45342857	Mean 2010-2001	1.81619048
12.10.1999	6.78	01.10.1999	0
Mean 1999-1991	6.78	Mean 1999-1991	0

OUTER BARSNESFJORD (75 m)			
Date	**Temperature (°C)**	**Date**	**Oxygen (mg/l)**
		2019	3.7
		2016	0.09
		2016	0.24
		2014	3.11
03.09.2013	7.227	03.09.2013	2.08
Mean 2019-2013	7.227	Mean 2019-2013	1.844
31.08.2010	6.968	31.08.2010	5.53
01.09.2009	8.425	31.08.2009	0.06
25.08.2008	8.158	01.09.2008	0.19
23.08.2007	7.951		
		24.08.2005	0.07
01.09.2004	7.065	25.08.2004	0.13
Mean 2010-2001	7.7134	Mean 2010-2001	1.196
12.10.1999	7.29		
		1993	0.2
		1993	3.9
Mean 1999-1991	7.29	Mean 1999-1991	2.05
17.09.1978	6.57	02.09.1978	3.64285714
Mean 1984-1978	6.57	Mean 1984-1978	3.64285714

INNER NAERØYFJORD (70 m)			
Date	**Temperature (°C)**	**Date**	**Oxygen (mg/l)**
01.09.2015	7.997	01.09.2015	0.40470588
11.02.2019	8.54692857	11.02.2019	0.66928571
Mean 2019-2013	8.27196429		0.5369958
03.09.2006	8.74	03.09.2006	1.97797
Mean 2010-2001	8.74	Mean 2010-2001	1.97797
19.11.1993	8.57	19.11.1993	0.88226
19.09.1994	8.36	19.09.1994	2.84
30.03.1996	6.78	30.03.1996	7.28
25.06.1996	7.44	25.06.1996	6.1
Mean 1999-1991	7.7875	Mean 1999-1991	4.275565

Appendix V: Meteorological raw data

Meteorological station	Year	Mean air temperature (°C)	Annual precipitation (mm/year)
Fjærland - Bremuseet	2019	5.9	1714.9
	2018	5.4	1760.3
	2017	5.6	2113.3
	2016	5.7	n.a.
	2015	5.9	2346
	2014	7.4	1782.9
	2013	4.5	1876.6
	Mean 2019-2013	5.771428571	1932.333333
Fjærland - Bremuseet	2010	3	1303.8
	2009	5.6	n.a.
	2008	5.8	1892.7
	2007	5.1	2233.1
	2006	6.1	1674
Fjærland - Skarestad	2005	n.a.	n.a.
	2004	6.4	1881.3
	2003	6.2	1955
	2002	6.1	1480.9
	2001	5.5	1583.9
	Mean 2010-2001	5.533333333	1750.5875
Fjærland - Skarestad	1999	6	2244.8
	1998	5.8	2061.3
	1997	6	2112
	1996	4.8	1101.3
	1995	5.6	1918.9
	1994	5.1	2215.2
	1993	5.2	1754.8
	1992	6.1	2279.5
	1991	5.9	1974.6
	Mean 1999-1991	5.611111111	1962.488889
Fjærland - Skarestad	1984	5.8	1622.6
	1983	5.5	2707.6
	1982	5.6	2037.1
	1981	3.6	1816.4
	1980	4.7	1843.4
	1979	3.7	1973.9
	1978	4.9	1832.3
	Mean 1984-1978	4.828571429	1976.185714

Meteorological station	Year	Mean air temperature (°C)	Annual precipitation (mm/year)
Sogndal - Selseng	2019		1563.3
	2018		1643.1
	2017		n.a.
	2016		1582.3
	2015		2100.6
	2014		1781.6
	2013		1795.6
	Mean 2019-2013		1744.416667
Sogndal - Selseng	2010		1127.6
	2009		1504.2
	2008		1722
	2007		1893.5
	2006		1467.5
	2005		1924.6
	2004		1558.1
	2003		1559.8
	2002		1224
	2001		1415.5
	Mean 2010-2001		1539.68
Sogndal - Selseng	1999		1899.2
	1998		1725.6
	1997		1647
	1996		942.5
	1995		1600.5
	1994		1693.8
	1993		1303.4
	1992		1845.3
	1991		1393.3
	Mean 1999-1991		1561.177778
Sogndal - Selseng	1984		1383.2
	1983		2071.9
	1982		1545.7
	1981		1414.5
	1980		1485.8
	1979		1570.7
	1978		1402.5
	Mean 1984-1978		1553.471429

Meteorological station	Year	Mean air temperature (°C)	Annual precipitation (mm/year)
Hafslo	2019		1025.2
	2018		1155.2
	2017		1158.5
	2016		1042.2
	2015		1380.2
	2014		1071.7
	2013		1078.9
	Mean 2019-2013		1130.271429
Hafslo	2010		792.6
	2009		n.a.
	2008		n.a.
	2007		n.a.
	2006		1065
	2005		n.a.
	2004		1073.9
	2003		1136.4
	2002		849
	2001		914
	Mean 2010-2001		971.8166667
Hafslo	1999		1312.6
	1998		1277.8
	1997		1104
	1996		676.8
	1995		1068.6
	1994		1227.6
	1993		973.5
	1992		1301.5
	1991		976.4
	Mean 1999-1991		1102.088889
Hafslo	1984		994.8
	1983		1504.4
	1982		1016.2
	1981		1011.7
	1980		1137.8
	1979		1121.2
	1978		976
	Mean 1984-1978		1108.871429

Meteorological station	Year	Mean air temperature (°C)	Annual precipitation (mm/year)
Vik I Sogn III	2019		1122
	2018		1132
	2017		1393.9
	2016		1002.7
	2015		1439.5
	2014		1081.6
	2013		1185.1
	Mean 2019-2013		1193.828571
Vik I Sogn III	2010		694.1
	2009		1129.7
	2008		1218.9
	2007		1441.9
	2006		1169.9
	2005		n.a.
	2004		1181.5
	2003		898.3
	2002		786
	2001		978
	Mean 2010-2001		1055.366667
Vik I Sogn III	1999		1349.4
	1998		1269
	1997		1295.7
	1996		651.2
	1995		1114.2
	1994		1249.9
	1993		1028.8
	1992		1368.6
	1991		1020.9
	Mean 1999-1991		1149.744444
Vik I Sogn III	1984		945.3
	1983		1558.1
	1982		1056.2
	1981		1060.7
	1980		1027.5
	1979		1132
	1978		1077
	Mean 1984-1978		1122.4

Meteorological station	Year	Mean air temperature (°C)	Annual precipitation (mm/year)
Sørebø	2019		1652
	2018		1822.7
	2017		2092.7
	2016		1641.4
	2015		2467.9
	2014		1857.6
	2013		1968.2
	Mean 2019-2013		1928.928571
Sørebø	2010		n.a.
	2009		n.a.
	2008		n.a.
	2007		n.a.
	2006		1993.2
	2005		2388.8
	2004		n.a.
	2003		1781.3
	2002		1547.8
	2001		1632.6
	Mean 2010-2001		1868.74
Sørebø	1999		2293.5
	1998		2076.5
	1997		2151.8
	1996		n.a.
	1995		n.a.
	1994		n.a.
	1993		n.a.
	1992		n.a.
	1991		n.a.
	Mean 1999-1991		2173.933333
Sørebø	1984		n.a.
	1983		n.a.
	1982		n.a.
	1981		n.a.
	1980		n.a.
	1979		n.a.
	1978		n.a
	Mean 1984-1978		

Meteorological station	Year	Mean air temperature (°C)	Annual precipitation (mm/year)
Jordalen - Nåsen	2019		1874.3
	2018		2019.7
	2017		2181.4
	2016		2064.8
	2015		2821.5
	2014		2292.1
	2013		2137.7
	Mean 2019-2013		2198.785714
Jordalen - Nåsen	2010		1236.7
	2009		1775.9
	2008		2160.3
	2007		2302.7
	2006		1912
	2005		2301.1
	2004		1880
	2003		1752.3
	2002		1526.3
	2001		1552
	Mean 2010-2001		1839.93
Jordalen - Nåsen	1999		2289.5
	1998		2053.6
	1997		1809.9
	1996		1103.9
	1995		1853.7
	1994		2003.9
	1993		1579.1
	1992		2159.9
	1991		1787
	Mean 1999-1991		1848.944444
Jordalen - Nåsen	1984		1706.9
	1983		2553.2
	1982		1838.7
	1981		1822.9
	1980		1717
	1979		1808.3
	1978		1706.5
	Mean 1984-1978		1879.071429

Meteorological station	Year	Mean air temperature (°C)	Annual precipitation (mm/year)
Aurland	2019		676.2
	2018		727.7
	2017		922.4
	2016		735.8
	2015		n.a.
	2014		n.a.
	2013		697.9
	Mean 2019-2013		752
Aurland	2010		574.3
	2009		569
	2008		n.a.
	2007		871.8
	2006		n.a.
	2005		785.6
	2004		629.5
	2003		634.5
	2002		541
	2001		591.6
	Mean 2010-2001		649.6625
Aurland	1999		790.2
	1998		789.4
	1997		687.6
	1996		435.1
	1995		736.1
	1994		799.1
	1993		694.2
	1992		856.4
	1991		691
	Mean 1999-1991		719.9
Aurland	1984		634.1
	1983		997.5
	1982		638.7
	1981		735.4
	1980		761.7
	1979		775.7
	1978		696.3
	Mean 1984-1978		748.4857143

Meteorological station	Year	Mean air temperature (°C)	Annual precipitation (mm/year)
Vangsnes II	2019	8.1	
	2018	8.1	
	2017	7.6	
	2016	7.9	
	2015	7.9	
	2014	9.3	
	2013	7	
	Mean 2019-2013	7.985714286	
Vangsnes II	2010	6.2	
	2009	7.7	
	2008	8.2	
	2007	7.4	
	2006	8.3	
	2005	7.5	
	2004	7.7	
	2003	7.7	
	2002	7.8	
	2001	6.9	
	Mean 2010-2001	7.54	
Vangsnes I	1999	n.a.	
	1998	n.a.	
	1997	n.a.	
	1996	6.5	
	1995	n.a.	
	1994	n.a.	
	1993	n.a.	
	1992	n.a.	
	1991	n.a.	
	Mean 1999-1991	6.5	
Vangsnes I	1984	7.4	
	1983	6.9	
	1982	7.2	
	1981	5.8	
	1980	6.7	
	1979	5.5	
	1978	6.6	
	Mean 1984-1978	6.585714286	

Meteorological station	Year	Mean air temperature (°C)	Annual precipitation (mm/year)
Takle	2019	8	
	2018	7.8	
	2017	7.8	
	2016	7.8	
	2015	8	
	2014	9	
	2013	7	
	Mean 2019-2013	7.914285714	
Takle	2010	5.8	
	2009	7.8	
	2008	8.1	
	2007	7.6	
	2006	8.4	
	2005	n.a.	
	2004	n.a.	
	2003	8	
	2002	8	
	2001	6.9	
	Mean 2010-2001	7.575	
Takle	1999	7.7	
	1998	7.1	
	1997	7.8	
	1996	6.5	
	1995	7	
	1994	6.9	
	1993	6.7	
	1992	7.7	
	1991	7.5	
	Mean 1999-1991	7.211111111	
Takle	1984	7.2	
	1983	7.1	
	1982	7.4	
	1981	6.1	
	1980	6.8	
	1979	5.7	
	1978	6.5	
	Mean 1984-1978	6.685714286	

Appendix VI: Final average LOI, hydrographical and meteorological values

	LOI (%)				Oxygen (mg/l)				Water temperature (°C)				Precipitation (mm/year)			
Tributary fjord basin	1978-1984	1991-1999	2001-2010	2013-2019	1978-1984	1991-1999	2001-2010	2013-2019	1978-1984	1991-1999	2001-2010	2013-2019	1978-1984	1991-1999	2001-2010	2013-2019
Fjærlandsfjord	3.1	3.4	3.3	3.7	-	-	-	-	-	-	-	-	1976.2	1962.5	1750.6	1932.3
Sogndalsfjord	8.7	9.2	9.1	-	6.1	4.2	3.6	4.0	7.4	7.9	8.3	8.3	1553.5	1561.2	1539.7	1744.4
Inner Barsnesfjord	8.6	8.0	9.7	10.7	-	0.0	1.8	0.2	-	6.8	7.5	7.1	1108.9	1102.1	971.8	1130.3
Outer Barsnesfjord	7.4	8.1	8.8	7.6	3.6	2.1	1.2	1.8	6.6	7.3	7.7	7.2	1108.9	1102.1	971.8	1130.3
Inner Ikjefjord	15.8	8.0	12.4	11.4	-	-	-	1.2	-	-	-	7.4	-	2173.9	1868.7	1928.9
Arnafjord system	3.9	3.9	4.0	4.0	-	-	-	-	-	-	-	-	1122.4	1149.7	1055.4	1193.8
Inner Nærøyfjord	9.9	9.7	7.9	8.8	-	4.3	2.0	0.5	-	7.8	8.7	8.3	1879.1	1848.9	1839.9	2198.8
Inner Aurlandsfjord	6.8	5.1	5.6	5.6	-	-	-	-	-	-	-	-	748.5	719.9	649.7	752.0

	Air temperature (°C)			
Meteorological station	1978-1984	1991-1999	2001-2010	2013-2019
Fjærland	4.8	5.6	5.5	5.8
Vangsnes	6.6	6.5	7.5	8.0
Takle	6.7	7.2	7.6	7.9

Affidavit

<u>Eidesstattliche Erklärung</u>

Hiermit erkläre ich an Eides statt, dass die vorliegende Abschlussarbeit

„Recent (0-40 years) environmental and climate change as interpreted by the spatial and temporal distribution of organic matter (LOI) in sediment cores from seven tributary fjords of the Sognefjord, Western Norway"

selbständig und ohne fremde Hilfe angefertigt habe. Ich habe dabei nur die in der Arbeit angegebenen Quellen und Hilfsmittel benutzt. Die Arbeit wurde in gleicher oder ähnlicher Form noch keiner anderen Prüfung vorgelegt und auch noch nicht veröffentlicht.

………………………………. ……………………………….

(Ort, (Abgabe-) Datum) (Unterschrift)

<u>Erklärung zu Eigentumsübertragung und Verwertungsrechte</u>

Hiermit erkläre ich mein Einverständnis, dass die Technische Hochschule Bingen die vorliegende Abschlussarbeit den Studierenden und interessierten Dritten zur Einsichtnahme zur Verfügung stellt und unter Nennung meines Namens (Jana Altenkirch) veröffentlichen darf.

………………………………. ……………………………….

(Ort, (Abgabe-) Datum) (Unterschrift)